The Ba/F3 transformation assay:

Characterization of a Novel CSF2RB-activating Variant,

and the Discovery of Acquired Mutations in Ba/F3 Cells.

By

Kevin Watanabe-Smith

A DISSERTATION

Presented to the Cancer Biology graduate program
and the Oregon Health & Science University
School of Medicine

in partial fulfillment of
the requirements for the degree of

Doctor of Philosophy

January 2017

School of Medicine

Oregon Health & Science University

CERTIFICATE OF APPROVAL

This is to certify that the PhD dissertation of

Kevin Watanabe-Smith

has been approved

_____
Brian Druker (Mentor)

_____
Melissa Wong (Committee Chair)

_____
Caroline Enns (Committee Member)

_____
Cary Harding (Committee Member)

_____
Matt Thayer (Committee Member)

_____
Jim Korkola (Examination Member)

_____
Anupriya Agarwal (Associate Member)

_____
Cristina Tognon (Associate Member)

Table of Contents

1 Introduction 4

1.1 Determining functional mutations in leukemia: The Ba/F3 transformation assay . 7

1.1.1 Background 7

1.1.2 The Ba/F3 cell line 10

1.1.3 Using Ba/F3 cells to assay transformation 12

1.1.4 The use of viruses in in vitro transformation assays and potential complications 14

1.1.5 Summary 18

1.2 The common beta chain: CSF2RB 19

1.2.1 CSF2RB activation and signaling 19

1.2.2 CSF2RB deficiencies and knockouts 21

1.2.3 CSF2RB overexpression and activating mutations 23

1.2.4 Summary 24

2 Discovery and functional characterization of a germline, CSF2RB-activating mutation in leukemia 30

2.1 Article 31

2.2 Materials & Methods 38

2.3 Figures 42

2.4 Tables 54

3 Analysis of acquired mutations in transgenes arising in Ba/F3 transformation assays: Findings and recommendations 62

3.1 Abstract 63

3.2 Introduction 64

3.3 Results 66

3.3.1 Experimental Design 66

3.3.2 Acquired mutations detected in transformed lines 67

3.3.3 CSF2RB R461C does not drive genomic instability 68

3.3.4 Transformation rate determined by limiting dilution analysis 69

3.3.5 Acquired mutations are exclusively observed in weakly transforming oncogenes 70

3.4 Discussion 70

3.5 Methods 76

3.6 Miscellaneous 78

3.7 Figures 81

3.8 Tables 86

4 Materials and Methods 92

4.1 Patient samples and genomic analysis 92

4.2 Cloning and construct creation 93

4.3 Cell Culture 94

4.3.1 Ba/F3 transformation assay 95

4.3.2 Genomic DNA extraction and Sanger sequencing 96

4.3.3 Protein lysis and immunoblot 97

4.3.4 Cycloheximide timecourse 98

4.3.5 Flow cytometry staining for CSF2RB 99

4.3.6 Small molecule inhibitor screen 99

4.3.7 Drug curves and Annexin-V readouts 100

4.3.8 6-thioguanine survival assay 100

4.3.9 Limiting dilution plates 101

4.4 Computational analysis and modeling 101

4.4.1 Statistical analysis 101

4.4.2 Transmembrane domain prediction 102

4.4.3 Multiple sequence alignment 102

4.4.4 Extreme limiting dilution analysis 102

4.4.5 Meta-literature review 102

5 Conclusions and Future Directions 104

5.1 Identification of R461C as the first CSF2RB-activating mutation in humans 104

5.1.1 CSF2RB R461C is a rare, germline variant 105

5.1.2 The implications of CSF2RB R461C for basic research 106

5.2 The continued use of the Ba/F3 transformation assay 107

5.2.1 Acquired mutations in transformed Ba/F3 cells..... 108

5.2.2 Relevance of weak transforming mutations 110

5.3 Summary 114

6 Appendix A: Alternate CSF2RB mutations at residue 461 117

6.1 Background 117

6.2 Results 118

6.3 Discussion 119

6.4 Figures 121

7 Appendix B: Discovery of a CSF2RA mutation inducing dimerization with CSF2RB 123

7.1 Background 123

7.2 Results 123

7.3 Discussion 124

7.4 Figures 127

8 References 129

List of Figures

Figure 1-1 Non-recurrently mutated genes in AML form a long tail. 26

Figure 1-2 CSF2RB signals through a dodecameric complex with a ligand and ligand-specific alpha chain. 27

Figure 1-3 CSF2RB activates signaling through JAK2/STAT5 and several other pathways. 28

Figure 1-4 CSF2RB mutations in all cancers as reported by TCGA. 29

Figure 2-1 CSF2RB R461C is discovered in a primary T-ALL sample. 42

Figure 2-2 R461 is a conserved residue in CSF2RB homologues. 43

Figure 2-3 CSF2RB R461C is a transforming mutation which results in receptor stabilization and formation of higher molecular weight complexes. 44

Figure 2-4 CSF2RB R461C transforms Ba/F3 cells. 46

Figure 2-5 CSF2RB R461C is enriched in Ba/F3 prior to gaining factor independence. ... 47

Figure 2-6 Residue R461 lies within the transmembrane domain of CSF2RB in most predictive models. 49

Figure 2-7 CSF2RB R461C is constitutively phosphorylated and activates canonical downstream pathways that are sensitive to JAK2 inhibition. 51

Figure 2-8 R461C cells are more sensitive to JAK-inhibitors than CSF2RB WT cells. 53

Figure 3-1 Experimental design schematic. 81

Figure 3-2 Compiled data from all IL-3 withdrawal experiments. 82

Figure 3-3 Ba/F3 cells expressing CSF2RB R461C do not demonstrate increased rates of mutagenesis. 83

Figure 3-4 Ba/F3 transformation rates vary by transgene but not by time in culture. 84

Figure 3-5 Acquired mutations occur in weak, but not strong, transforming transgenes. .. 85

Figure 6-1 R461A and R461S drive factor-independent growth in Ba/F3 cells. 121

Figure 6-2 CSF2RB R461A and R461S drive surface accumulation similar to R461C. ... 122

Figure 7-1 CSF2RA G343D results in Ba/F3 transformation when combined with functional CSF2RB. 127

List of Tables

Table 2-1 Co-occuring mutations in the T-ALL patient..... 54

Table 2-2 Antibodies used in this study 55

Table 2-3 Complete results of the small-molecule inhibitor screen. 56

Table 2-4 Mutations found in primary leukemic samples 61

Table 3-1 Frequency of sequence validation in Ba/F3 transformation studies (2014-2016) 86

Table 3-2 Complete table of studies using the Ba/F3 transformation assay (2014-2016) – Frequency of sequencing outgrown Ba/F3 lines..... 87

Table 3-3 Constructs used in this study 89

Table 3-4 Sequence results of Ba/F3 lines from bulk withdrawal assays. 90

Abbreviations

$\Delta\beta_c$	Truncated beta-common (CSF2RB)
β-me	Beta-mercaptoethanol (2-mercaptoethanol)
6-TG	6-thioguanine
ABL	Abelson tyrosine protein kinase
aCML	Atypical chronic myeloid leukemia
AKT	Serine/threonine protein kinase
ALK	Anaplastic lymphoma receptor tyrosine kinase
ALL	Acute lymphoblastic leukemia
AML	Acute myelogenous leukemia
ATCC	American Type Culture Collection
AZD1480	JAK2 specific inhibitor
B-ALL	B-cell acute lymphoblastic leukemia
Ba/F3	Murine, pro-B cell line
BALB/c	Common albino mouse strain
BCR	Breakpoint cluster region
BCR-ABL	Oncogene formed by fusion of BCR and ABL
BION-1	Monoclonal antibody directed towards CSF2RB
BLAST	Basic local alignment search tool
BSA	Bovine serum albumin
CLUSTALO	Clustal Omega – a multiple sequence alignment program
CML	Chronic myelogenous leukemia
CNL	Chronic neutrophilic leukemia
COSMIC	Catalogue of somatic mutations in cancer
Cre-loxP	Site specific recombinase using Cre recombinase and LoxP sites
CRISPR	Clustered regularly interspaced short palindromic repeats
CRLF2	Cytokine receptor-like factor 2
CSF1R	Colony stimulating factor 1 receptor

CSF2	Colony Stimulating Factor 2
CSF2RA	Colony stimulating factor 2 receptor alpha subunit
CSF2RB	Colony stimulating factor 2 receptor beta common subunit
CSF2RB2	Colony stimulating factor 2 receptor beta common subunit (murine specific)
CSF3R	Colony stimulating factor 3 receptor
CSL311	Monoclonal antibody directed toward CSF2RB
D10	DMEM-based cell culture media using 10% FBS
DMEM	Dulbecco's modified eagle medium
DMSO	Dimethyl sulfoxide
DNA	Deoxyribonucleic acid
EDTA	Ethylenediaminetetraacetic acid
EGFR	Epidermal growth factor receptor
ELDA	Extreme limiting dilution analysis
ENU	N-ethyl-N-nitrosourea
EPOR	Erythropoietin receptor
ERBB2	Erb-B2 receptor tyrosine kinase 2
ERK	MAPK1 (Extracellular signal-regulated kinase)
FACS	Fluorescence activated cell sorting
FBS	Fetal bovine serum
FGFR	Fibroblast growth factor receptor
FLT3	Fms related tyrosine kinase 3
FLT3-ITD	FLT3 internal tandem duplication
GAPDH	Glyceraldehyde-3-phosphate dehydrogenase
GD2	A carbohydrate antigen enriched in some tumors
gDNA	Genomic DNA
GFI	Growth factor independence
GFP	Green fluorescent protein
GM-CSF	Granulocyte-macrophage colony stimulating factor (CSF2)
HapMap	International haplotype map project

HAT	Hypoxanthine-aminopterin-thymidine medium
hCSF2RA	Human CSF2RA
hCSF2RB	Human CSF2RB
HEPES	4-(2-hydroxyethyl)-1-piperazineethanesulfonic acid
HPRT	Hypoxanthine Phosphoribosyltransferase 1
HT	Hypoxanthine-thymidine medium
IC_{50}	Concentration of an inhibitor where response is reduced to 50%
IL-3	Interleukin 3
IL-5	Interleukin 5
IL-7	Interleukin 7
IL3RA	Interleukin 3 receptor subunit alpha
IL5RA	Interleukin 5 receptor subunit alpha
IL7R	Interleukin 7 receptor
IRES	Internal ribosome entry site
JAK	Janus kinase
KIT	KIT Proto-oncogene receptor tyrosine kinase
LIF	Leukemia inhibitory factor
MAF	Minor allele frequency
MAPK	Mitogen-activated protein kinase
MDS	Myelodysplastic syndrome
MEK	Mitogen-activated protein kinase kinase
MFI	Mean fluorescence intensity
MPL	MPL Proto-oncogene, thrombopoietin receptor (myeloproliferative leukemia protein)
mRNA	Messenger ribonucleic acid
MSV	Murine sarcoma virus
MSCV	Murine stem cell virus
mTOR1	Mammalian target of rapamycin 1
MuLV	Murine leukemia virus

p210	BCR-ABL fusion transcript coding for a 210kDa protein
PAP	Pulmonary alveolar proteinosis
PCA	Personal cell analysis system (Guava PCA, Millipore)
PCR	Polymerase chain reaction
PDGFRα	Platelet derived growth factor receptor alpha
PDGFRβ	Platelet derived growth factor receptor beta
PE	Phycoerythrin
PI3K	Phosphatidylinositol 3-kinase
PTEN	Phosphatase and Tensin homolog
R10	RPMI-based cell culture media containing 10% FBS
RET	Ret proto-oncogene
RIKEN	Rikagaku Kenkyūsho – Japanese research institute
RPMI	Roswell Park Memorial Institute medium
RSV	Rous sarcoma virus
S6	Ribosomal protein s6
SNP	Single nucleotide polymorphism
SNV	Single nucleotide variation
SOCS-1	Suppressor of cytokine signaling 1
src	SRC proto-oncogene (c-src); v-src is an activated form of c-src in RSV
STAT	Signal transducer and activator of transcription
T-ALL	T-cell acute lymphoblastic leukemia
TCGA	The Cancer Genome Atlas
TM	Transmembrane domain
WEHI-3	Murine cell line, secrets IL-3
WEHI-CM	Conditioned media from WEHI-3 cells (contains IL-3)
WT	Wildtype

Acknowledgements

No man is an island entire of itself; every man
Is a piece of the continent, a part of the main; -John Donne

The research performed in my graduate training would not be possible without the researchers that preceded me. Many of them are named in the coming pages, but the unsung heroes of research are the librarians, the National Institutes of Health, and groups that maintain public databases. Without them I would never be able to write this dissertation. And thank you to every teacher and instructor, from Canby school district to George Fox University and OHSU, I know I wasn't the easiest student to teach yet I appreciated your dedication.

I am most grateful to have been mentored by Dr. Brian Druker, the very definition of a humble yet confident scientist, who could not have been more understanding and supportive through every twist and turn in my graduate training. I also had the fortune to have two additional mentors: Dr. Anupriya Agarwal has been a great teacher of the scientific method and troubleshot more of my failed experiments than I care to admit. Dr. Cristina Tognon always challenged me to fully understand my assumptions and to consider the next step in both my research and in my career.

The Druker lab group is full of so many wonderful individuals. Sarah Bowden, Zoë Schmidt, and Lola Bichler have handled countless administrative forms allowing me to focus on my research. Our lab has been excellently managed by Rebecca Smith, Olga Ryabinina, and Kara Johnson. Kara specifically has my first point of contact for every question over the past five years. Dr. Bill Chang and Dr. Jessica Leonard have answered every clinically relevant question I've had while sharing a laboratory bay with me. I was also lucky to work with two talented and hardworking summer students, Corinne Togiai and Jamila Godil. There are many other members of the Druker lab that I can't possibly thank them all but it has been a joy to work with and learn from everyone.

I am grateful for the class of graduate students I entered PMCB with, who spent hours editing my grants and qualification exam proposals. I would like to particularly thank my fellow graduate students in the Druker lab: Nathalie Javidi-Sharifi, Marilynn Chow, Chelsea Jenkins, and David Edwards. They have been an invaluable source of support and friendship, and I feel fortunate for knowing each one. Marilynn and I entered both graduate school and the Druker lab the same year; we've shared the ups and downs of every year, and she's covered so many weekend experiments for me that we had to establish an official form.

I want to thank my dissertation committee for engaging with every theory I presented: Dr. Melissa Wong, Dr. Caroline Enns, Dr. Matt Thayer, Dr. Cary Harding, Dr. Jim Korkola, and former members Dr. Bill Skach and Dr. Ujwal Shinde. I am especially grateful for Dr. Wong, Dr. Allison Fryer, Dr. Jackie Wirz, Dr. Shannon McWeeney, and Dr. Steven Bedrick who have gone above and beyond in sharing their wise counsel and advice.

I have been blessed with a family that has loved, encouraged, and believed in me my entire life. And most of all, I'm thankful for my wife Denae, who has supported and loved me through my best, my worst, and everything in-between. I don't know what adventure will come next, but I know we will always journey together. I can't wait.

Abstract

Hematologic malignancies are predominantly caused by genetic aberrations resulting in the unregulated proliferation or blocked differentiation of hematopoietic progenitors. The identification and characterization of growth-activating mutations, or driver mutations, has resulted in the development of targeted therapeutics that dramatically improve patient survival and decrease treatment-related toxicity. However, the most common types of leukemia lack a recurrent and defining driver mutation, meaning that the continued development of targeted therapies will require the characterization of novel and rare leukemic variants. The most common assay used to characterize the functional impact of novel mutations found in leukemia is the *in vitro* Ba/F3 transformation assay, which was used in the work described herein to screen primary CSF2RB mutations found across all leukemia subtypes. While characterizing one activating mutation it was discovered that acquired mutations in the transgene could arise in the Ba/F3 assay, potentially resulting in false-positive data. This observation was investigated in detail and recommendations stemming from this inquiry are also provided.

In this dissertation, the discovery of the first CSF2RB-activating human variant found in the germline of a pediatric T-cell acute lymphoblastic leukemia patient is presented. *In vitro*, CSF2RB R461C transforms Ba/F3 cells to factor-independent growth through ligand-independent activation and stabilization of CSF2RB. CSF2RB R461C increases downstream

activation of JAK2/STAT-5, and inhibition of JAK2 results in apoptosis, making this a potentially actionable clinical variant.

During the course of characterizing CSF2RB R461C, the frequent trend for Ba/F3 cells to acquire additional mutations in CSF2RB during the factor withdrawal assay was noted. This observation was validated by additional experiments including other receptor activating mutations. Failure to account for these acquired mutations in the Ba/F3 assay could affect the efficacy of screening for functional mutations in leukemia, resulting in wasted researcher time and false positives.

To date, acquired mutations are largely confined to weak transforming oncogenes, as determined by limiting dilution analysis of Ba/F3 cells. Based upon insights from these studies, the Ba/F3 transformation assay would be substantially improved with two recommendations. First, every transformed Ba/F3 cell line should be sequenced for the full length of the transgene of interest. Second, researchers should adopt limiting dilution assays of Ba/F3 cells when characterizing transforming mutations and report rates of transformation. It is unclear at this time what relevance a mutation's rate of transformation has on disease, but that question can only be addressed by additional testing of a wide range of mutations.

The research in this dissertation characterizes a rare variant in leukemia and recommends improvements for the most common model system used to screen novel mutations. The investigation of rare mutations in leukemia is an essential step in the pursuit of

individualized and targeted therapies. Recommendations provided herein will improve future studies of functional leukemic mutations, ensuring reported results are useful and reproducible.

1 Introduction

Leukemia is characterized by the accumulation of immature leukocytes (blasts) from a single hematopoietic subtype, often as the result of a genetic aberration increasing proliferation or inhibiting differentiation of the founder clone. Subtypes of leukemia can be classified by the duration of time to progression (chronic or acute) and the over-represented hematopoietic subtype (myeloid or lymphoid), and each subtype can be further distinguished by surface markers expressed by the clonal population. Leukemia originates in the bone marrow and alters normal hematopoiesis. Patients present with symptoms resulting from the reduction of functional cells in specific hematopoietic lineages (anemia, neutropenia, bruising) or the excess of leukocytes (ischemia, stroke). White blood cell counts represent the simplest measure for leukemia burden, with percent blasts and bone marrow cellularity being a more granular measurement. Treatment is highly specialized based on subtype, but is generally characterized by induction chemotherapy regimens. For specific leukemia subtypes and risk stratification groups, treatment will also include allogeneic or autologous bone marrow transplant or radiation. The use of targeted inhibitor therapy is a relatively new development made possible by years of basic research characterizing the causes behind individual leukemias. Each leukemia subtype carries a unique assortment of genetic alterations. The identification and characterization of these genetic lesions has enabled therapeutic targeting of specific oncogenic mutations and has improved patient outcomes,

with the greatest clinical advancements having been achieved for chronic myelogenous leukemia (CML).

Almost every case of CML features a balanced translocation between chromosomes 9 and 22, resulting in the expression of a fusion oncogene *BCR-ABL*. The resultant fusion protein, BCR-ABL, is the driving force behind CML, thus a drug that limits the capacity for BCR-ABL to function would be the universal treatment. One cancer subtype, one driving mutation, one drug to treat every patient; the dream of the '90s was alive in Portland, Oregon, home to the paradigm shifting clinical trial for imatinib (Gleevec), a targeted BCR-ABL inhibitor. While the success of molecularly targeted therapy in CML remains unquestioned, other leukemia subtypes are not as responsive to single targeted inhibitors. The mutational landscape of the most common form of leukemia, acute myeloid leukemia (AML), is not characterized by a single, recurrent genetic lesion. Individual cases of AML are heterogeneous, with only three mutations recurrent in 11-28% of patients[1]. Sequencing of 200 AML patients revealed 1,600 non-recurrent single nucleotide variants (SNVs) in coding regions, so-called n-of-1 mutations[1]. This large number of rare lesions is commonly referred to as the long tail of mutations in leukemia (Figure 1-1). In contrast to BCR-ABL in CML, AML patients present with several potentially functional mutations, and targeting one recurrent mutation like FLT3-ITD does not bring about the same improvements in outcome that imatinib brought to CML. Instead, researchers must identify the rare and unique functional mutations in a patient, that long tail of mutations, continuing

the pursuit of new combinations of therapies tailored for each patient. Identification and characterization of rare, functional mutations requires a robust and scalable model system such as the Ba/F3 transformation assay. The work presented in this dissertation hinges on the use of the Ba/F3 transformation assay to characterize one functional mutation in the long tail of leukemia, and the discovery of a previously unrecognized complication that could confound findings using this model.

The research described herein covers the cytokine receptor CSF2RB (Colony Stimulating Factor 2 Receptor Beta[1]) and the germline mutation R461C[2] found in a pediatric leukemia patient. Within Ba/F3 cell lines, this mutation leads to increased protein stability and ligand-independent activation of CSF2RB, driving a cancer-like cellular proliferation. Details concerning the mechanism of this signaling are presented as well as findings on targeted inhibitors with promising preliminary efficacy for future leukemic patients with the same mutation.

Additionally, during these studies a reproducible flaw in the Ba/F3 transformation assay was identified, whereby the cell lines acquired additional mutations within the gene of interest. This phenomenon was investigated further and found to be a reproducible flaw in the context of weakly-transforming receptor mutations. These acquired mutations could result in false-positive reports, cases where a non-functional variant appears function

---

[1] aka. Cytokine Receptor Common Subunit Beta.
[2] Arginine at position 461, mutated to a cysteine.

through acquisition of additional mutations. Alternatively, even functional mutations could be impacted by additional mutations, resulting in the incorrect characterization of the signaling and inhibitor-sensitivities of a particular mutation.

This phenomenon represents a confounding variable in hundreds of studies, potentially leading to irreproducible research and the waste of investigator funds and efforts. It is imperative that this flaw be addressed in future research studies. A simple protocol addition—sequencing the transgene of outgrown Ba/F3 lines—can be used to mitigate this phenomenon and improve the reproducibility of future research.

1.1 Determining functional mutations in leukemia: The Ba/F3 transformation assay

1.1.1 Background

1.1.1.1 Genetic alterations drive cancer

In 1909 Francis Peyton Rous, a researcher at the Manhattan-based Rockefeller Institute[3], found a case of infectious sarcoma in a chicken brought to him by a concerned farmer[2]. The cause of this cancer would later be found to be a virus (named Rous Sarcoma Virus or RSV), an odd finding thought not to be relevant to human biology until the 1964 discovery

[3] Later renamed Rockefeller University

of a cancer-causing virus in humans: the Epstein-Barr virus in Burkitt's lymphoma[3]. Rous would go on to win the 1966 Nobel Prize in Physiology or Medicine[4] while researchers continued to search for what turned out to be rare cases of virally-driven cancers[2].

Rous' discovery continues to be relevant today as future researchers discovered the oncogenic portion of RSV was the gene v-src, which originated from the chicken genome[4], not the virus[5] (reviewed in [6]). The implication being that cancer is not just a result of viral infection, but is caused by variations in the very genes within the afflicted organism. The driving force behind the vast majority of cancers are genetic mutations; carcinogens are mutagens[7].

1.1.1.2 Validation of driver mutations

While a remarkable finding, knowing that cancer is caused by mutations is not very useful if we cannot determine which mutation is the offending lesion. This is the problem that faced researchers George Daley and David Baltimore in 1988 while they studied the gene fusion product BCR-ABL[8]. At that time, BCR-ABL[5] was known to be the product of t(9;22)[9], the balanced translocation between chromosomes 9 and 22[11] that forms the Philadelphia chromosome characteristic of chronic myelogenous leukemia (CML)[12]. We now know that the modified ABL tyrosine kinase is constitutively activated due to oligomerization of

---

[4] v-src denotes virally activated src, c-src is the normal gene.

[5] BCR refers to the breakpoint cluster region on chromosome 22[9], and ABL to the tyrosine kinase coded by the murine leukemia virus discovered by Herbert Abelson[10].

the BCR domains, driving cellular proliferation[13]. But at the time, while all of the above evidence pointed to BCR-ABL as the driver behind CML leukemogenesis, it was only a correlation and not proof of causation. What was necessary was an experiment where researchers added BCR-ABL to a simplified system, controlled for all other factors, and observed a transformation to oncogenic growth.

Transformation assays existed prior to 1988, the most prominent using murine NIH-3T3 fibroblasts. NIH-3T3 cells[14], and similar lines derived in George Todaro's laboratory in the 1960's with the 3T3 protocol (3 day Transfer of $3x10^5$ cells)[15, 16], demonstrated an inability to grow beyond a monolayer due to contact inhibition. The addition of murine sarcoma virus (MSV) or murine leukemia virus (MuLV) could transform these cells to lose contact inhibition and form growth foci[14], generating an *in vitro* assay allowing for the detection of oncogenic transformation. RSV was later shown to drive transformation using this same assay[17]. Daley and Baltimore tested BCR-ABL[6] in the NIH-3T3 assay and found that it failed to drive growth foci[18], while at the same time another group demonstrated that BCR-ABL could drive transformation in primary mouse bone marrow cells[7][19]. This led to the hypothesis that while BCR-ABL could not transform fibroblasts, it could transform a hematopoietic line which would be consistent with its role as a putative driver of leukemia.

---

[6] Specifically, Daley and Baltimore used p210, the most common form of BCR-ABL fusion in CML.
[7] In this assay, "transformation" is determined by anchorage independent growth while suspended in agar.

Various hematopoietic-based transformation assays had been established by 1988 and they were largely based around the transformation of growth factor-dependent cells to factor independence[8]. From 1985 to 1987 there were five published models showing factor-dependent lines that could be transformed by the viral copy of ABL, v-abl (p160): primary mast cells (IL-3 dependent)[20], IO_3 and E1c cells derived from Fr-MuLV infected mice (IL-3 dependent)[21], 32D cells (IL-3 dependent)[22], FDC-P1 cells (IL-3/GM-CSF dependent)[23], and A4 T-cells (IL-2 dependent)[24]. Some of these lines remain in use today, but none so much as Ba/F3 cells.

1.1.2 The Ba/F3 cell line

Ba/F3 cells were originally derived by Ronald Palacios in 1985[25], from harvests of murine bone marrow that were cultured in IL-3 supplemented media[9] for the purposes of isolating B-cell precursors[29]. In this respect, Palacios was quite successful and characterized four such lines[10] that showed: low expression of the B-cell antigen B220; immunoglobulin still in the germline configuration; and no detectable myeloid Mac-1, mature B-cell marker LIF, or T-cell markers CD5 and CD8a. These markers indicate pro-B lymphocytes but the cells lack the heavy chain rearrangement characteristic of the stage.

---

[8] While growth factor independence (GFI) assays are distinct from the more traditional contact-inhibition transformation assays, both these and other methods testing the oncogenic potential of a gene product are referred to as transformation assays.

[9] Specifically, the IL-3 used for derivation and culture was not purified IL-3 but the cheaper conditioned media[26] from the IL-3 secreting WEHI-3 cell line[27]. WEHI-3 cells are derived from the myelomonocytic leukemia of a BALB/c mouse. The line was created at their namesake institution, the Walter and Eliza Hall Institute in Australia[28].

[10] The lines were: CB/Bm 7, Ba/C1, Bc/Bm 11, and L/B AgA2.

Consequentially, they are classified as either lymphoid precursors[30] or pro-B lymphocytes[25]. These lines were fully dependent on IL-3 for sustained growth, and died within 24-36 h without the factor[25].

The more complicated part of Ba/F3 cells is that their origin is actually untold. The name is first published by Baltimore's lab, in collaboration with Palacios, in 1986[30] as a line derived from mouse bone marrow and having the same features Palacios described in the earlier clones. The name indicates the mouse of origin, BALB/c, and the specific clone[25]. The history of this cell line became even murkier in 2014 when SNP profiling was performed on several common cell lines to detect contamination. While Ba/F3 cells are a unique clone and were not contaminated with any other line, they also did not match the SNP profile of BALB/c-derived lines but instead C3H-derived lines[11][31]. Consequentially, the BioResource Center cell repository at RIKEN publicly observed that "to the best of our bibliographical search, we could identified [sic] no paper describing the establishment of Ba/F3 cell line, i.e., there is no paper demonstrating that [the] Ba/F3 cell line was derived from [a] BALB/c mouse strain"[32]. Additionally, the male gender of this cell line is not publicly clear save for a 2002 study on Myc-induced aneuploidy[12], which published Ba/F3 karyotypes with Y chromosomes[34].

---

[11] Coincidentally the same mouse strain that 32D cells were derived from

[12] Ba/F3 cells are normally diploid in culture[33].

Regardless, and almost in spite of the lack of documentation, Ba/F3 cells became a standard of hematopoietic research. Ba/F3 cells rapidly divide and grow in suspension, allowing for shorter experiments and removing the need for trypsin. The cells are easy to transduce or transfect by retrovirus, lentivirus, or electroporation, and cellular proliferation is a simple readout for any experiment.

1.1.3 Using Ba/F3 cells to assay transformation

In 1986, researchers in Baltimore's lab performed the first series of transformation assays using the Ba/F3 cell line[30]. The Ba/F3 protocol was not significantly different from those used in myeloid models[20, 21, 23], but it was the first using a lymphoid cell line. Ba/F3 cells were infected with Murine Leukemia Virus (MuLV) containing v-abl, cultured for 3 days in WEHI-conditioned media (WEHI-CM), and then transferred to media without IL-3. Growing clones were isolated for expansion within two weeks. Cells expressing v-abl continued to grow, cells expressing v-src (as found in RSV) grew poorly with partial IL-3 independence, and vector-control cells died within two days. Outgrown cultures did not express IL-3 mRNA and media conditioned by these cells could not sustain the growth of normal Ba/F3 cells in the absence of IL-3, indicating that transformation was not the result of activating growth factor secretion but instead activation of a pathway downstream of IL-3 signaling.

With the Ba/F3 assay established, Daley tested the transformative capacity for BCR-ABL while refining the Ba/F3 protocol[8]. Daley's protocol used five steps now standard in

Ba/F3 transformation assays: Infection, Expansion, Selection, Washing, and Monitoring. Ba/F3 cells are infected with replication-deficient retroviruses containing the gene of interest or relevant controls, as well as a selectable marker like the fluorescent GFP or G418-resistant neomycin. Ba/F3 cells are then expanded in culture for 48 h in WEHI-CM prior to selection for infected clones (Daley used 7-10 days of G418 treatment). Once the selected cells demonstrate stable growth they are washed 2-3 times in IL-3-free media and monitored for growth over 2-3 weeks. Ba/F3 cells expressing BCR-ABL achieved factor-independent growth within 5-10 days, while non-infected Ba/F3 cells did not generate spontaneously transformed clones[8]. This assay, along with an earlier study on primary cells[19], finally established BCR-ABL as a functional oncogene.

The use of Ba/F3 cells in a transformation assay to test potential oncogenes has become ubiquitous in leukemia research with prominent findings including activating mutations in MPL (myelofibrosis)[35], CSF3R (chronic neutrophilic leukemia)[36], JAK1/2 (pediatric ALL)[37], JAK3 (acute megakaryoblastic leukemia)[38], rearrangements in CRLF2 (Down syndrome-associated ALL)[39] and JAK2-TEL fusions (T-ALL)[40]. Ba/F3 transformation assays have also become prominent in other malignancies, validating the oncogenicity of KIT[41] and PDGFRα[42, 43] mutations in gastrointestinal stromal tumor, ALK mutations in neuroblastoma[44], and ERBB2 mutations in lung adenocarcinoma[45].

Ba/F3 cells are transformed by a variety of oncogenes, and they also become addicted to the continued action of that oncogene[46]. This allows for the simple and rapid screening of

targeted inhibitors while using the viability or proliferation of transformed Ba/F3 cells as a readout. Ba/F3 cells were used in establishing FLT3 as a target of sorafenib[47], ponatinib as a pan-FGFR inhibitor[48], and preclinical efficacy for the JAK-inhibitor ruxolitinib[49]. The same method can identify additional mutations that render an oncogene resistant to targeted inhibitors like gefitinib-resistant EGFR mutations in lung adenocarcinoma[50] or imatinib-resistant KIT mutations in AML[51]. If combined with an ENU random mutagenesis screen, Ba/F3 cells can even be used to proactively predict BCR-ABL mutations that provide resistance to kinase domain inhibitors[52, 53].

1.1.4 The use of viruses in *in vitro* transformation assays and potential complications

1.1.4.1 Methods of gene transfer in Ba/F3 cells

One variation in the Ba/F3 transformation assay relevant to this dissertation is whether the method of gene delivery is viral or non-viral. The earliest NIH-3T3 transformation assay in 1969 used existing murine retroviruses[14] and Baltimore's lab cloned retroviruses for the first Ba/F3 assays[8, 30]. Over time, researchers developed alternative techniques, including incubating cells with plasmid and calcium-phosphate[54] or using phosphatidylserine vesicular fusion[55-57]. But in 1982, researchers discovered genes could be efficiently and simply transferred into cells by short electrical pulses, or electroporation[58]. Electroporation[40-42] and retroviral infection[35, 44] became the

two most prominent forms of gene transfer in Ba/F3 cells, with the selection of one over the other seemingly a result of laboratory preference. A meta-analysis of Ba/F3 transformation studies published 2014-2016 (Table 3-1, Table 3-2) indicates that viral infection (14 of 24 studies), and specifically retroviral infection (12 of 24), is the most common method currently used for gene transfer, with electroporation a distant second (6 of 24).

1.1.4.2 Retroviral infection and spontaneous transformation: The work of Carol Stocking

The use of retroviruses to infect Ba/F3 cells is theoretically problematic. Retroviral genomes are prone to acquire mutations during reverse transcription or cause mutations in infected cells through insertional mutagenesis. Murine retroviruses have a baseline mutation rate of 1 SNV for every 10,000 base pairs during reverse transcription[59]. In a transformation assay, an acquired mutation could potentially alter a normal gene into a functional oncogene, resulting in a false positive result and potentially irreproducible results. Early research into this possibility examined instances of spontaneous transformation: cases where a minority of infected cells achieve factor-independent growth.

In 1985, Thomas Gonda's laboratory infected FDC-P1 cells[13] to express GM-CSF and observed factor-independent growth even in the presence of GM-CSF antiserum[60]. This

[13] Murine, myeloid precursor line dependent on IL-3 or GM-CSF.

was remarkable as the initial event driving transformation appeared dispensable. Wolfram Ostertag tried to replicate these results and found that some, but not all, GM-CSF expressing FDC-P1 clones demonstrated a similar effect[61]. This spontaneous transformation of a minority of cells to factor-independent growth would become a theme in the early career of a researcher working with Ostertag, Carol Stocking. Stocking's findings bear striking similarities to those detailed in this dissertation, both in the subject of CSF2RB and in investigating hypotheses for acquired mutations in factor-dependent cell lines.

Stocking defined the rates of spontaneous transformation in two factor-dependent lines (murine D35 and human TF-1) and found a 20x increase in transformation rate following intense retroviral infection[14][62, 63]. For D35 cells transformed by retroviral infection, 10 of 11 clones were sustained by activating the secretion of a soluble growth factor, usually through transposon insertions near the activated gene. The 11th clone was detailed in a follow-up study to express a truncated form of CSF2RB ($\Delta\beta_c$) while the other copy of CSF2RB was fully deleted[15][64]. $\Delta\beta_c$ was capable of increasing FDC-P1 transformation by four orders of magnitude[16][64, 65]. This outgrowth was noted to be slow, taking 6-7 days[64], and an additional study showed that $\Delta\beta_c$ expression in FDC-P1 cells could not

---

[14] The retroviruses did not drive expression of any oncogenes, limiting this investigation to insertional mutagenesis.
[15] The two copies of CSF2RB2, the murine-exclusive beta chain that can replace CSF2RB for IL-3 signaling, are adjacent to CSF2RB in the mouse genome and were also disrupted.
[16] From $5x10^{-8}$ to $3x10^{-4}$[64], or from $1.7x10^{-8}$ to $6.8x10^{-5}$[65].

sustain factor-independent growth when immediately assayed 24 h after infection[65]. The most surprising result was that Cre-*loxP* excision of $\Delta\beta_c$ from transformed FDC-P1 cells did not remove the capacity for factor-independent growth in 7 of 8 clones. The single revertant clone was remarkably hypersensitive to reintroduction of $\Delta\beta_c$, with transformation rates 1000x higher than naïve FDC-P1 cells when reinfected[65].

This series of complicated results were difficult to summarize into a single cohesive theory, and perhaps because of this difficulty the study was overlooked and never meaningfully cited[17]. Clearly $\Delta\beta_c$ was oncogenic in FDC-P1 cells, yielding a 4000-6000x increase in transformation to factor-independent growth. On the other hand, these cells were not immediately transformed by the truncated receptor, nor were they dependent on its continued expression. The single revertant clone was key to the authors' conclusion that $\Delta\beta_c$ is somehow causing or cooperating with a wide library of additional, persistent genetic mutations that could replace the need for $\Delta\beta_c$ entirely. However, conclusions regarding the presence of genetic mutations are speculative as none of these cells were sequenced (an understandable omission in 2001). Ultimately, this study, and a similar one by Stocking using PDGFRβ[69], indicated a pernicious tendency for retrovirally-infected receptor constructs to reliably but slowly transform factor-dependent cells, possibly through the acquisition of additional mutations. In spite of these findings, current studies using the

---

[17] Prassolov, V *et al.* 2001 was cited 4 times (once to reference the activating potential of CSF2RB[66] and three times as the source for a construct[67-69]) and always by papers where Stocking was an author.

Ba/F3 transformation assay have not sequenced the gene of interest following transformation (Table 3-1), making the assay similarly vulnerable to the same confounding results.

1.1.5 Summary

The Ba/F3 transformation assay is a storied and essential model system for cancer researchers. However, it has not been the subject of scrutiny matching its prominence and use within the field. This dissertation critiques the Ba/F3 transformation assay, identifying a recurrent flaw that has not been previously reported: the unexpectedly frequent tendency for transgenes tested in the Ba/F3 system to acquire additional mutations (Chapter 3). This finding is worrisome, given the widespread use of this assay, but also understandable as it was hypothesized in historical studies. Based upon the research described in this thesis, recommendations for researchers to mitigate this flaw in future studies are presented.

This discovery of acquired mutations in the Ba/F3 assay was made while using the assay for its intended purpose. This model enabled an in-depth investigation of a novel variant in CSF2RB (Chapter 2), which represents the first identified CSF2RB activating variant found in a human subject.

1.2 The common beta chain: CSF2RB

1.2.1 CSF2RB activation and signaling

Colony stimulating factor 2 receptor beta common subunit (CSF2RB)[18] is a single-pass, type-1 cytokine receptor. In contrast to the other colony stimulating factor receptors[19], CSF2RB does not contain a kinase domain and signals by forming hetero-trimers with one of 3 ligands and 3 alpha chains. IL-3, IL-5, GM-CSF and their ligand-specific alpha chains[20] all signal through CSF2RB, which acts as the primary signaling component. These ligands have largely overlapping and broad roles in inducible hematopoiesis[70] by regulating proliferation, differentiation, and survival[71]. After the ligand binds its high-affinity receptor (CSF2RB in complex with the ligand-specific alpha chain), associated JAK2 kinases transphosphorylate and then continue to phosphorylate additional tyrosine residues on CSF2RB (Figure 1-2). These sites allow for the docking of proteins and activation of several downstream pathways, notably JAK2/STAT5, Ras/Raf/MAPK, and PI3K/AKT (Figure 1-3).

The most exhaustive structural characterization of CSF2RB is in the context of GM-CSF signaling, where the final activated complex appears to be a dodecamer composed of 2 hexamers, each containing 2 alpha chains, 2 beta chains and 2 ligands (Figure 1-2). The

---

[18] Other common names include CD131, beta common cytokine receptor, or simply beta common (β_c)
[19] CSF1R is a kinase, and both CSF1R and CSF3R signal through the formation of homodimers.
[20] IL3RA, IL5RA, and CSF2RA, respectively.

dodecameric complex is necessary as each hexamer forms a horseshoe shape[70], leaving the cytoplasmic CSF2RB tails too distant to enable JAK cross-phosphorylation. The dodecamer forms an "M" shape where the proximity of CSF2RB intracellular domains mimics those observed in other activated receptors[72], allowing the activation of JAK and other downstream pathways.

Granulocyte-macrophage colony-stimulating factor (GM-CSF) signals through binding CSF2RB and granulocyte-macrophage colony-stimulating factor receptor subunit alpha (GMRα, CSF2RA). GM-CSF signaling results in a wide array of pro-myeloid effects, though it is unique in promoting the expansion of neutrophils. Interleukin 3 (IL-3) uniquely acts to drive production of hematopoietic stem cells, mast cells and basophils[71, 73], while also having largely overlapping roles with GM-CSF. Interleukin 5 (IL-5) is the most restricted cytokine, specifically driving eosinophil proliferation and activation[74].

Clinical applications of GM-CSF have been the subject of substantial research. From the early 1990s, recombinant GM-CSF[21] has been sporadically used to treat neutropenia[76], stimulate myeloid reconstitution following chemotherapy or transplantation and peripheral mobilization of progenitors prior to harvest for transplantation[77]. GM-CSF has also been used to prime an immune response in neuroblastoma patients prior to treatment with anti-GD2 antibodies[78]. However, in AML patients, the use of GM-CSF in combination with

[21] GM-CSF synthesized in yeast (sargramostim), bacteria (molgramostim), or murine cells (regramostim)[75].

chemotherapy resulted in reduced rates of complete remission[79]. Recently, oncolytic viruses engineered to express GM-CSF increased median survival in patients with solid tumors[80, 81], consistent with the findings that GM-CSF can drive immunological invasion[82][22]. These paradoxical roles for GM-CSF reflect a cytokine with broad and context-dependent functions.

1.2.2 CSF2RB deficiencies and knockouts

For the breadth of pathways and cell types influenced by CSF2RB signaling, the signals also seem surprisingly redundant with alternate pathways which compensate for their loss. Pulmonary alveolar proteinosis (PAP), a strikingly rare disease with an incidence below 1 in 150,000[85], is an autoimmunological disorder resulting from the production of GM-CSF directed antibodies. The absence of GM-CSF signal reduces alveolar macrophage function, leading to surfactant accumulation and dyspnea[86]. Standard treatments include whole lung lavage[87] or GM-CSF inhalation[88], with a 5-year survival rate for treated patients of 94%[85].

One case report detailed a patient of consanguineous birth possessing a homozygous frameshift mutation (R211fs) in CSF2RB, a region in the protein distal of the transmembrane (TM) domain, which would code for a non-functional receptor[89]. The

[22] Though the generation of GM-CSF in KRAS-mutant pancreatic ductal carcinoma drives accumulation of myeloid cells that suppress antitumor immunity[83, 84].

same mutation was found heterozygously in both parents, indicating the patient was likely born without a functional CSF2RB gene. This patient was asymptomatic until she developed adult onset PAP at 36 years old[23]. Remarkably, the inability to signal through CSF2RB did not noticeably impact the patient for 36 years. When the deficiency finally manifested, it occurred in a disease fully accounted for by the loss of GM-CSF signaling, making IL-3 and IL-5 appear increasingly dispensable. On the other hand, the rareness of PAP caused by CSF2RB deficiency (only two reported cases of a very rare but treatable disease) suggests there is some additional, selective pressure to preserve CSF2RB function.

Several knock-out mouse lines have been generated investigating CSF2RB signaling, and the results paint a similar picture of minimal phenotypes. CSF2RB knockout mice lost affinity to GM-CSF and IL-5, though they retained IL-3 affinity as mice possess a second gene (CSF2RB2[24]) capable of acting as the beta chain of an IL-3 receptor. CSF2RB deficient mice had fewer eosinophils (likely due to loss of IL-5 signaling) and symptoms similar to PAP (loss of GM-CSF signaling)[91]. Mice deficient in CSF2RB2 had minor decreases in IL-3 affinity but showed no obvious hematopoietic abnormalities[92]. To get around the compensatory receptors, mice deficient in the IL-3 ligand were created and showed no changes in hematopoiesis but did have slightly altered parasitic[73] and general immune

[23] The patient underwent bilateral lung transplant, only to recur 9 months later when donor alveolar macrophages were replaced by host macrophages[90].
[24] Alternate names: IL3R, βIL-3, IL3RB2

responses[93, 94]. The ultimate mouse model was deficient in both CSF2RB and CSF2RB2, and showed no phenotypes other than those previously observed (decrease in eosinophils, PAP symptoms, minor changes in immune response), indicating that CSF2RB signaling is not essential for hematopoiesis[95].

1.2.3 CSF2RB overexpression and activating mutations

Given the hematopoiesis-promoting effects of CSF2RB signaling, it is unsurprising that the CSF2RB family of receptors are consistently expressed in the majority of leukemias. A subset of AMLs show increased receptor expression, correlating with unfavorable phenotypes. The vast majority of AMLs show expression of CSF2RB, and 23% of AMLs present with high CSF2RB expression, correlating with an increased fraction of cycling blasts[96]. IL3RA is overexpressed in 45% of AMLs and B-ALLs, and in AML this overexpression correlated with increased blast cycling and a poorer prognosis[97].

Since CSF2RB is widely expressed or even overexpressed in leukemia, it would be reasonable to suspect it could carry activating mutations driving leukemic outgrowth. Several *in vitro* studies have demonstrated the ability for point mutations to drive ligand-independent activation of CSF2RB. Particularly, screens focused on the membrane spanning and adjacent regions of CSF2RB identified a dozen mutations driving signals of varying strength[98]. While these activating mutations in the transmembrane domain have been used to characterize CSF2RB downstream signaling, little is known about the actual transmembrane domain itself[71]. The domain is commonly defined as residues 444-

460[99] owing to computational domain modeling in a 1998 study[98], corresponding to a single-pass alpha helix domain. More advanced and modern modeling platforms indicate a larger domain to be more plausible, likely including residues 442-463 (Figure 2-6)[100]. The number of activating mutations within the transmembrane region is consistent with findings that such mutations frequently lead to ligand-independent receptor activation[101-103]. In spite of these *in vitro* findings, CSF2RB mutations in leukemia are practically non-existent.

The Cancer Genome Atlas (TCGA) shows CSF2RB mutations to be rare events in every cancer type—with the possible exception of melanoma (7% of cases)—and no observed mutations in leukemia[104, 105]. The catalogue of somatic mutations in cancer (COSMIC) reports only a single CSF2RB coding mutation[25] in 749 cases of AML[106]. Even more striking, the TM domain identified through *in vitro* screens as a hotspot for activating mutations, is completely unmutated across the entire TCGA dataset (Figure 1-4).

1.2.4 Summary

CSF2RB is a widely-acting cytokine receptor, driving hematopoietic expansion and activation. It can be mutationally activated in *in vitro* screens and is frequently overexpressed in leukemia. Given the redundant or non-essential roles played by CSF2RB,

[25] A missense D852A mutation in the cytoplasmic domain, which has been confirmed somatic but has not been tested *in vitro*.

it represents an excellent target for therapeutics with minimal toxicity. In spite of these findings, a functional CSF2RB mutation has not been reported in any case of cancer. In this dissertation, evidence for and characterization of the first instance of an activated CSF2RB variant found in a human patient are presented. These findings will impact future studies involving genomic sequencing of leukemia patients, as well as basic research into the mechanisms of CSF2RB activation and signaling.

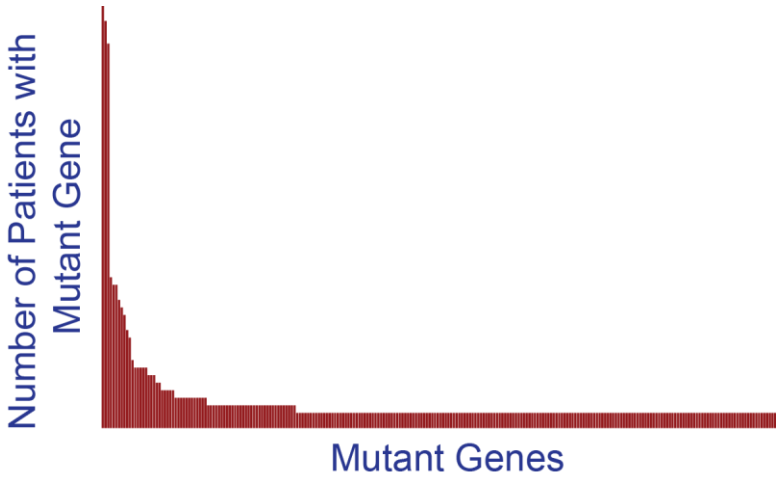

Figure 1-1 Non-recurrently mutated genes in AML form a long tail.

Number of AML patients with mutations in a given gene as reported by TCGA. The long tail to the right indicates the number of rarely mutated genes found in AML. Figure courtesy of Jeff Tyner[107].

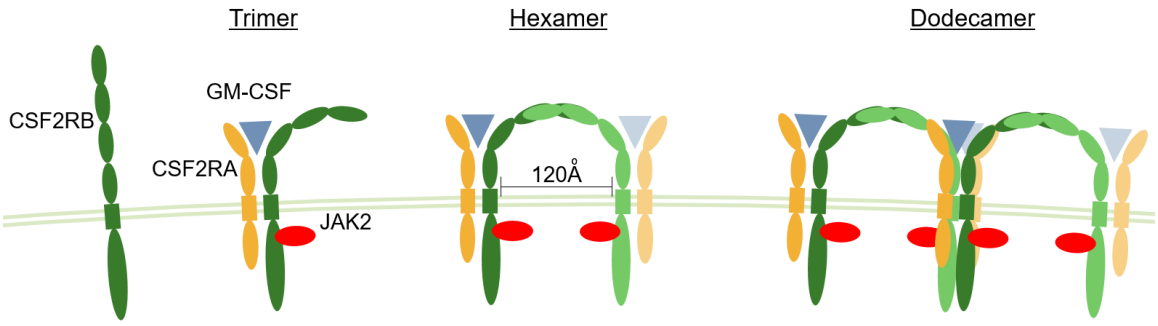

Figure 1-2 CSF2RB signals through a dodecameric complex with a ligand and ligand-specific alpha chain.

CSF2RB is a single-pass transmembrane receptor for IL-3, IL-5 and GM-CSF. In each case, the high-affinity receptor is formed by the combination of CSF2RB with a ligand-specific alpha chain (IL3RA, IL5RA, CSF2RA). JAK2 dimerization is essential for cross-phosphorylation and phosphorylation of additional tyrosine residues on the cytoplasmic tail of CSF2RB. In a hexameric conformation the two CSF2RB chains are too distant to allow JAK2 activation. The final signaling complex is dodecameric, where the proximity of intracellular CSF2RB chains and associated JAK2 kinases activates downstream signaling. Figure inspired by [108].

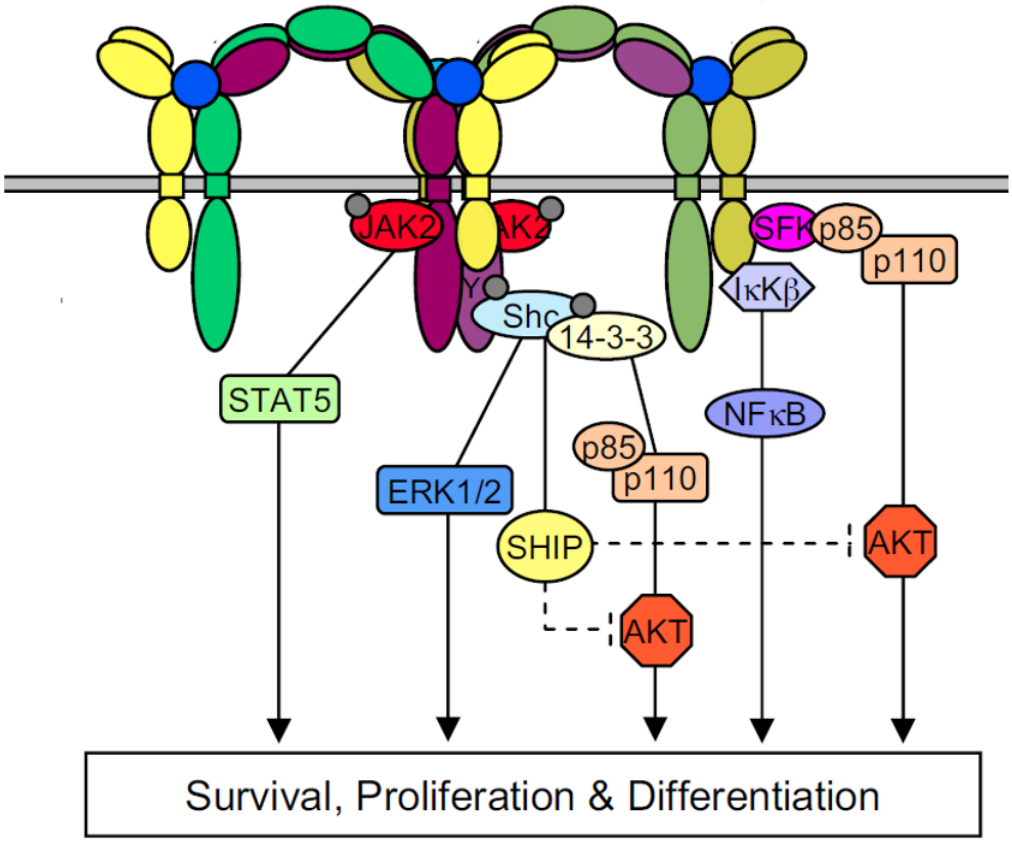

Figure 1-3 CSF2RB activates signaling through JAK2/STAT5 and several other pathways.

CSF2RB activation first results in activation of JAK2 and STAT5. Activated JAK2 also phosphorylates additional tyrosine residues on CSF2RB, allowing docking of additional signaling molecules and activation of several pathways including MEK/ERK and PI3K/AKT. Figure created by Michelle Perugini[109].

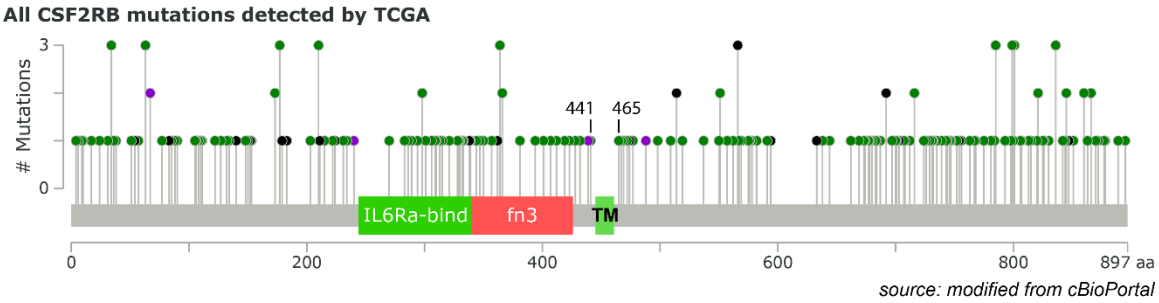

Figure 1-4 CSF2RB mutations in all cancers as reported by TCGA.

Every CSF2RB mutation reported in TCGA is visualized above. The annotations of transmembrane domain and surrounding residues were added for this figure.

2 Discovery and functional characterization of a germline, CSF2RB-activating mutation in leukemia

Kevin Watanabe-Smith, Cristina Tognon, Jeffrey W. Tyner, Jules P.P. Meijerink, Brian J. Druker, Anupriya Agarwal

This manuscript was published September, 2016 in *Leukemia* (Vol.30, Issue 9, 1950-1953).
I designed the experiments detailed in this manuscript with mentoring from the other authors. I exclusively and personally performed every experiment and analyzed every piece of data. I drew conclusions from the results and wrote the manuscript, with feedback and editing from the other authors.

2.1 Article

Colony stimulating factor 2 receptor beta (CSF2RB) is the shared beta-chain receptor and essential signaling component for IL-3, IL-5 and GM-CSF receptor activation. In the context of GM-CSF signaling, the ligand-specific alpha chain (CSF2RA) complexes with CSF2RB and GM-CSF ligand, forming a dodecameric complex in which the proximity of CSF2RB subunits allows associated JAK2 kinases to trans-phosphorylate[71]. CSF2RB signals through several pathways including JAK2/STAT5, PI3K/mTOR and MEK/ERK to promote survival, proliferation and differentiation (reviewed in [110]). Both spontaneous transformation[64, 111] and random mutagenesis[64, 98] screens have shown that CSF2RB mutations can result in ligand-independent activation *in vitro*. However, these predicted oncogenic mutations have never been observed clinically. In fact, the only phenotypic CSF2RB mutations reported are recessive, loss-of-function, germline mutations in pulmonary alveolar proteinosis[89]. As oncology moves toward an age of personalized and molecularly-targeted treatment it will require the identification and *in vitro* characterization of targetable genetic lesions. Here we describe the first case of a leukemia patient harboring a germline, CSF2RB-activating point mutation (R461C) and identify small molecule inhibitors with therapeutic potential against this mutation.

We obtained a pediatric T-cell acute lymphoblastic leukemia (T-ALL, Figure 2-1A) with informed consent approved by the Institutional Review Boards of Oregon Health & Science University and Erasmus University Medical Center - Sophia Children's Hospital. We

isolated mononuclear cells and performed deep sequencing as previously described[36], uncovering the CSF2RB R461C mutation at a 54% allele burden (Figure 2-1B and C). The patient also presented with somatic NOTCH1-truncation, NOTCH1 missense, and PTEN point mutations, all recurrent and leukemia-associated mutations[106] (other observed mutations in Table 2-1). R461C was later confirmed by Sanger sequencing as a heterozygous, germline variant using a minimal residual disease day 79 sample for normal DNA (Figure 2-1D). CSF2RB R461C has never been previously described in cancer patients (including public databases) but is listed as a SNP in the 1000 Genomes database[112] (rs371045078) at a low allele frequency (MAF=0.000998, 5 observations in 1000 Genomes[112]; MAF=0.000272, 33 observations in the Exome Aggregation Consortium[113]) in exclusively heterozygous cases. Prior work has established that cancer-predisposing mutations exist in the germline of healthy individuals at frequencies as high as 1.1%, but those frequencies elevate to over 8% in children and adolescents with cancer, most of which demonstrate no family history of cancer[114]. Congenital mutations in CSF3R have also been observed to precede the development of acute myeloid leukemia[115]. In addition, there are numerous reports of families with gain-of-function germline mutations in receptors with similar biology as CSF2RB (e.g., CSF3R[116], EPOR[117], MPL[118]) and in many of these pedigrees the affected family members do not develop overt leukemia, though they sometimes exhibit elevated blood counts.

The location of this variant, within the putative membrane-spanning portion of the receptor, is of particular interest as this region is a hot spot for activating mutations *in vitro*[98]. Previously, mutations altering the number of membrane-spanning or membrane-adjacent unpaired cysteines have been shown to activate the IL-7 receptor in T-ALL[119] and RET in medullary thyroid carcinoma[120]. CSF2RB has been shown to be partially activated *in vitro* by replacement of the extracellular domain with a short, cysteine-containing sequence[64]. Lastly, multiple sequence alignment of CSF2RB homologues demonstrated that arginine 461 is conserved across most mammals (Figure 2-2) increasing the potential that R461C could have functional relevance and cooperate with canonical leukemogenic mutations. Accordingly, we hypothesized that R461C could activate CSF2RB-signaling and contribute to the patient's leukemia.

We cloned CSF2RB R461C into the pMXs-IRES-Puro plasmid and transfected into IL-3-dependent murine Ba/F3 cells by electroporation. Stably transfected cells were selected using two weeks of continual 2μg/ml puromycin selection prior to performing IL-3 withdrawal transformation assays as previously described[36]. R461C conferred factor-independent growth while wild-type (WT) CSF2RB did not (Figure 2-3A, Figure 2-4). The full CSF2RB transgene was sequence confirmed in two biologically replicate, IL-3 independent cell lines and used for further studies.

We identified that CSF2RB R461C expression resulted in an accumulation of surface CSF2RB protein, relative to WT, prior to IL-3 withdrawal when assayed by flow cytometry (Figure 2-5). Furthermore, immunoblot analysis showed that the R461C protein is significantly increased in IL-3-independent cells relative to WT cells grown in IL-3 (Figure 2-3B, details and all antibodies included Supplemental methods and Table 2-2). As both exogenous versions of CSF2RB were expressed by identical promoters we rationalized that the accumulation was due to changes in CSF2RB protein stability. We performed cycloheximide time course experiments using 100ug/ml cycloheximide in DMSO followed by staining with PE-conjugated anti-CSF2RB to determine alterations in surface protein stability. The R461C mutant possessed a prolonged surface half-life relative to WT CSF2RB (6.5 vs 3.6 hours; Figure 2-3C). Given the presence of a novel cysteine and increased stability in the R461C mutant, we investigated disulfide-linked receptor oligomerization by immunoblot under non-reducing conditions. Comparing the WT- and R461C-expressing cells, we observed CSF2RB-containing complexes of ~500 kDa that showed a reduced intensity when 2-mercaptoethanol was added to the lysate (normally CSF2RB runs at 125 kDa, Figure 2-3D), indicating R461C enables novel disulfide interactions with additional CSF2RB monomers or other endogenous receptors.

Previous studies have shown that mutations within receptor transmembrane domains can result in constitutive receptor oligomerization and activation[118-120]. The role of the CSF2RB transmembrane domain in receptor stability and signal transduction has not been

characterized[71]. Even the boundaries of the membrane-spanning region have not been empirically studied, though it is commonly assumed to span residues 444-460 based on early domain modeling[98]. Various modern models consistently predict a much larger domain (Figure 2-6), including residue 461, suggesting R461C might be within the transmembrane domain and alter receptor-receptor interactions. Another possibility is that the loss of a charged residue near the membrane boundary could result in shifting or fluidity of the transmembrane domain of the mutant receptor.

Using immunoblot and co-immunoprecipitation analysis, we showed that transformed Ba/F3 cells expressing CSF2RB R461C exhibited constitutive receptor phosphorylation and signaled through several pathways, including STAT5, PI3K/mTOR1, and MEK/ERK (Figure 2-7A and B). To identify therapeutically targetable pathways we utilized a 104 small molecule inhibitor library screen, as previously described[36, 121], and compared IC_{50} values for R461C-expressing cells to WT-expressing cells. JAK inhibitors (Tofacitinib, Ruxolitinib, and AZD1480) constituted the three top hits in the screen (Figure 2-7C, Figure 2-8A-C, full screen Table 2-3). These treatments were specific and cytotoxic, inducing apoptosis in R461C-expressing cells (Figure 2-7D and Figure 2-8D). While these inhibitors have a differential specificity for targeting JAK kinases (Tofacitinib: JAK2/3, Ruxolitinib: JAK1/2, AZD1480: JAK2), the strongest target is JAK2. We also observed reduced levels of total JAK2 in R461C cells (Figure 2-7B), which is consistent with JAK2 activation and then degradation through a STAT5/SOCS-1 negative feedback loop[122].

These results suggest a dependency on the JAK/STAT pathway that is consistent with ligand-independent activation of CSF2RB in R461C-expressing cells. Targeted inhibition of JAK2 using AZD1480 quickly reduced levels of phosphorylated STAT5, validating the specific nature of the inhibition and highlighting JAK2 as the key mediator of CSF2RB R461C signaling (Figure 2-7E).

In sequencing 449 primary hematopoietic malignancies, we found 7 additional CSF2RB mutations (Table 2-4) but none were membrane spanning and all 7 were incapable of transforming Ba/F3 cells (data not shown). Several other CSF2RB-activating mutations have been observed *in vitro*, but have not been observed in primary patient samples. CSF2RB R461C is a rare germline variant and recent studies of germline cancer-predisposing mutations have not included CSF2RB[114], possibly because of the lack of previous evidence showing the oncogenic potential of CSF2RB. Our data would support the inclusion of CSF2RB in future studies. CSF2RB R461C is a transforming mutation *in vitro*, and further investigation is necessary to determine its status as a predisposing or cooperative congenital mutation.

CSF2RB has previously been shown to become factor-independent through *in vitro* mutagenesis screens. One such screen successfully predicted R461C to be an active variant[98] (though insufficient to transform Ba/F3 cells in a short-term withdrawal assay), demonstrating the potential for predictive mutagenesis screens. In spite of this *in vitro* evidence, there has never before been a reported case of cancer with a CSF2RB-activating

mutation. We have demonstrated for the first time that a targetable CSF2RB variant found in a human leukemia confers factor-independent growth, receptor phosphorylation and accumulation, and constitutive JAK/STAT pathway activation. Our findings contribute to ongoing efforts to identify potential germline predisposition mutations in pediatric cancers, and are consistent with observations that genetic alterations activating cytokine receptor pathways are common in leukemia. Our research highlights the need for basic research to investigate and characterize the functional role of the CSF2RB transmembrane domain in signaling and recycling of the receptor. Finally, JAK inhibitors blocked the growth of R461C-transformed cells, thereby providing a therapeutic rationale to consider JAK inhibitors in any future cases of CSF2RB-activated leukemias.

2.2 Materials & Methods

2.2.1.1 Patient samples and genomic analysis

Clinical samples were obtained with informed consent approved by the Institutional Review Boards of Oregon Health & Science University and Erasmus University Medical Center - Sophia Children's Hospital. Bone marrow or blood samples from patients with acute leukemia were separated using a Ficoll gradient followed by red blood cell lysis. Cells were cultured in RPMI-1640 medium (Invitrogen) containing 10% fetal bovine serum (FBS, Atlanta Biologicals), L-glutamine (Invitrogen), fungizone (Invitrogen), penicillin/streptomycin (Invitrogen), and 10^{-4}M 2-mercaptoethanol (Sigma).

Genomic DNA was isolated from cryopreserved patient sample material using Qiagen DNeasy columns. DNA was fragmented by sonication using an S2 Sonicator (Corvaris). Fragmented DNA was then processed according to the SeqEZ protocol (Nimblegen/Roche), which is based on the TruSeq protocol (Illumina). Solution capture was performed using a custom DNA probe capture library previously described[36]. The libraries were sequenced on a HiSeq 2000 sequencer (Illumina) followed by FASTQ assembly using the CASAVA pipeline (Illumina). Sequence capture, library preparation, and deep sequencing were performed by the OHSU Massively Parallel Sequencing Shared Resource.

Sanger sequencing of CSF2RB mutations was confirmed by PCR amplification of CSF2RB exons 10 and 11 using M13-tagged primers (Exon10&11F gtaaaacgacggccagCCCTGAGGT CGATTTCCC, Exon10&11R caggaaacagctatgaccGGACAGAGACAAGAGAGGCAG) followed by sequencing with M13 forward (GTAAAACGACGGCCAGT) and reverse (CAGGAAACAGCTATGACC) primers.

2.2.1.2 Cell culture

Ba/F3 cells were obtained from ATCC and grown in RPMI 1640 medium with 10% FBS, L-glutamine, fungizone, penicillin-streptomycin, and15% WEHI-conditioned medium (a source of IL3).

2.2.1.3 Ba/F3 transformation assay

The CSF2RB R461C mutation was cloned as previously described[36] into the pMXs-IRES-Puro plasmid. 2.5e7 pro-B Ba/F3 cells were electroporated in a 0.4mm cuvette at 300V for two 25ms pulses with 40µg of plasmid. Stably transfected cells were selected using two weeks of continual 2µg/ml puromycin selection. Parental Ba/F3 cells or those stably expressing CSF2RB WT or R461C were washed three times and re-suspended in RPMI 1640 with 10% FBS, L-glutamine, fungizone and penicillin-streptomycin. Viable cell counts were obtained using a propidium iodide exclusion on a Guava Personal Cell Analysis System (Millipore). Genomic DNA was harvested from outgrown lines and the expressed transgene was confirmed by Sanger sequencing.

2.2.1.4 Immunoblot analysis

Immunoblotting was performed as previously described[36] (all antibodies used in this study are listed in Table 2-2). Prior to lysis, cells were starved overnight in 0.1% FBS. Cells were lysed in Cell Lysis Buffer (Cell Signaling) containing Complete Mini Protease Inhibitor Cocktail Tablets (Roche), Phosphatase Inhibitor Cocktail 2 (Sigma) and Phenylmethanesulfonyl fluoride solution (Sigma) and quantitated using a Bradford protein assay (Bio-Rad). Most samples were mixed with a concentrated protein loading dye containing 8% 2-mercaptoethanol prior to loading; for non-reducing gels the protein lysate was mixed with a 2-mercaptoethanol-free dye. Immunoprecipitations were performed with anti-CSF2RB or rabbit IgG isotype control.

2.2.1.5 Cycloheximide time course

Ba/F3 cells were treated with 100µg/ml cycloheximide in DMSO for the indicated times before washing in PBS with 0.5% FBS and staining for 45 minutes with PE-conjugated anti-CSF2RB antibody. Cells were analyzed by flow cytometry (BD FACSAria IIIu and BD LSR II) for mean fluorescence intensity and normalized to untreated controls.

2.2.1.6 Transmembrane domain prediction

Consensus coding sequences for wildtype and R461C CSF2RB were analyzed by the indicated modeling programs. Top predictions that maintained a single transmembrane domain and type-I orientation are listed.

2.2.1.7 Small-molecule kinase inhibitor screen

A library (previously described[121]) of 104 small-molecule kinase inhibitors across three 384-well plates was used to determine inhibitors that specifically inhibited the growth of R461C-expressing cells. Cells were maintained in their culture media, where only WT cells were supplemented with 15% WEHI-conditioned media. Cells were plated at 400 cells per well in 50µl total volume (8,000 cells per mL) and incubated for 3 days at 37°C, 5% CO_2 and then subjected to a CellTiter 96 AQ_{ueous} One solution, tetrazolium-based, cell proliferation assay (Promega). All values were normalized to cells incubated in the absence of drug and IC_{50} values were calculated from the resulting kill curves of each drug gradient. Biologically replicate WT and R461C lines were run on this assay, with R461C-specific drugs identified as drugs with the largest percent difference in IC_{50} between WT and R461C cells.

2.3 Figures

A

Clinical details for CSF2RB-mutated T-ALL patient	
Age	14
Gender	F
Diagnosis	Immature T-ALL
WBC blasts per µl	511,000
Karyotype	46, XX, t(7;11)(q34;p12), inc[15]
Immunophenotype Markers	CD1a-,CD2+, Cytoplasmic CD3+, Surface CD3-, weak CD4+, weak CD5+, CD7+, CD8+, CD10+, CD99+, CD117-

B

Deep sequencing results - CSF2RB R461C

	Reads	Percent Total	Forward Reads	Reverse Reads
WT allele	48	46%	22	26
Mut allele	57	54%	20	37
Total	105			

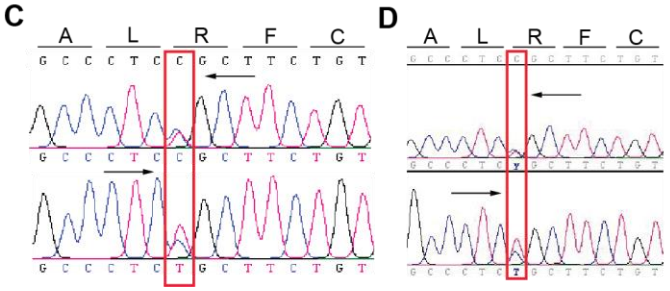

Figure 2-1 CSF2RB R461C is discovered in a primary T-ALL sample.

(A) Clinical details for the CSF2RB-mutated patient. (B) Deep sequencing reads of a primary T-ALL sample for the R461C mutation. (C) Sanger sequencing confirmation of the observed mutation following PCR amplification of the patient's leukemic gDNA. (D) Sanger sequencing of the same mutation using a day 79 minimal residual disease blood sample from the same patient indicates the mutation is germline.

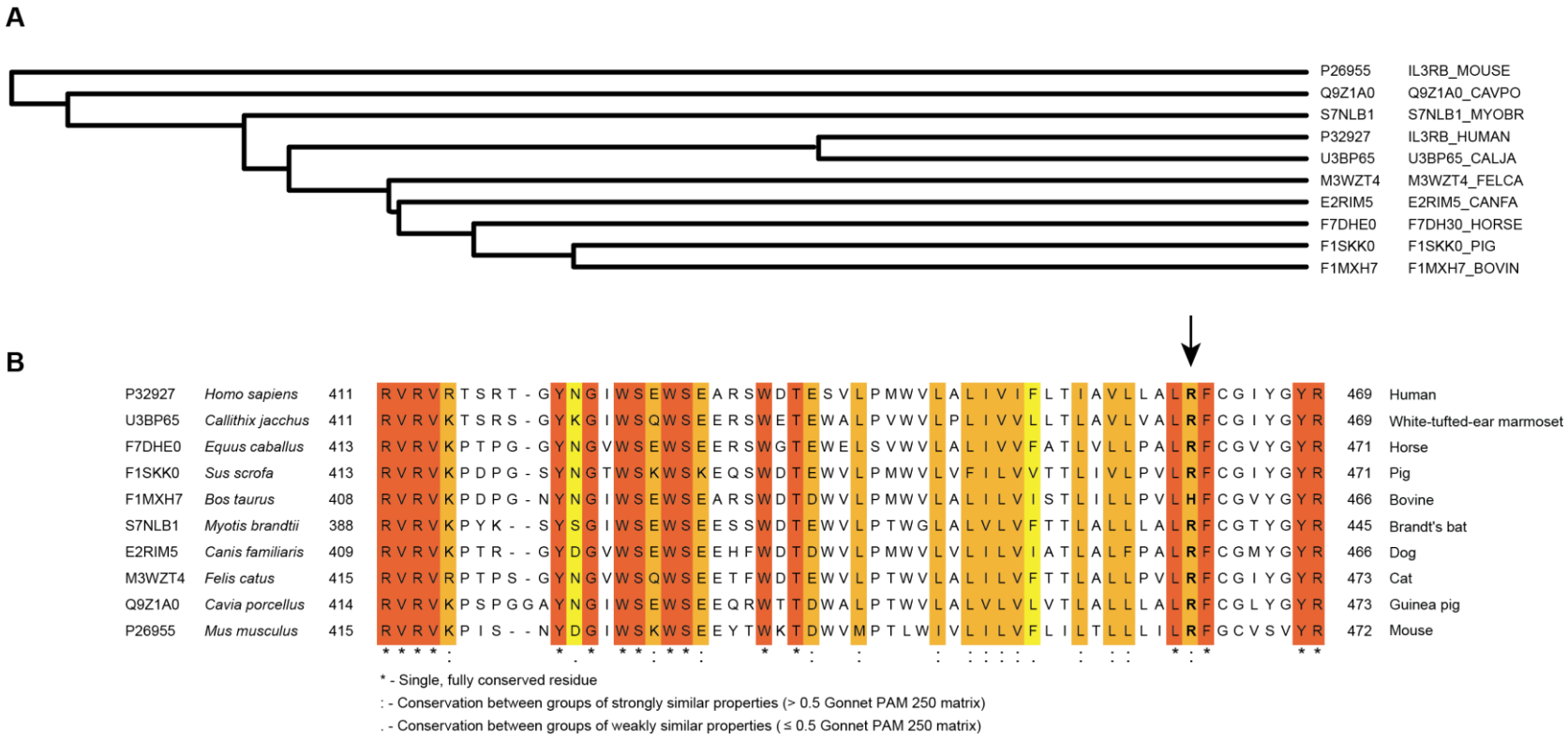

Figure 2-2 R461 is a conserved residue in CSF2RB homologues.

(A) Taxonomic distribution of mammalian species used for multiple sequence alignment. (B) Multiple sequence alignment for mammalian CSF2RB homologues. Alignment performed using CLUSTALO, 25.2% of positions were identical.

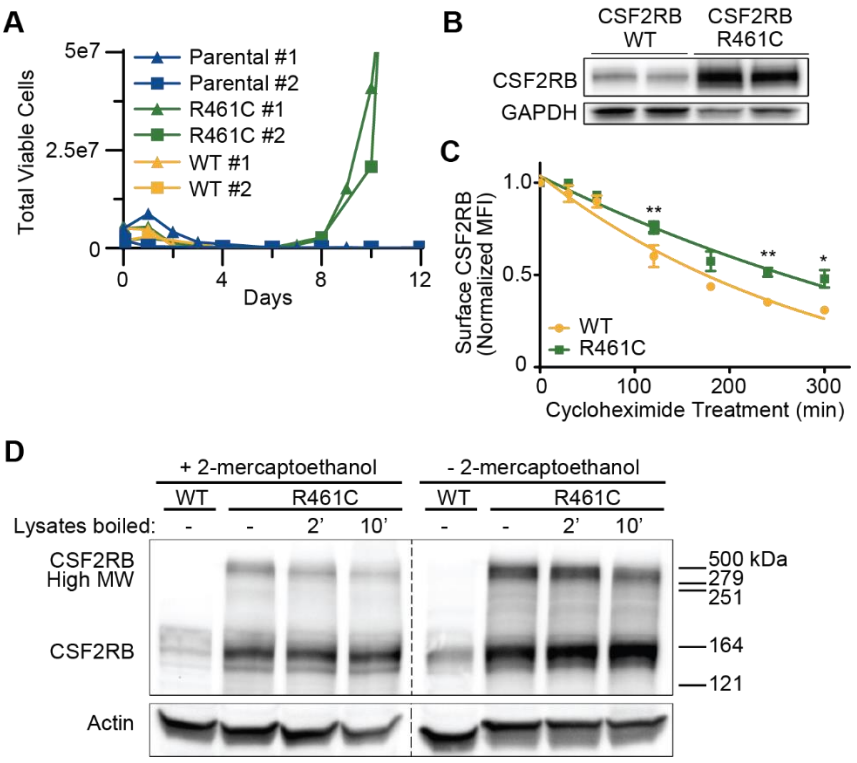

Figure 2-3 CSF2RB R461C is a transforming mutation which results in receptor stabilization and formation of higher molecular weight complexes.

Biologically replicate Ba/F3 lines expressing CSF2RB WT or R461C were monitored for growth in the absence of IL-3. Validation experiments in Supplemental Figure 3. (B) CSF2RB immunoblot of transformed Ba/F3 lines. Prior to lysis the cells were starved overnight in 0.1% FBS. WT cells were grown in IL-3 supplemented media prior to overnight starvation. (C) Ba/F3 cells expressing CSF2RB WT or R461C were treated with cycloheximide and stained with PE-conjugated anti-CSF2RB antibody and analyzed by flow cytometry (BD FACSAria IIIu and BD LSR II). Normalized mean fluorescence intensity (MFI) is shown over time (*$p<0.05$, **$p<0.01$). (D) Protein lysates were analyzed by immunoblot to determine the presence of high molecular weight, CSF2RB-containing complexes. Treatment with a reducing agent (2-mercaptoethanol) is compared with lysate

boiling at 95°C. WT cells were grown in IL-3 supplemented media and prior to lysis all lines were starved overnight in 0.1% FBS.

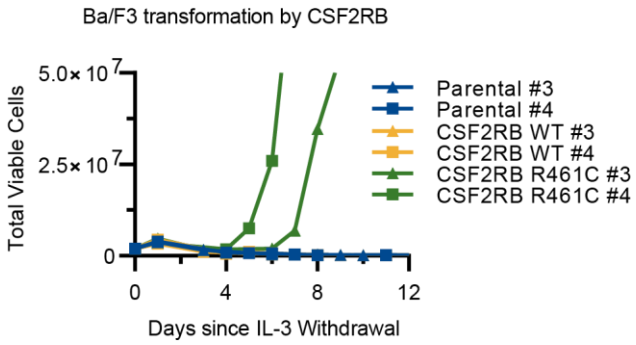

Figure 2-4 CSF2RB R461C transforms Ba/F3 cells.

Validation of the capacity of CSF2RB R461C to rapidly transform Ba/F3 cells following IL-3 withdrawal, as shown in Figure 1A. Cells were infected using a MIG-CSF2RB construct by retrovirus, and then sorted for GFP+ cells. Outgrowth monitored by frequent counting of viable cells using Guava ViaCount (Millipore).

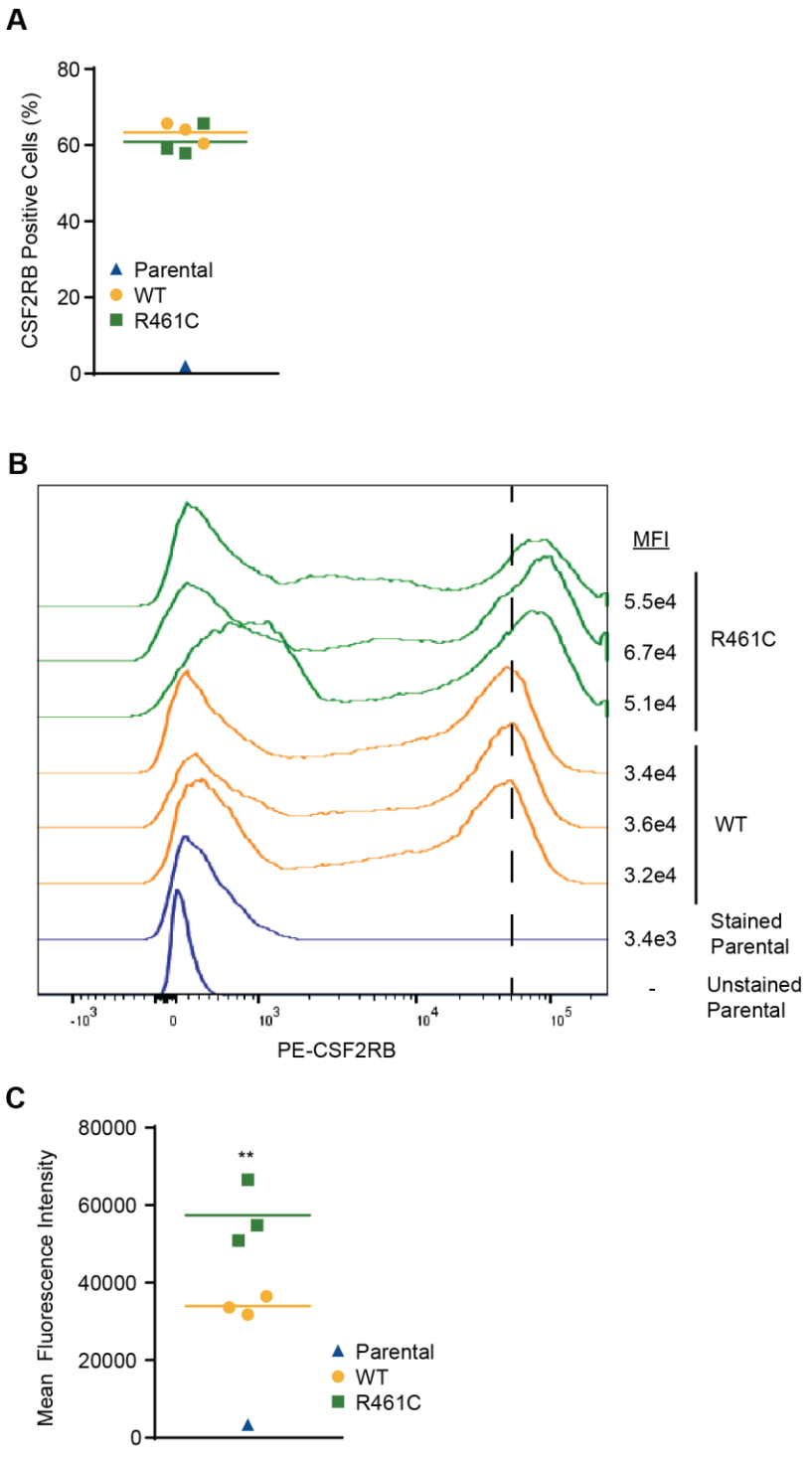

Figure 2-5 CSF2RB R461C is enriched in Ba/F3 prior to gaining factor independence.

(A) Ba/F3 cells transfected with WT or R461C CSF2RB and puromycin-selected were stained for CSF2RB and analyzed by flow cytometry. Percent of cells positive for surface CSF2RB displayed for three biological replicates. (B) Histograms for intensity of PE-conjugated CSF2RB across biologically replicate lines, with mean fluorescent intensity (MFI) for positive cells shown at right. Stained and unstained parental Ba/F3 cells shown are as controls. Dotted line drawn at WT peak for reference. (C) MFI of PE-CSF2RB for 10,000 cells in each sample (**$p<0.01$ WT vs R461C).

A

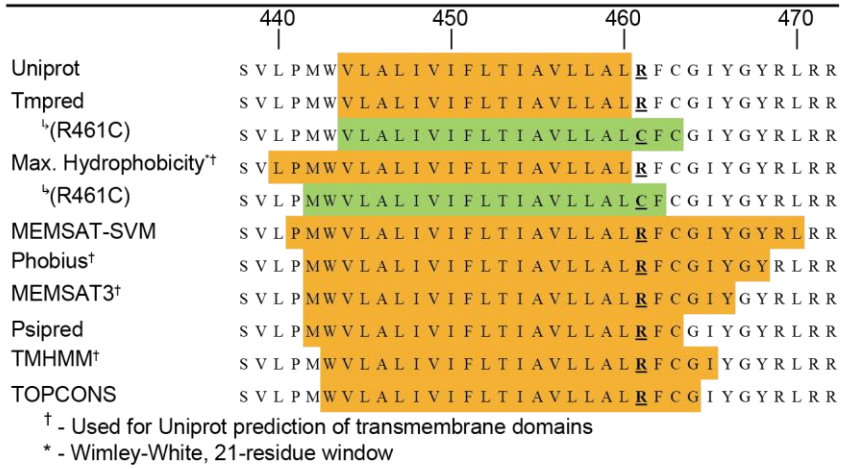

B

Model	Website	Predicted TM domain WT	R461C
Uniprot	www.uniprot.org/uniprot/P32927	444-460	n/a
Tmpred	www.ch.embnet.org/software/TMPRED_form.html	444-460	444-463
Max. Hydrophobicity	http://www.tulane.edu/~biochem/WW/PepDraw/	440-460	442-462
MEMSAT-SVM	bioinf.cs.ucl.ac.uk/psipred/	441-470	441-468
Phobius	phobius.sbc.su.se/	442-468	442-468
MEMSAT3	bioinf.cs.ucl.ac.uk/psipred/	442-466	442-466
Psipred	bioinf.cs.ucl.ac.uk/psipred/	442-463	442-462
TMHMM	www.cbs.dtu.dk/services/TMHMM/	443-465	443-465
TOPCONS	topcons.cbr.su.se	443-464	443-464

Figure 2-6 Residue R461 lies within the transmembrane domain of CSF2RB in most predictive models.

(A) Illustration of transmembrane domain prediction models for CSF2RB (predicted domain in orange, residue 461 shown in bold). Uniprot uses no single model but a combination of four. The TMPred and maximum hydrophobicity window approaches yielded differing results for the WT (orange) and R461C (green) sequence. (B) List of prediction platforms, results, and servers used in this study. Uniprot[99], TmPred[123],

Max Hydrophobicity[124], MEMSAT-SVM[125-128], Phobius[129, 130], MEMSAT3[125-128] Psipred[128, 131], TMHMM[132, 133], TOPCONS[134]

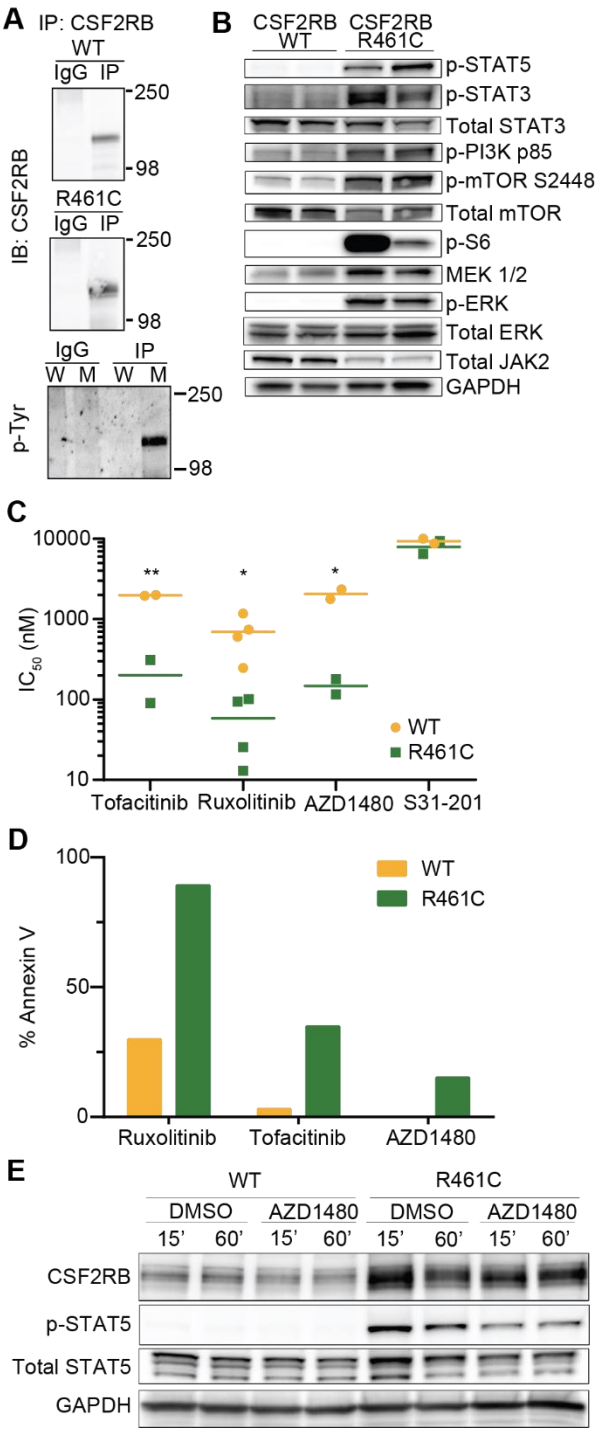

Figure 2-7 CSF2RB R461C is constitutively phosphorylated and activates canonical downstream pathways that are sensitive to JAK2 inhibition.

(A) CSF2RB was immunoprecipitated from transformed Ba/F3 lysates starved overnight in 0.1% FBS and probed for CSF2RB or phosphorylated tyrosine residues on replicate blots (W – WT lysate, M – R461C mutant lysate). WT cells were grown in IL-3 supplemented media. (B) Immunoblot analysis for activation of canonical CSF2RB signaling members across biologically replicate lysates. WT cells were grown in IL-3 supplemented media and all lines were starved overnight in 0.1% FBS. (C) Biologically replicate WT and R461C lines were screened on a small molecule inhibitor library and the top three hits (determined by % IC_{50} difference between the two lines) were the JAK-inhibitors Tofacitinib, Ruxolitinib and AZD1480. The STAT3 inhibitor S31-201 was equally ineffective on both WT and R461C (*$p<0.05$, **$p<0.01$). WT cells were grown and tested in IL-3 supplemented media. Key inhibitors are validated in Supplemental Figure 6A-C, full inhibitor panel results are found in Supplemental Table 3. (D) Lines were treated with indicated JAK-inhibitors (Ruxolitinib 350nM, Tofacitinib 350nM, AZD1480 1μM) for 48 hours and analyzed for apoptotic induction using Annexin V staining and flow cytometry (Guava PCA). 24 hour reads are shown in Supplemental Figure 6D. (E) Cells were starved overnight in 0.1% FBS and then treated with the JAK2 specific inhibitor AZD1480 (500nM) for the indicated time and immunoblotted for CSF2RB downstream signaling. WT cells were maintained in IL-3 supplemented media prior to starvation and treatment.

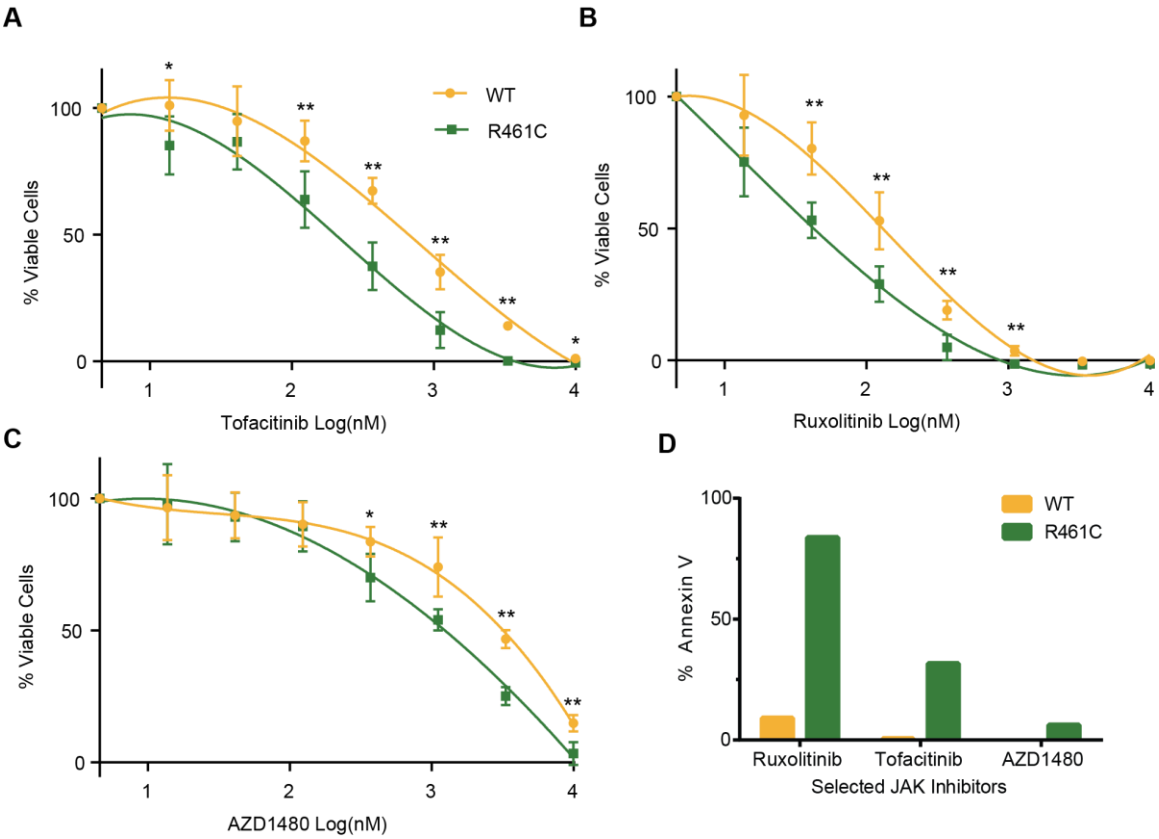

Figure 2-8 R461C cells are more sensitive to JAK-inhibitors than CSF2RB WT cells.

(A-C) Ba/F3 cells were exposed to increasing concentrations of JAK-inhibitor for 72 hours prior to assessment of viability by a colorimetric assay. Normalized viability shown across drug concentrations (*$p<0.05$, **$p<0.01$). (D) Ba/F3 lines were treated for 24 hours with indicated JAK-inhibitors (Ruxolitinib 350nM, Tofacitinib 350nM, AZD1480 1μM) and analyzed for apoptotic induction using Annexin V staining and flow cytometry (Guava PCA). 48 hour reads shown in Figure 2D.

2.4 Tables

Table 2-1 Co-occuring mutations in the T-ALL patient

Gene	CDS change	Amino acid change	Type	COSMIC status	Somatic confirmation
CSF2RB	C1381T	R461C	Missense	Not found	Germline
PTEN	C737G	P246R	Missense	Full match	Somatic
NOTCH1	C6856GC	L2286A…	Frameshift insertion	Not found	Somatic
NOTCH1	T4847A	I1616N	Missense	Full match	Somatic (subpopulation)
LHCGR	T47A	L16Q	Missense	Full match	Germline
TRAT1	C361T	R121C	Missense	Full match	Germline
IGF1R	G361T	E121*	Nonsense	Not found	N/A (not tested)
LRRK2	G1033A	D345N	Missense	Not found	N/A (not tested)
MAST3	T2374C	S792P	Missense	Not found	N/A (not tested)
NEK5	T2120G	L707R	Missense	Not found	N/A (not tested)
PHKG2	G1174A	D392N	Missense	Not found	N/A (not tested)
POMK	T401G	V134G	Missense	Not found	N/A (not tested)

All mutations in the patient that passed read quality filters and SNP exclusion criteria (MAF<0.001). Mutations were checked in COSMIC to determine if it was previously reported in a cancer case. Six mutations were investigated with Sanger sequencing of leukemic and normal DNA samples and determinations of germline or somatic status are listed. Sanger validation of Notch1 I1616N was faint in the leukemic sample, potentially indicating a subpopulation.

Table 2-2 Antibodies used in this study

Target	Antibody	Vendor	Clone	Species	Primary Dilution	Secondary Antibody	Secondary Dilution	Predicted Size (kDa)
CSF2RB	sc-678	Santa Cruz	K-17	Rb	1:200	HRPαRb	1:5000	130
CSF2RB (PE-conjugated)	306104	Biolegend		Ms	1:50	n/a	n/a	n/a
CSF2RB (Immunoprecipitation)	sc-678	Santa Cruz	K-17	Rb	1:25	n/a	n/a	n/a
Normal rabbit IgG (Immunoprecipitation)	sc-2027	Santa Cruz		Rb	1:12.5	n/a	n/a	n/a
p-Tyrosine	05-321	Millipore	4G10	Ms	1:5000	HRPαMs	1:5000	n/a
p-STAT5 (Y694)	9351	Cell Signaling		Rb	1:1000	HRPαRb	1:5000	90
p-STAT3 (Y705)	9131	Cell Signaling		Rb	1:1000	HRPαRb	1:5000	79, 85
Total STAT3	9139	Cell Signaling		Ms	1:1000	HRPαMs	1:5000	79, 86
p-PI3 Kinase (p85 Y458, p55 Y199)	4228	Cell Signaling		Rb	1:1000	HRPαRb	1:5000	60, 85
p-mTor (S2448)	5536	Cell Signaling	D9C2 XP	Rb	1:1000	HRPαRb	1:5000	289
mTOR	2983	Cell Signaling	7C10	Rb	1:1000	HRPαRb	1:5000	289
p-S6 Ribosomal Protein (S235/236)	4858	Cell Signaling	D57.2.2E XP	Rb	1:1000	HRPαRb	1:5000	32
MEK1/2	9122	Cell Signaling		Rb	1:1000	HRPαRb	1:5000	45
p-p44/42 MAPK (ERK1/2) (T202/Y204)	9101	Cell Signaling		Rb	1:1000	HRPαRb	1:5000	42, 44
Total p44/42 MAPK (ERK 1/2)	9102	Cell Signaling		Rb	1:1000	HRPαRb	1:5000	42, 44
Total Jak2	3230	Cell Signaling	D2E12 XP	Rb	1:1000	HRPαRb	1:5000	125
GAPDH	AM4300	ThermoFisher	6C5	Ms	1:5000	HRPαMs	1:5000	36
Actin	T 6074	Sigma	B512	Ms	1:10000	HRPαMs	1:5000	54

A list of all antibodies used in these experiments.

Table 2-3 Complete results of the small-molecule inhibitor screen.

		Calculated IC50 (nM)						
EffectiveDrug	**Targets**	**WT1 IC50**	**WT2 IC50**	**Avg WT**	**R461C 3 IC50**	**R461C 4 IC50**	**Avg R461C**	**%Diff**
Ruxolitinib (INCB018424)_2	JAK	604	246	**425**	26	13	**19**	**4.5%**
JAK Inhibitor I	JAK	677	258	**468**	33	23	**28**	**6.1%**
AZD1480	JAK-2	2345	1779	**2062**	179	116	**147**	**7.1%**
Tofacitinib (CP-690550)	JAK	1996	1951	**1974**	90	310	**200**	**10.1%**
Ruxolitinib (INCB018424)_1	JAK	1176	742	**959**	94	101	**98**	**10.2%**
NVP-ADW742_1	IGF1R	10000	10000	**10000**	742	1480	**1111**	**11.1%**
Bosutinib (SKI-606)	Src, Abl	10000	10000	**10000**	632	1951	**1291**	**12.9%**
JNJ-28312141	CSF1R/FLT3	10000	10000	**10000**	1906	852	**1379**	**13.8%**
Lapatinib_2	ERB2/EGFR	10000	10000	**10000**	1289	1699	**1494**	**14.9%**
NF-kB Activation Inhibitor	NF-kB	205	230	**218**	18	57	**38**	**17.3%**
Pazopanib (GW786034)_2	VEGFR/c-KIT	10000	9121	**9561**	2345	1231	**1788**	**18.7%**
Canertinib (CI-1033)	EGFR/ERB2	10000	10000	**10000**	1661	2400	**2030**	**20.3%**
GDC-0941_2	PI3K	3021	2189	**2605**	725	458	**592**	**22.7%**
PRT062607	Syk	7080	8711	**7896**	2043	1550	**1796**	**22.8%**
Masitinib (AB-1010)	KIT/PDGFR	10000	10000	**10000**	3163	2631	**2897**	**29.0%**
Cediranib (AZD2171)	VEGFR	10000	7763	**8882**	2755	2513	**2634**	**29.7%**
Quizartinib (AC220)_2	FLT3	6919	9121	**8020**	2345	2571	**2458**	**30.7%**
Trametinib (GSK1120212)	MEK1/2	332	502	**417**	124	149	**136**	**32.7%**
Dovitinib (CHIR-258)	FLT3/ c-KIT/FGFR1/ FGFR3/VEGFR1,2,3,/ PDGFR/CSF1R	3982	1381	**2682**	872	913	**892**	**33.3%**
Cytopia (CYT387)	JAK1/JAK2	1446	1231	**1339**	725	364	**545**	**40.7%**
Ibrutinib (PCI 32765)	BTK	10000	10000	**10000**	3163	5130	**4146**	**41.5%**
Arsenic Trioxide		10000	9121	**9561**	3891	4899	**4395**	**46.0%**
Quizartinib (AC220)_1	FLT3	3163	5249	**4206**	1863	2090	**1977**	**47.0%**
Crizotinib (PF-2341066)_2	ALK	2456	1906	**2181**	1350	742	**1046**	**48.0%**
JNJ-7706621	CDK/cyclin, AuroraA and B	2631	5013	**3822**	1996	1863	**1930**	**50.5%**

Neratinib (HKI-272)	ERB2/EGFR	6311	6762	**6536**	576	6027	**3302**	**50.5%**
Midostaurin (PKC412)	PKC	1149	814	**981**	795	230	**513**	**52.2%**
KU-55933	PI3K/mTOR/ATM	10000	6167	**8083**	5755	2693	**4224**	**52.3%**
17-AAG (Tanespimycin)	Hsp90	647	220	**433**	264	192	**228**	**52.6%**
GSK-1838705A	IGF1R and ALK	3312	3632	**3472**	1996	1661	**1828**	**52.7%**
Axitinib (AG-013736)	VEGFR1,2,3/PDGFR/cKIT	2292	2043	**2167**	1515	956	**1235**	**57.0%**
NVP-ADW742_2	IGF1R	10000	10000	**10000**	4468	7414	**5941**	**59.4%**
Tivozanib (AV-951)	VEGFR	10000	8129	**9065**	6919	3891	**5405**	**59.6%**
Pelitinib (EKB-569)	ERB1,2,4	1996	1231	**1614**	833	1097	**965**	**59.8%**
Saracatinib (AZD0530)	Src/Fyn/Lyn/Blk/Fgr/Lck	10000	10000	**10000**	2043	10000	**6021**	**60.2%**
Ponatinib (AP24534)_1	BCR/ABL T315I /FLT3/RET/KIT/FGFR/PDGFR	280	220	**250**	182	123	**152**	**61.0%**
GDC-0941_1	PI3K	6167	4899	**5533**	2139	4678	**3409**	**61.6%**
Erlotinib_2	EGFR/JAK2V617F	10000	10000	**10000**	2345	10000	**6173**	**61.7%**
Vargetef	VEGFR, PDGFR, FGFR	2139	10000	**6069**	448	7245	**3847**	**63.4%**
KI20227	CSF1R, VEGFR, c-KIT PDGFRB	8512	8711	**8612**	7763	3237	**5500**	**63.9%**
Pazopanib (GW786034)_1	VEGFR/c-KIT	10000	10000	**10000**	4572	8319	**6445**	**64.5%**
Gefitinib_2	EGFR	10000	10000	**10000**	5130	7763	**6447**	**64.5%**
Erlotinib_1	EGFR/JAK2V617F	10000	10000	**10000**	5371	7587	**6479**	**64.8%**
MK-2206	AKT1,2,3	10000	10000	**10000**	3091	10000	**6546**	**65.5%**
SU11274	MET	4787	5130	**4958**	3389	3237	**3313**	**66.8%**
Vandetanib (ZD6474)	VEGFR, EGFR, RET	10000	10000	**10000**	3468	10000	**6734**	**67.3%**
Rapamycin_1	mTOR, IL2	16	11	**14**	10	9	**9**	**68.2%**
PI-103	P13K	1231	913	**1072**	469	1001	**735**	**68.5%**
GW-2580_1	CSF1R	10000	10000	**10000**	10000	3803	**6901**	**69.0%**
LY-333531	PKCB	4899	4572	**4735**	3237	3389	**3313**	**70.0%**
Ponatinib (AP24534)_2	BCR/ABL T315I /FLT3/RET/KIT/FGFR/PDGFR	244	212	**228**	198	125	**161**	**70.8%**
MLN120B	IKKB	5000	5000	**5000**	2275	5000	**3638**	**72.8%**
INK-128	mTOR	36	22	**29**	20	22	**21**	**73.0%**
Lapatinib_1	ERB2/EGFR	10000	10000	**10000**	5013	10000	**7506**	**75.1%**
Selumetinib (AZD6244)	MEK1	10000	10000	**10000**	8914	6167	**7540**	**75.4%**
Rapamycin_2	mTOR, IL2	10	9	**10**	7	8	**8**	**78.5%**

Afatinib (BIBW-2992)	ERB2/EGFR	1203	892	**1048**	677	978	**828**	**79.0%**
Azacytidine		10000	10000	**10000**	6311	10000	**8155**	**81.6%**
VX-745	p-38a MAPK	10000	10000	**10000**	6311	10000	**8155**	**81.6%**
NVP-TAE684	ALK	1739	2755	**2247**	1550	2139	**1844**	**82.1%**
Elesclomol	Hsp90/apoptosis	7	6	**7**	6	5	**6**	**83.3%**
S31-201	STAT3	10000	8711	**9355**	6458	9334	**7896**	**84.4%**
AT7519	CDK	2043	1480	**1761**	1779	1231	**1505**	**85.5%**
GSK-1904529A_2	IGF1R and IR	10000	10000	**10000**	10000	7245	**8623**	**86.2%**
Foretinib (XL880)	MET, VEGFR2,KDR	2292	1996	**2144**	1906	1821	**1864**	**86.9%**
Gefitinib_1	EGFR	10000	10000	**10000**	7587	10000	**8793**	**87.9%**
PHA-665752	c-Met	1821	2043	**1932**	1480	1996	**1738**	**90.0%**
KW-2449	FLT3/ABL/FGFR1/AuroraA	1586	1906	**1746**	1203	1996	**1600**	**91.6%**
H-89	PKA	4075	10000	**7037**	5889	7414	**6652**	**94.5%**
BEZ235	PI3K/mTOR	8	7	**8**	8	7	**7**	**95.7%**
Imatinib	BCR/ABL, KIT	10000	9551	**9775**	8711	10000	**9355**	**95.7%**
Crenolanib_1	PDGFRA/B	1289	1231	**1260**	1176	1260	**1218**	**96.6%**
ABT-737	Bcl-2	10000	10000	**10000**	10000	9334	**9667**	**96.7%**
Crenolanib_2	PDGFRA/B	1550	1176	**1363**	1048	1661	**1354**	**99.4%**
Carbozantinib (XL184)	MET and VEGFR2	10000	10000	**10000**	10000	10000	**10000**	**100.0%**
CHIR-99021	GSK3-B	10000	10000	**10000**	10000	10000	**10000**	**100.0%**
CI-1040 (PD184352)	MEK/MAPK	10000	10000	**10000**	10000	10000	**10000**	**100.0%**
Dasatinib_1	BCR/ABL, SRC, c-Kit	1000	1000	**1000**	1000	1000	**1000**	**100.0%**
Dasatinib_2	BCR/ABL, SRC, c-Kit	1000	1000	**1000**	1000	1000	**1000**	**100.0%**
Doramapimod (BIRB 796)	MAPK	10000	10000	**10000**	10000	10000	**10000**	**100.0%**
GDC-0879	B-RAFV600E/pERK	10000	10000	**10000**	10000	10000	**10000**	**100.0%**
GS-1101 (CAL-101)	PI3K	10000	10000	**10000**	10000	10000	**10000**	**100.0%**
GSK-1904529A_1	IGF1R and IR	10000	10000	**10000**	10000	10000	**10000**	**100.0%**
GSK690693	AKT	10000	10000	**10000**	10000	10000	**10000**	**100.0%**
GW-2580_2	CSF1R	10000	10000	**10000**	10000	10000	**10000**	**100.0%**
JNJ-38877605	c-MET	10000	10000	**10000**	10000	10000	**10000**	**100.0%**
Linifanib (ABT-869)	VEGFR/PDGFR/KDR/CSF1R	10000	10000	**10000**	10000	10000	**10000**	**100.0%**
MGCD-265	MET/VEGFR/Tie2	10000	10000	**10000**	10000	10000	**10000**	**100.0%**
Motesanib (AMG-706)	VEGFR1,2,3/PDGFR/cKIT/RET	10000	10000	**10000**	10000	10000	**10000**	**100.0%**

Nilotinib_1	BCR-ABL/KIT/LCK/EPHA/DDR	10000	10000	**10000**	10000	10000	**10000**	**100.0%**
Nilotinib_2	BCR-ABL/KIT/LCK/EPHA/DDR	10000	10000	**10000**	10000	10000	**10000**	**100.0%**
PHT-427	AKT, PDPK1	10000	10000	**10000**	10000	10000	**10000**	**100.0%**
RAF265 (CHIR-265)	B-RAF/VEGFR	10000	10000	**10000**	10000	10000	**10000**	**100.0%**
Regorafenib (BAY 73-4506)	c-KIT/VEGFR1,2/B-Raf/RET/PDGFR	10000	10000	**10000**	10000	10000	**10000**	**100.0%**
Roscovitine (CYC-202)	cdc/cdk/cyclin	10000	10000	**10000**	10000	10000	**10000**	**100.0%**
SB-431542	ALK5	10000	10000	**10000**	10000	10000	**10000**	**100.0%**
SGX-523	MET	10000	10000	**10000**	10000	10000	**10000**	**100.0%**
Sorafenib_1	VEGFR, PDGFR, RAF	10000	10000	**10000**	10000	10000	**10000**	**100.0%**
Sorafenib_2	VEGFR, PDGFR, RAF	10000	10000	**10000**	10000	10000	**10000**	**100.0%**
STO609	CAMKK	10000	10000	**10000**	10000	10000	**10000**	**100.0%**
Sunitinib_1	PDGFR, VEGFR, KIT, RET, CSF1R, FLT3	1000	1000	**1000**	1000	1000	**1000**	**100.0%**
Sunitinib_2	PDGFR, VEGFR, KIT, RET, CSF1R, FLT3	1000	1000	**1000**	1000	1000	**1000**	**100.0%**
TG100-115	PI3K	10000	10000	**10000**	10000	10000	**10000**	**100.0%**
Vatalanib (PTK787)	VEGFR, KIT, PDGFR	10000	10000	**10000**	10000	10000	**10000**	**100.0%**
Vemurafenib (PLX-4032)_1	B-Raf(V600E), C-Raf	10000	10000	**10000**	10000	10000	**10000**	**100.0%**
Vemurafenib (PLX-4032)_2	B-Raf(V600E), C-Raf	10000	10000	**10000**	10000	10000	**10000**	**100.0%**
Vismodegib (GDC-0449)	hedgehog	10000	10000	**10000**	10000	10000	**10000**	**100.0%**
XAV-939	TNKS1, 2 (wnt b-catenin pathway)	10000	10000	**10000**	10000	10000	**10000**	**100.0%**
PP242	mTOR	514	332	**423**	563	296	**430**	**101.6%**
Crizotinib (PF-2341066)_1	ALK	2755	1623	**2189**	2456	2090	**2273**	**103.8%**
MLN8054	Aurora A	2400	2400	**2400**	2952	2043	**2497**	**104.1%**
DBZ	Notch	8711	10000	**9355**	10000	10000	**10000**	**106.9%**
PD173955	BCR-ABL, SRC	3312	3803	**3558**	4468	3716	**4092**	**115.0%**
Alisertib (MLN8237)	Aurora A	296	469	**382**	604	276	**440**	**115.1%**
Velcade (Bortezomib)	proteasome inhibitor	1623	693	**1158**	1176	1623	**1399**	**120.9%**
YM-155	survivin	1000	618	**809**	1000	1000	**1000**	**123.6%**
BMS-345541	IKK	2292	4366	**3329**	3803	5496	**4650**	**139.7%**
A-674563	AKT	709	777	**743**	1661	725	**1193**	**160.5%**
Flavopiridol	cdk	241	152	**197**	448	187	**317**	**161.5%**

SNS-032 (BMS-387032)	CDK2	1001	852	**927**	1906	1231	**1569**	**169.3%**
BI-2536	PLK1	36	30	**33**	159	56	**108**	**324.8%**
Barasertib (AZD1152-HQPA)	Aurora B	116	64	**90**	340	276	**308**	**342.5%**
Tozasertib (VX-680)	pan-Aurora	48	79	**63**	205	332	**269**	**425.1%**

Biologically replicate WT and R461C lines were run on a screen of 104 small-molecule kinase inhibitors as previously described1. R461C cells were IL-3 independent and tested in IL-3 free media, while WT cells were grown and tested in IL-3 supplemented media. Colorimetric viability readouts (MTS) at 72 hours are used to compute IC50 values. Average WT and R461C IC50 are compared and the table is sorted for percent difference between the two. The top ranked inhibitors are those most selective for CSF2RB R461C.

Table 2-4 Mutations found in primary leukemic samples

Diagnosis	CCDS Change	Amino Acid Change	Location
AML	G145A	D49N	Extracellular
Ph- aCML	G553A	A185T	Extracellular
Ph+ CML	T626C	V209A	Extracellular
T-ALL	C1381T	R461C	Membrane spanning or adjacent
B-ALL	G1570T	V524L	Cytoplasmic
B-ALL	C1661T	T544M	Cytoplasmic
AMML - M4	G1940T	G647V	Cytoplasmic
AML - M5	G1940T	G647V	Cytoplasmic
B-ALL	C2497G	L833V	Cytoplasmic

* Leukemia patient cohort consists of 449 total leukemias:
184 MPN, 147 AML, 108 ALL (92 B-ALL, 16 T-ALL, 5 undefined lymphoid leukemias), 10 other

A list of all CSF2RB missense mutations found in patients and tested in the Ba/F3 transformation assay; only R461C transformed Ba/F3 cells. The composition of the 449 leukemia cohort is listed by diagnosis type.

3 Analysis of acquired mutations in transgenes arising in Ba/F3 transformation assays: Findings and recommendations

Kevin Watanabe-Smith, Jamila Godil, Anupriya Agarwal, Cristina Tognon, Brian Druker

This manuscript was submitted November 21st, 2016 to *Oncotarget*, where it has been accepted for publication following minor revision. I formulated and designed the complete experimental approach in this manuscript with feedback from Dr. Tognon. I developed the protocols for limiting dilution analysis and 6-TG survival assays, which were not previously performed in our laboratory. I performed all of the experiments, with the exception of one iteration of the methodology outlined in Figure 3-1, which was performed by Jamila Godil (a summer student I mentored). I analyzed the data with Jamila Godil and personally drew conclusions from the results. I wrote the manuscript with feedback and editing from the other authors.

3.1 Abstract

The identification and functional validation of potentially oncogenic mutations in leukemia is an essential step toward a future of personalized targeted therapy. To assess the oncogenic capacity of individual mutations, reliable and scalable *in vitro* experimental approaches are required. Since 1988, researchers have used the IL-3 dependent Ba/F3 transformation assay to validate the oncogenic potential of mutations to drive factor-independent growth. Here we report a previously unrecognized phenomenon whereby Ba/F3 cells, engineered to express weakly transforming mutations, present with additional acquired mutations in the expressed transgene following factor withdrawal. Using four mutations with known transformative capacity in three cytokine receptors (CSF2RB, CSF3R and IL7R), we demonstrate that the mutated receptors are highly susceptible to acquiring additional mutations. These acquired mutations of unknown functional significance are selected by factor withdrawal but appear to exist prior to the removal of growth factor. This anomaly has the potential to confound efforts to both validate and characterize oncogenic mutations in leukemia, particularly when it is not standard practice to sequence validate cDNAs from transformed Ba/F3 lines. We present specific recommendations to detect and mitigate this phenomenon in future research using Ba/F3 transformation assays, along with methods to make the Ba/F3 assay more quantitative.

3.2 Introduction

In 1988, George Daley and David Baltimore established that BCR-ABL—the gene fusion product found in almost every case of chronic myelogenous leukemia (CML)[135]—was oncogenic using the murine Ba/F3 cell line[8]. This cell line, derived from pro-B bone marrow cells, required interleukin 3 (IL-3) for normal proliferation and survival[25]. Stable expression of BCR-ABL in Ba/F3 cells blocked apoptosis and promoted proliferation, resulting in IL-3 independent growth[8] and, as a result, a new transformation assay was created. The Ba/F3 system was a superior model for hematopoietic malignancies in contrast to earlier NIH 3T3 growth-foci formation assays, where the BCR-ABL fusion was insufficient to transform fibroblasts[18].

In a typical Ba/F3 transformation assay, Ba/F3 cells are infected by a retrovirus or electroporated with a plasmid, driving expression of a gene of interest. Cells expressing the transgene are selected for by FACS or antibiotic treatment based on additional markers within the vectors, and then washed to remove IL-3 from the culture medium to initiate a cytokine-independent growth assay. Growth is monitored for two or three weeks. If cells continue to proliferate it is concluded that the transgene is transformative and an active oncogene. The resulting transformed Ba/F3 cells are frequently used for pathway analysis to characterize mechanisms of oncogenic signaling or to test the effects of selective targeted inhibitors on cell growth and survival[46]. A meta-analysis of all articles, published between 2014 and 2016, using the Ba/F3 system indicates that the cells are not sequenced following

oncogenic transformation to detect the presence of additional mutations in the expressed transgene[136-159] (Table 3-1, Table 3-2).

While testing a transforming CSF2RB mutation in a previous study[100], we noted that CSF2RB R461C-expressing cells demonstrated two reliable phenotypes: IL-3 independent growth and acquired mutations in the CSF2RB transgene following IL-3 withdrawal. Interestingly, when the CSF2RB wildtype-expressing cells spontaneously transformed it was only through the acquisition of a previously characterized transforming mutation (V449E)[160]. Conversely, R461C-expressing cells acquired a series of divergent mutations that were found throughout the receptor.

These observations led us to expand our investigation to include additional genes with well-established activating mutations in order to determine the prevalence and rate of acquired mutations that occur in this system. We found that acquired mutations are not unique to CSF2RB R461C but are similarly present in CSF3R variants. These acquired mutations are more common in weakly-transforming constructs. Withdrawal of IL-3 serves as a selective pressure to enrich for acquired mutations, but our data suggest these mutations exist prior to factor withdrawal. In contrast to earlier findings[65], we find no evidence that the time spent in culture between viral infection and factor withdrawal influences transformation rate. We recommend that future studies using the Ba/F3 transformation assay verify the complete sequence of the ectopically expressed transgene prior to pathway characterization

and publication of results. These recommendations are particularly critical for weakly or slowly transforming mutations, where acquired mutations appear to be most prevalent.

3.3 Results

3.3.1 Experimental Design

Three cytokine receptors harboring four unique oncogenic mutations along with wild type control receptors were selected for this study based upon their well-established transformation capability (Table 3-3). CSF2RB R461C is a germline mutation found in a T-ALL patient and shown to activate ligand-independent signaling *in vitro*[100]. CSF3R T618I is a prominent mutation in CNLs and aCMLs and leads to ligand-independent activation[36]. CSF3R truncation mutations (including W791X) have also been reported in both CNL and aCML[36], resulting in surface receptor accumulation through altered endocytosis and degradation[115, 161]. IL7R 243InsPPCL was described in a B-ALL patient[162] and is one of a group of mutations in pediatric ALLs that activate IL7R by introducing unpaired cysteine residues in the membrane-proximal region of the receptor that cause constitutive dimerization[119]. Expression of BCR-ABL fusion or empty vector served as positive and negative controls, respectively, for transformation of Ba/F3 cells in our assays.

The schematic diagram in Figure 3-1 describes the protocol used to create and collect samples for subsequent sequence verification. Retrovirally infected Ba/F3 cells were sorted

by GFP-positive FACS 48-hours post-infection and a series of limiting dilution plates were created. On day 9, a second series of limiting dilution plates were created. On day 10 each flask was triple-washed and split into replicate flasks to monitor IL-3 independent growth. Cells undergoing IL-3 withdrawal were monitored using a Guava ViaCount for 21 days. While variability was evident between biological replicates, technical replicate flasks from the same infected cell line exhibited near identical outgrowth curves (Figure 3-2A). Time to factor-independent growth is represented by the number of days to reach 500% of viable cells in the initial culture (Figure 3-2B).

Genomic DNA (gDNA) was immediately harvested from every outgrown line once factor-independent proliferation was evident. Genomic DNA was harvested from cell lines cultured in IL-3 containing media at the point of factor withdrawal (day 10) and also at day 31, which represents the complete length of the transformation assay. Transgenes were PCR amplified from gDNA using vector-specific primers, Sanger sequencing was performed, and all mutations from every cell line were comprehensively catalogued.

3.3.2 Acquired mutations detected in transformed lines

Sanger sequencing of these cell lines revealed acquired mutations in the one CSF2RB WT line that transformed (1 of 3) and every CSF3R WT line (4 of 4), all of which transformed (Figure 3-2C, Table 3-4). The majority of CSF2RB R461C lines (4 of 5) and CSF3R W791X lines (3 of 4) also presented with a variety of additional acquired mutations (Figure 2C). The CSF3R T618I lines were the most rapidly transforming and did not contain

acquired mutations, nor did the slightly slower-growing IL7R 243InsPPCL lines. The empty vector (negative control) transformed once and sequencing revealed a contamination with IL7R Ins243PPCL in both replicate flasks, demonstrating the ability to detect cross-contamination in our experimental design. In all but one case (11 of 12), replicate withdrawal flasks exhibited identical acquired mutations upon sequencing (Table 3-4), indicating the acquired mutations were likely present prior to IL-3 withdrawal. To rule out the possibility that acquired mutations are merely a function of time in culture, we sequenced the transgene of cells on the day of withdrawal (day 10, baseline) and again following 21 days in culture with IL-3 (day 31, cultured). Sequencing revealed mutations in only 1 of 15 cultured lines (Table 3-4), indicating that the acquired mutations do not provide a competitive, proliferative advantage while growing in IL-3-supplemented media.

3.3.3 CSF2RB R461C does not drive genomic instability

The high rate of acquired mutations in CSF2RB R461C, both reported here and observed in our prior experiments, led us to question if the variant caused widespread mutagenesis or genomic instability. To address this, we performed a 6-thioguanine (6-TG) survival assay following retroviral infection. In this assay, only cells that possess a higher capability to induce mutations through genomic instability or other mechanisms will be capable of mutationally inactivating HPRT to survive 6-TG treatment. We observed no increase in survival for CSF2RB R461C cells compared to controls (ENU-treated and no infection) or

any other transformed cell line (Figure 3-3), indicating that the CSF2RB R461C mutation is not causing genetic instability.

3.3.4 Transformation rate determined by limiting dilution analysis

In contrast to bulk Ba/F3 transformation assays, a limiting dilution assay has the ability to pinpoint the proportion of infected cells capable of surviving IL-3 withdrawal. Using this more quantitative assay we investigated whether acquired mutations are more common in lines with weaker rates of transformation. Limiting dilution plates were visually scored for growth after three weeks. Plating efficiency was calculated from plates diluted to 1 cell per well in media containing IL-3. The remaining plates were used to calculate the ratio of transforming cells (displayed as transformation rate X, where 1 in X cells are capable of factor-independent growth) with 95% confidence intervals using Extreme Limiting Dilution Analysis (ELDA) as previously described[163].

A previous study investigating another *in vitro* transforming CSF2RB mutation found that the transformation rate of infected cells increased with the time in culture after viral infection and before factor withdrawal[65]. In our study, we observed no consistent effect of culture time on transformation rate with any of the mutations tested (Figure 3-4A). Transformation rate estimates were calculated and these results demonstrated reliable differences between individual mutations (Figure 3-4B). These data are also summarized by the median transformation rate, which is calculated after combining the transformation rates of the technical replicates for each mutation. Transformation rate correlated with time

to outgrowth, but also served as a more quantitative measure to assess the relative functional impact of a given mutation. These data highlight the quantitative difference between strongly transforming mutations (CSF3R T618I, BCR-ABL) and weakly transforming mutations (IL7R 243InsPPCL, CSF3R W791X, CSF2RB R461C).

3.3.5 Acquired mutations are exclusively observed in weakly transforming oncogenes

Mutations that possess a weaker ability to transform cells (less than 1 in every 200 cells, Figure 3-5A) or a slower time to outgrowth (5 days or longer to reach a 5x increase over the initial cell number, Figure 3-5B) account for every case of acquired mutations in this study. While a weakly transforming mutation does not always indicate the presence of acquired mutations, our data indicate that strongly transforming mutations do not present with additional mutations.

3.4 Discussion

In a previous study, we observed that exogenous expression of the CSF2RB R461C transgene frequently presented with additional acquired mutations in the gene following selection of Ba/F3 cells to IL-3-independent cell growth. As a result of this observation, we expanded our investigation to include other transforming mutations and determine if: 1) acquired mutations also arose in other transgenes, 2) whether the mutations were present

prior to IL-3 withdrawal, 3) if they were enriched in weakly transforming oncogenes, and 4) if the time in culture following infection impacted the transformation rate.

Our study indicates that weakly transforming mutations in both CSF2RB and CSF3R frequently present with acquired mutations. While this could be indicative of the large number of potentially activating mutations in each gene[36, 98, 160], it is striking that CSF3R T618I does not present with acquired mutations and expression of CSF2RB WT only infrequently results in factor-independent growth. Instead, it appears that the frequencies of these mutations are dependent on the transformation rate intrinsic to each specific oncogene.

Our data indicate that the majority of these mutations likely exist prior to factor withdrawal—replicate withdrawal flasks present with identical mutations in almost every case—but only expand to levels detectable by Sanger sequencing in the absence of IL-3. Selection of factor independent Ba/F3 cells in the absence of IL-3 has been previously proposed, possibly as the result of enrichment for cells with stronger activation of downstream signaling[164]. Retroviral infection and reverse transcription is an inherently mutagenic process[165], making it an inevitability that an infected cell line has a library of clonal mutations in the infected transgene. The number of these clonal mutations would by increased by the use of high viral titers. Based on our data, we calculate that in many cases the strength of the intended mutation (CSF3R T618I) gives up to 70% of clones (1 in every 1.4 cells) the capacity to survive factor withdrawal (Figure 3B). In these cases acquired

mutations would never expand beyond the mutation detection threshold of Sanger sequencing, which is around 5-10%[166]. In other cases, the acquired mutations can be functionally active, turning a non-transforming gene into a putative oncogene, as observed with the V449E mutation found in the CSF2RB wildtype receptor (Table 3-4). Then in a third, more complex case there are oncogenic constructs that are functionally active—both CSF2RB R461C and CSF3R W791X have higher transformation rates than their WT counterparts—but regularly present with acquired mutations following transformation. In this third case, the acquired mutations could be passenger mutations resulting from the rare clone capable of factor-independent growth (as rare as 1 in 60,000 cells in CSF2RB R461C; Figure 3-4B), or they could be functional mutations that drive factor independent growth, resulting in clonal expansion detectable by Sanger sequencing. Distinguishing between the passenger mutations and the functionally active acquired mutations would require laborious empirical investigation, detracting from the scalability of this model system and thus making it an impractical solution. We have not attempted to determine the functionality of observed acquired mutations, though specific extracellular deletions have been previously shown to result in receptor activation of CSF2RB[64, 65].

Another potential complication in transformation assays is the acquisition of mutations outside of the intended transgene. Other researchers have detailed the potential for IL9Rα mutant Ba/F3 cells to gradually reach growth factor independence through the acquisition of recurrent JAK1 mutations[167]. Additionally, the use of retroviruses can result in

insertional mutagenesis, possibly disrupting tumor suppressor genes resulting in factor-independent growth. These artifacts would not be detected in our experimental design, but underscore the importance of screening biological replicates to control for false-positives. Non-transgenic mutations could also be controlled for by inducible transgene expression, but this would not solve the problem of acquired mutations within the transgene.

It is not clear what constitutes a weakly transforming mutation which drives oncogenic growth in only a subset of infected cells. The Ba/F3 model has traditionally been very effective for screening mutations in growth factor receptors[35, 36, 41, 45, 119], but in these cases of weakly transforming mutations an alternative cell line could yield more robust results. It is possible that weak mutations are barely capable of transforming cells to become factor independent, possibly requiring a high level of expression, and the majority of cells fail to reach that state. It is also possible that some mutations need a second, cooperating mutation as proposed by earlier studies[65].

Stocking and colleagues have previously described a truncated form of CSF2RB, $\Delta\beta_c$, that was capable of transforming FDC-P1 factor-dependent cells[62, 64]. In a follow-up study[65], they described two striking observations. First, 7 of 8 $\Delta\beta_c$ transformed lines could have $\Delta\beta_c$ removed by Cre-Lox excision and maintain factor independent growth. Second, $\Delta\beta_c$ lines showed no increase in transformation (by limiting dilution analysis) 24 hours after infection, but a substantial increase 10 days after infection (from $1.0x10^{-8}$ to $6.8x10^{-5}$). This led the authors to conclude that $\Delta\beta_c$ was either mutagenic—capable of

creating oncogenic lesions to sustain growth—or synergistic with a spectrum of potential secondary mutations that could replace dependence on the original transgene[65]. While we do not see an effect of culture time on transformation rate in our study, and CSF2RB R461C does not appear cause genomic instability by 6-TG selection, it is possible that some mutations have the ability to synergize with a larger library of secondary cooperating mutations that might be selected in a transformation assay.

In any case, determining the significance of acquired mutations would require time-consuming independent validation. Yet the presence of these unintended mutations has the potential to confound our ability to functionally characterize potentially transforming mutations. Researchers are increasingly using transformed Ba/F3 cells to screen oncogenes for drug sensitivity[46]. In these experiments, an acquired mutation could dramatically alter results, stressing the importance of understanding this phenomenon. At this time, we cannot propose a method that eliminates the appearance of acquired mutations. Our previous study mitigated this effect by using electroporation instead of retroviral infection, avoiding the potential for reverse-transcription induced mutagenesis. However, some of these electroporated lines still presented with acquired mutations, and there is insufficient evidence to determine if this approach reduced their frequency.

We recommend that every outgrown Ba/F3 line should be sequenced to validate the sequence of the full transgene, ensuring reproducible results and reducing the risks of characterizing artificial oncogenes. Even in lines that repeatedly transform, biological

replicates are prone to frequent acquired mutations. This sequence validation is particularly important for all mutations that are weakly transforming. We present our criteria for classifying a weakly transforming mutation by limiting dilution analysis (fewer than 1 in every 200 cells sustaining factor-independent growth), or time to outgrowth (lines that take more than 4 days post-factor withdrawal to reach 5x the number of viable cells in the starting culture). However, these measures could vary by protocol or laboratory and we cannot conclude that strongly transforming genes never acquire mutations. Transformation rate as determined by limiting dilution analysis would also represent a valued addition to the Ba/F3 assay. Widespread adoption of this measure in future studies would allow detailed investigation into correlations between transformation rate and clinical relevance of weakly transforming mutations.

The Ba/F3 transformation assay remains an invaluable tool for the functional validation of activating mutations found in primary leukemias. We report a previously unrecognized phenomenon where weak transforming mutations are susceptible to acquiring additional mutations within the transgene of interest. These acquired mutations could jeopardize attempts to characterize the signaling mechanisms and drug sensitivities of leukemic oncogenes. We propose an addition to the standard Ba/F3 protocol and suggest the sequencing of the full transgene in outgrown cells to detect confounding mutations and improve the reproducibility of future studies. Additional research should be directed toward methods that reduce the incidence of acquired mutations in these critical assays.

Special attention should be paid to whether the use of retroviruses increases this phenomenon, as this method is the most frequently used in current studies (Table 3-1). A larger study covering additional leukemic oncogenes would indicate if acquired mutations occur in non-cytokine receptors, and would help define the range of studies that could be affected by this phenomenon.

3.5 Methods

3.5.1.1 Cell Culture

Ba/F3 cells were obtained from ATCC and grown in RPMI 1640 medium with 10% FBS, L-glutamine, fungizone, penicillin-streptomycin, and 15% WEHI-conditioned medium (a source of IL-3). Frozen vials of cells, previously in culture less than 30 cumulative days, were freshly thawed for each experiment.

3.5.1.2 Ba/F3 transformation assay

Gene constructs were cloned as previously described[36] into a MSCV-IRES-GFP retroviral vector[168] and confirmed by Sanger sequencing. Retrovirus was created by transfecting plasmids into 293T/17 cells along with the pIK6.1MCV.ecopac.UTD helper plasmid. Virus was harvested and used to infect Ba/F3 cells in two rounds of retroviral spin inoculation. Infected Ba/F3 cells were 42% GFP-positive on average, as determined by FACS. Percent of GFP-positive cells following infection varied primarily by replicate set and minimally by transgene (average per non-control transgene ranged from 38-50%). The number of vector

copies integrated into each line is unknown, but Table 3-4 indicates some lines possessed more than one copy. High rates of infection were necessary to enable sorting of GFP-positive cells by FACS 48-hours post-infection and subsequent plating for limiting dilution analysis. For factor-independent transformation assays, Ba/F3 cells were washed three times and re-suspended in RPMI 1640 with 10% FBS, L-glutamine, fungizone and penicillin-streptomycin. Viable cell counts were obtained using a propidium iodide exclusion on a Guava Personal Cell Analysis System (Millipore). Genomic DNA was harvested using the DNeasy Blood and Tissue Kit (Qiagen).

3.5.1.3 Transgene amplification and sequencing

Transgenic DNA was amplified from genomic DNA extracts using vector specific primers (MigFwd – CCCTTTGTACACCCTAAGCCTCCGCC, MigRev – GGAAAGACCCCTAGAATGCTCGTCAA), AccuPrime Taq DNA polymerase, high fidelity (ThermoFisher Scientific) and a modified "slowdown PCR" thermocycler protocol[169]. Sanger sequencing (Eurofins) was performed with transgene-specific internal primers and analyzed using LaserGene 14 Seqman Pro (DNASTAR).

3.5.1.4 Limiting dilution analysis

Cells were counted and resuspended in IL-3 free media prior to dilution. Diluted cells were plated in 96-well plates with IL-3-free or IL-3-containing media. Wells were visually inspected once a week for three weeks to identify cell growth. All data was analyzed using

the elda function provided with the statmod package (version 1.4.26) in R (version 3.3.2)[163].

3.5.1.5 6-thioguanine survival assay

Ba/F3 cells were cultured in HAT-supplemented media (100μM sodium hypoxanthine, 0.4μM aminopterin, 16μM thymidine, Gibco) for 4 days to select for HPRT-expressing cells. Cells were then allowed to recover for 5 days in HT-supplemented media (100μM sodium hypoxanthine, 16μM thymidine, Gibco) prior to culturing in regular Ba/F3 media. Ba/F3 cells were infected with retrovirus 14 days prior to 6-TG exposure. Positive control cells were treated overnight with 50μg/ml ENU 6 days prior to 6-TG exposure. Biologically replicate lines were screened for 6-TG survival in the following conditions: 2 96-well plates seeded at 1 cell per well without 6-TG (plating efficiency calculations), 2 96-well plates at 1000 cells per well with 20μM 6-TG, and 2 96-well plates at 5000 cells per well with 20μM 6-TG. Wells were visually assessed for growth 14 days later and the number of cells surviving through HPRT-inactivation was determined using ELDA.

3.6 Miscellaneous

3.6.1.1 Abbreviations

CSF2RB, Colony stimulating factor 2 receptor beta common subunit; CSF3R, Colony stimulating factor 3 receptor; IL7R, Interleukin 7 receptor; BCR-ABL, Breakpoint cluster region – Abelson tyrosine-protein kinase 1 fusion; CML, Chronic myelogenous leukemia;

IL-3, Interleukin-3; FACS, Fluorescence activated cell sorting; ALL, Acute lymphoblastic leukemia; T-ALL, T-cell acute lymphoblastic leukemia; B-ALL B-cell acute lymphoblastic leukemia; CNL, Chronic neutrophilic leukemia; aCML, Atypical chronic myelogenous leukemia; GFP, Green fluorescent protein; HPRT, Hypoxanthine phosphoribosyltransferase 1; 6-TG, 6-thioguanine; ENU, N-ethyl-N-nitrosourea; ELDA, Extreme limiting dilution analysis; $\Delta\beta_c$, truncated beta-common receptor (CSF2RB).

3.6.1.2 Authorship

KWS and CT designed experiments, KWS and JG performed experiments and analyzed data, KWS wrote the manuscript, AA and BD advised on experimental design and provided critical feedback, all authors reviewed the manuscript.

3.6.1.3 Acknowledgements

The authors would like to acknowledge Dr. Bill Chang and Dr. Tamilla Nechiporuk for critical feedback in writing and editing the manuscript, Dr. Haijiao Zhang for providing CSF3R constructs and insights on CSF3R activation.

3.6.1.4 Conflicts of interest

The authors have no conflicts of interest to disclose.

3.6.1.5 Funding

This work was funded by a Howard Hughes Medical Institute Investigator award and NIH/NCI MERIT award (R37CA065823) to B.J.D., NIH/NCI R00 award (5R00CA151670-04) to A.A. and a V foundation scholar award to A.A. K.W.S. was supported by a T32 program training grant (5T32GM071338-08), Knight Cancer Institute stipend award, the Allan Price memorial ARCS scholar award and a Tartar Trust fellowship.

3.7 Figures

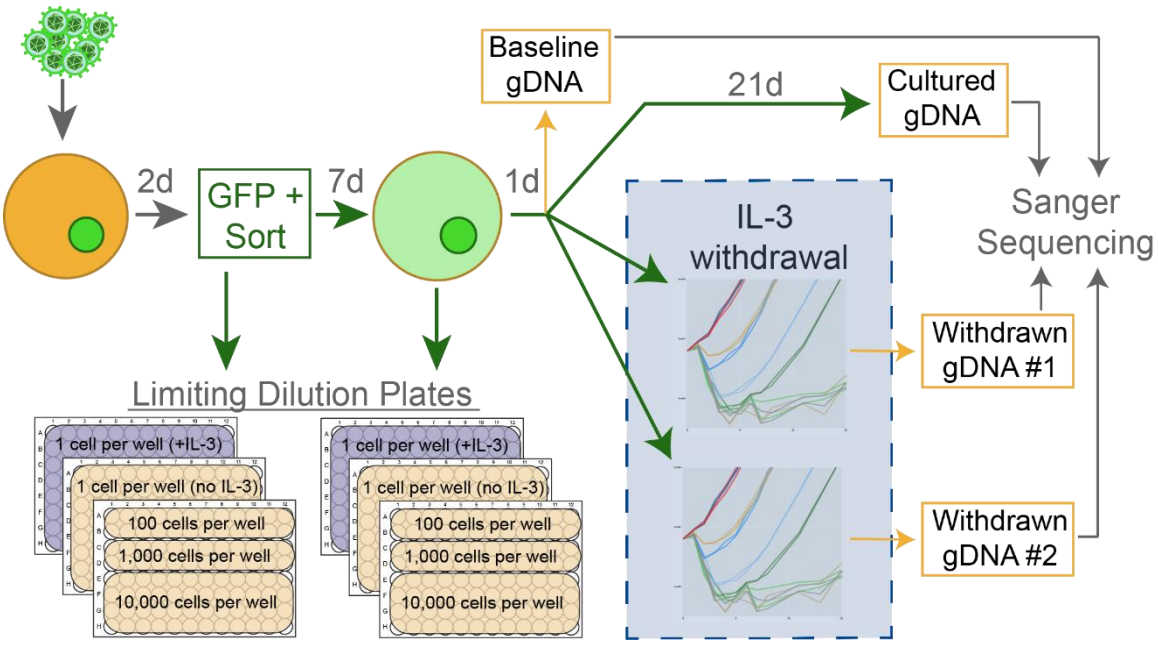

Figure 3-1 Experimental design schematic.

Ba/F3 cells are infected using freshly harvested retrovirus which drives the expression of GFP and the transgene of interest. Infected cells are selected for GFP-expression on day 2, and the first set of limiting dilution plates are created. On day 9 a second set of limiting dilution plates are started, and on day 10 the cells are triple-washed then monitored for IL-3 independent growth over 21 days in two technically replicate flasks. Genomic DNA (gDNA) is harvested from cell lines in IL-3 on day 10 (baseline) and day 31 (cultured). As cells proliferate in the absence of IL-3, gDNA is harvested to detect acquired mutations. This workflow was repeated for every construct to create a minimum of three biologically replicate lines.

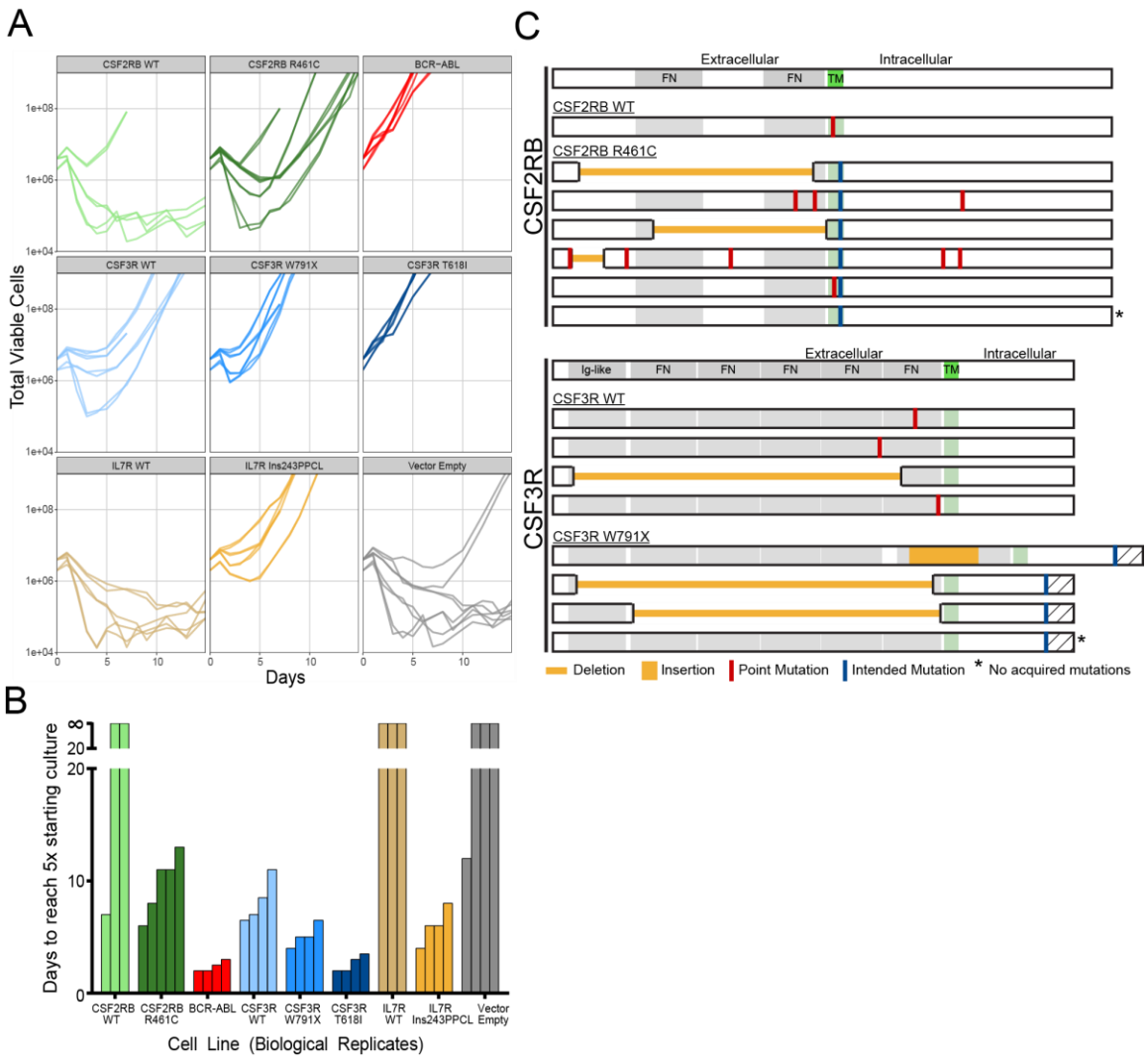

Figure 3-2 Compiled data from all IL-3 withdrawal experiments.

(A) Outgrowth curves for every replicate in this study, separated by transgene and mutation. The outgrown vector empty line was sequenced and found to be contaminated with IL7R Ins243PPCL. (B) Time to outgrowth can be summarized as the number of days to reach a viable cell count 5-times the number of cells initially seeded in each flask at the start of the experiment. Lines that did not grow within the 21-day period are shown above the break. (C) Mutations detected in outgrown lines after transformation to factor-independent growth. Every transformed line for CSF2RB WT, R461C and CSF3R WT, W791X are shown, including lines that did not acquire additional mutations (*).

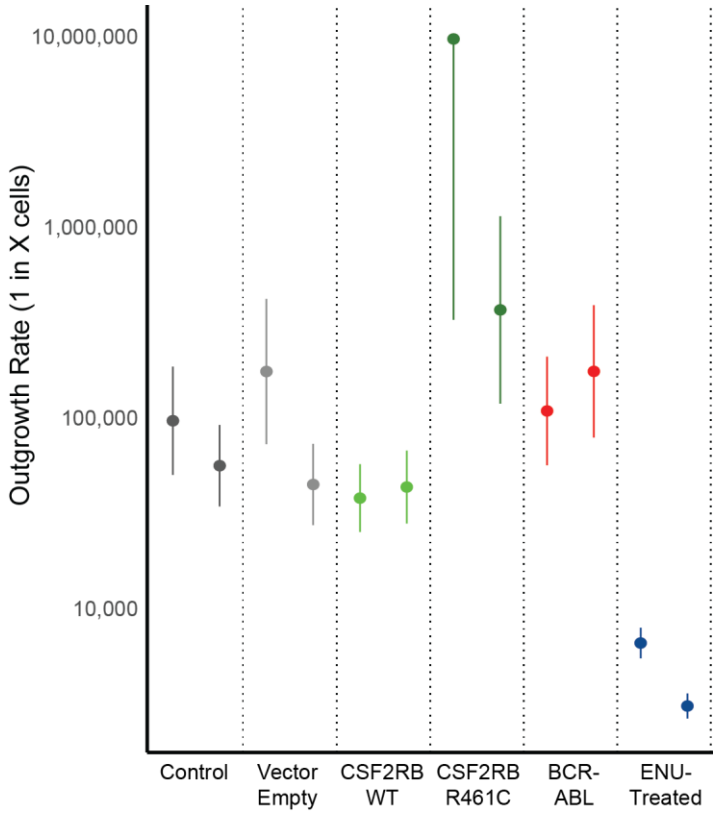

Figure 3-3 Ba/F3 cells expressing CSF2RB R461C do not demonstrate increased rates of mutagenesis.

Outgrowth rate and 95% confidence intervals are shown for biologically replicate lines. Outgrowth rate is expressed as 1 in X cells have mutationally inactivated HPRT to survive 6-TG treatment, thus a higher outgrowth rate indicates a less mutagenic condition. Mutagenesis induced by ENU-treatment was used as a positive control.

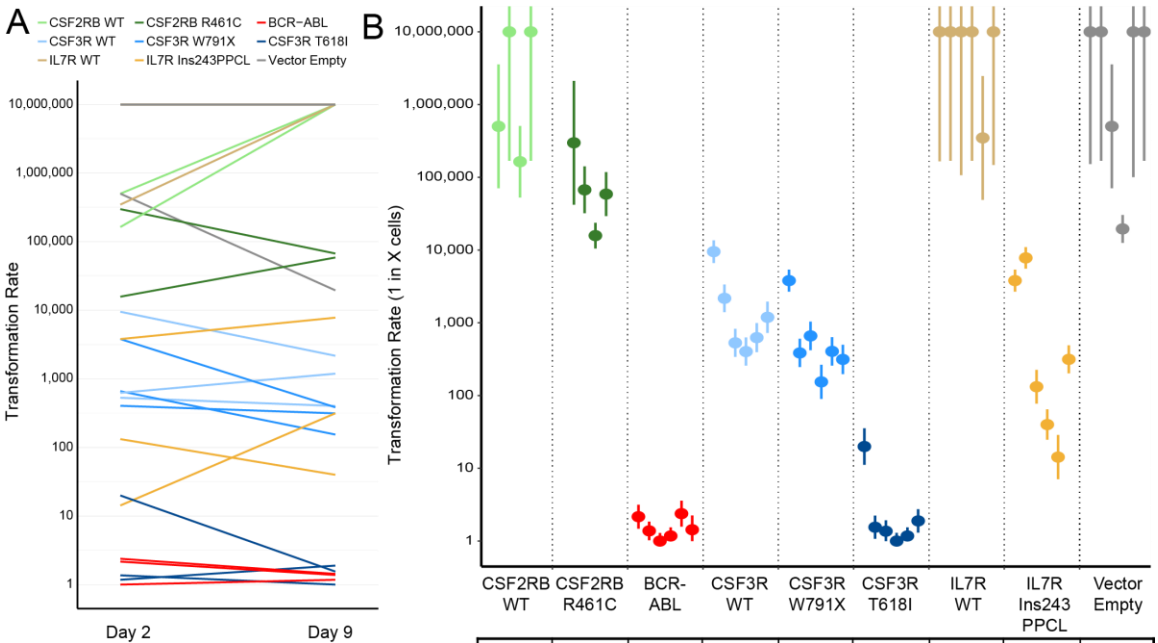

	CSF2RB WT	CSF2RB R461C	BCR-ABL	CSF3R WT	CSF3R W791X	CSF3R T618I	IL7R WT	IL7R Ins243 PPCL	Vector Empty
Median transformation rate	670,340	61,390	1.7	870	386	1.4	~1E7	118	~1E7
Transforming cell frequency	1.49E-6	1.63E-5	5.98E-1	1.15E-3	2.59E-3	7.03E-1	1.00E-7	8.50E-3	1.00E-7

Figure 3-4 Ba/F3 transformation rates vary by transgene but not by time in culture.

(A) Transformation rates calculated for each biologically replicate cell line are shown for plates started 2 days and 9 days after retroviral infection. The transformation rate is expressed as 1 in X cells capable of transforming to IL-3 independent growth, therefore a higher transformation rate indicates a weakly transforming cell line. No consistent trend is observed between days post-infection and transformation rate. (B) Transformation rate and 95% confidence intervals for every replicate. The median rates across biologically replicate samples are shown below, along with the frequency of transforming cells (inverse of transformation rate). Lines that exhibited no observable transformation are shown with a rate of $1.0x10^7$.

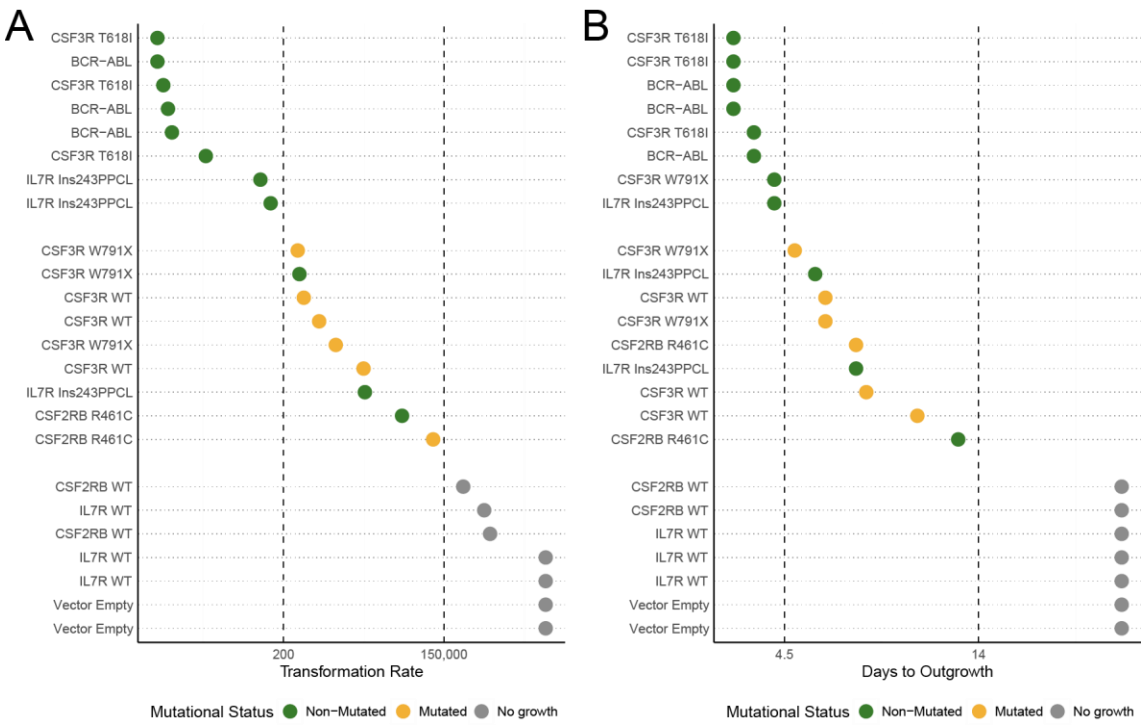

Figure 3-5 Acquired mutations occur in weak, but not strong, transforming transgenes.

(A) Cell lines are ordered by transformation rate and colored based on mutational status as observed from sanger sequencing of bulk outgrowth assays of the same lines. (B) Cell lines are ordered by days to outgrowth (time to reach a 5-times increase in viable cells over the starting cell number) and colored based on mutational status. BCR-ABL was not fully sequenced due to length and structural complexity.

3.8 Tables

Table 3-1 Frequency of sequence validation in Ba/F3 transformation studies (2014-2016)

Frequency of sequence validation in Ba/F3 transformation studies (2014-2016)	
Characteristics	PubMed Articles (%)
Publication Year	
2014	8 (33)
2015	9 (38)
2016	7 (29)
Search Term	
Ba/F3	23 (96)
Baf3	1 (4)
Method of transduction	
Retrovirus	12 (50)
Lentivirus	2 (8)
Electroporation	6 (25)
Unclear	4 (17)
Sequencing outgrown Ba/F3 lines	
Transgene sequence confirmed	0 (0)
Transgene not sequenced	24 (100)

Source: PubMed articles matching "Ba/F3" or "Baf3", published 2014-2016, and using Ba/F3 cells for the purpose to establish transformative potential of genetic products. Data current as of 10-26-16

Table 3-2 Complete table of studies using the Ba/F3 transformation assay (2014-2016) – Frequency of sequencing outgrown Ba/F3 lines.

Supplemental Table 1

Studies using the Ba/F3 transformation assay (2014-2016) – Frequency of sequencing outgrown Ba/F3 lines

PMID	Year	Journal	Title	Method of transduction	Sequenced transgene of outgrown lines
27672444	2016	Cell Discov	NTRK2 activation cooperates with PTEN deficiency in T-ALL through activation of both the PI3K-AKT and JAK-STAT3 pathways.	Retrovirus	No
27174491	2016	Leukemia	MEK and PI3K-AKT inhibitors synergistically block activated IL7 receptor signaling in T-cell acute lymphoblastic leukemia.	Electroporation	No
26854029	2016	Nat Commun	KRAS insertion mutations are oncogenic and exhibit distinct functional properties.	Retrovirus	No
26703895	2016	Exp Hematol	Ph-like ALL-related novel fusion kinase ATF7IP-PDGFRB exhibits high sensitivity to tyrosine kinase inhibitors in murine cells.	Retrovirus	No
26701727	2016	Oncotarget	Activating JAK1 mutation may predict the sensitivity of JAK-STAT inhibition in hepatocellular carcinoma.	Lentivirus	No
26630010	2015	PNAS	Augmentor α and β (FAM150) are ligands of the receptor tyrosine kinases ALK and LTK: Hierarchy and specificity of ligand-receptor interactions.	Retrovirus	No
26544513	2015	Oncotarget	Mutant HRAS as novel target for MEK and mTOR inhibitors.	Retrovirus	No
26455322	2016	Oncogene	PDGFRB mutants found in patients with familial infantile myofibromatosis or overgrowth syndrome are oncogenic and sensitive to imatinib.	Electroporation	No
26370156	2015	Cancer Discov	RICTOR Amplification Defines a Novel Subset of Patients with Lung Cancer Who May Benefit from Treatment with mTORC1/2 Inhibitors.	Unclear	No
26216197	2016	Leukemia	Contribution of JAK2 mutations to T-cell lymphoblastic lymphoma development.	Lentivirus	No
26206867	2015	Clin Cancer Res	EGFR Exon 18 Mutations in Lung Cancer: Molecular Predictors of Augmented Sensitivity to Afatinib or Neratinib as Compared with First- or Third-Generation TKIs.	Retrovirus	No
26040420	2015	Cell Mol Life Sci	PI3 kinase is indispensable for oncogenic transformation by the V560D mutant of c-Kit in a kinase-independent manner.	Retrovirus	No
25546157	2015	J Clin Endocrinol Metab	RET fusion as a novel driver of medullary thyroid carcinoma.	Unclear	No
25538044	2015	Blood	The thrombopoietin receptor P106L mutation functionally separates receptor signaling activity from thrombopoietin homeostasis.	Electroporation	No
25515960	2015	Blood	The role of the Janus-faced transcription factor PAX5-JAK2 in acute lymphoblastic leukemia.	Electroporation	No
25294908	2014	Clin Cancer Res	Identification of recurrent FGFR3-TACC3 fusion oncogenes from lung adenocarcinoma.	Retrovirus	No

PMID	Year	Journal	Title	Method of transduction	Sequenced transgene of outgrown lines
25193870	2014	Blood	JAK3 mutants transform hematopoietic cells through JAK1 activation, causing T-cell acute lymphoblastic leukemia in a mouse model.	Retrovirus	No
25146434	2015	Leuk Lymphoma	Identification of mutant alleles of JAK3 in pediatric patients with acute lymphoblastic leukemia.	Electroporation	No
24825865	2014	Blood	Integrated genomic sequencing reveals mutational landscape of T-cell prolymphocytic leukemia.	Unclear	No
24608088	2014	PLoS One	Activating FLT3 mutants show distinct gain-of-function phenotypes in vitro and a characteristic signaling pathway profile associated with prognosis in acute myeloid leukemia.	Unclear	No
24398328	2014	Blood	Germ-line JAK2 mutations in the kinase domain are responsible for hereditary thrombocytosis and are resistant to JAK2 and HSP90 inhibitors.	Retrovirus	No
24367893	2014	Leuk Res	Sensitivity of SNX2-ABL1 toward tyrosine kinase inhibitors distinct from that of BCR-ABL1.	Retrovirus	No
24315414	2014	Mol Oncol	Functional characterization of a novel FGFR1OP-RET rearrangement in hematopoietic malignancies.	Retrovirus	No
23752188	2014	Oncogene	PDGFRA alterations in cancer: characterization of a gain-of-function V536E transmembrane mutant as well as loss-of-function and passenger mutations.	Electroporation	No

Source: PubMed articles matching “Ba/F3” or “Baf3”, published 2014-2016, and using Ba/F3 cells for the purpose to establish transformative potential of genetic products. Data current as of 10-26-16

Table 3-3 Constructs used in this study

Constructs used in this study	
Gene	**Mutation**
CSF2RB	WT
CSF2RB	R461C
CSF3R	WT
CSF3R	T618I
CSF3R	W791X
IL7R	WT
IL7R	243InsPPCL
Empty Vector	n/a
BCR-ABL	BCR-ABL (p210)

Table 3-4 Sequence results of Ba/F3 lines from bulk withdrawal assays.

Sequence results of outgrown Ba/F3 lines						
Gene	Variant	Il-3 independent transformation	Baseline gDNA	Cultured gDNA	Withdrawn gDNA #1	Withdrawn gDNA #2
CSF2RB	WT	+	✓	n/a	V449E	V449E
		-				
		-				
	R461C	+	✓	n/a	Del H43-S417	Del H43-S417
		+	✓	n/a	K389R, YN420CS, R657G	K389R, YN420CS, R657G
		+	✓	n/a	Del S161-S438	100% - Del L30-M81 50% - T27T, P118T, G285R, L626L, E653K
		+	✓	✓	50% - F451S	50% - F451S
		+	✓	✓	✓	✓
CSF3R	WT	+	✓	n/a	S581C	S581C
		+	✓	✓	80% - E524K	80% - E524K
		+	✓	✓	50% - Del A33-P558	50% - Del A33-P558
		+	✓	✓	50% - T618I	50% - T618I
	T618I	+	✓	n/a	✓	✓
		+	✓	✓	✓	✓
		+	✓	✓	✓	✓
		+	✓	✓	✓	✓
	W791X	+	✓	n/a	Internal 111aa duplication (bounds unclear)	Internal 111aa duplication (bounds unclear)
		+	✓	✓	50% - E524K, 50% - Del L38-T609	50% - E524K, 50% - Del L38-T609
		+	✓	✓	✓	✓
		+	✓	50% - Del W187-I564	50% - Del L129-E622	50% - Del L129-E622
IL7R	WT	-				
		-				
		-				
		-				
	Ins243PPCL	+	✓	n/a	✓	✓
		+	✓	✓	✓	✓
		+	✓	✓	✓	✓
		+	✓	✓	✓	✓
Vector	Empty	+	✓	✓	Contamination: IL7R Ins243PPCL	Contamination: IL7R Ins243PPCL
		-				
		-				
		-				

✓ - Full transgene sequenced, no variants detected

Table 3-4 Sequence results of Ba/F3 lines from bulk withdrawal assays.

Sequence results of outgrown Ba/F3 lines from bulk withdrawal assays. Where a mixed read is evident (double peaks on Sanger trace) the estimated mutational burden is provided. This includes one cell line where Sanger sequencing detected a near-heterozygous deletion, alongside a point mutation within the deleted region on the non-deleted copy.

4 Materials and Methods

4.1 Patient samples and genomic analysis

Clinical samples were obtained with informed consent approved by the Institutional Review Boards of Oregon Health & Science University and Erasmus University Medical Center - Sophia Children's Hospital. Bone marrow or blood samples from patients with acute leukemia were separated using a Ficoll gradient followed by red blood cell lysis. Cells were cultured in RPMI-1640 medium (Invitrogen) containing 10% fetal bovine serum (FBS, Atlanta Biologicals), L-glutamine (Invitrogen), fungizone (Invitrogen), penicillin/streptomycin (Invitrogen), and 10^{-4}M 2-mercaptoethanol (Sigma).

Genomic DNA was isolated from cryopreserved patient sample material using Qiagen DNeasy columns. DNA was fragmented by sonication using an S2 Sonicator (Corvaris). Fragmented DNA was then processed according to the SeqEZ protocol (Nimblegen/Roche), which is based on the TruSeq protocol (Illumina). Solution capture was performed using a custom DNA probe capture library previously described[36]. The libraries were sequenced on a HiSeq 2000 sequencer (Illumina) followed by FASTQ assembly using the CASAVA pipeline (Illumina). Sequence capture, library preparation, and deep sequencing were performed by the OHSU Massively Parallel Sequencing Shared Resource.

Sanger sequencing of CSF2RB mutations was confirmed by PCR amplification of CSF2RB exons 10 and 11 using M13-tagged primers (Exon10&11F gtaaaacgacggccagCCCTGAGGTCGATTTCCC, Exon10&11R caggaaacagctatgaccGGACAGAGACAAGAGAGGCAG) followed by sequencing with M13 forward (GTAAAACGACGGCCAGT) and reverse (CAGGAAACAGCTATGACC) primers.

4.2 Cloning and construct creation

Human CSF2RB in the Gateway-compatible pENTR223 vector was ordered from the Harvard PlasmID repository (HsCD00073687). Variants were created using the QuikChange II XL Site-Directed Mutagenesis Kit (Agilent Technologies, Santa Clara, California). Constructs were cloned into destination vectors (pMXs-IRES-Puro, MSCV-IRES-GFP) using the Gateway LR Clonase II Enzyme (ThermoFisher Scientific, Invitrogen, Waltham, Massachusetts). Plasmids were grown in One Shot TOP10 Chemically Competent E. *coli* (ThermoFisher Scientific, Invitrogen) and purified using QIAprep Spin Miniprep Kit or Maxiprep Kit (Qiagen, Hilden, Germany). Concentrations of plasmid purifications were quantified using a Nanodrop ND-1000 (ThermoFisher Scientific). PCR amplification for sequencing used AccuPrime Taq DNA polymerase, high fidelity (ThermoFisher Scientific, Invitrogen) and a modified "slowdown PCR" thermocycler protocol[169]. Sequence confirmation of constructs was performed using Sanger sequencing

(Eurofins Genomics, Luxembourg, Luxembourg) and analyzed using LaserGene 14 Seqman Pro (DNASTAR, Madison, Wisconsin).

4.3 Cell Culture

Ba/F3 cells were obtained from ATCC and grown in filtered R10 + Wehi media (RPMI 1640 + L-Glutamine medium [Gibco 11875, ThermoFisher Scientific] with 10% Fetal Bovine Serum [Atlanta Biologicals, Flowery Branch, Georgia], 2% L-glutamine [200mM, ThermoFisher Scientific, Gibco], 1% penicillin-streptomycin [10,000 U/ml, ThermoFisher Scientific, Gibco], 0.1% Amphotericin B [250µg/ml amphotericin B, 205µg/ml sodium deoxycholate, ThermoFisher Scientific, Gibco], and 15% WEHI-conditioned media [a source of IL3]). During withdrawal assays, Ba/F3 cells were maintained in R10 media (same as R10 + WEHI but with no WEHI-conditioned media).

Ba/F3 cells were counted using Guava ViaCount (EMD Millipore, Billerica, Massachusetts) on a Guava Personal Cell Analysis flow cytometer (EMD Millipore) or Muse Cell Analyzer (EMD Millipore). Cells were split to concentrations of $1x10^5$-$3x10^5$/ml every 1-3 days.

293T/17 cells were grown in D10 media (Dulbecco's Modified Eagle Medium [DMEM, Gibco 11995, ThermoFisher Scientific] with 10% FBS, 2% L-glutamine, 1% penicillin-streptomycin, 0.1% Amphotericin B). Cells were split prior to reaching confluence every 2-4 days using Trypsin-EDTA (0.05%, ThermoFisher Scientific, Gibco) and Dulbecco's phosphate-buffered saline (DPBS, ThermoFisher Scientific, Gibco) to 5-15% confluence.

4.3.1 Ba/F3 transformation assay

Ba/F3 transformation assays were performed either by electroporation followed by puromycin selection, or retroviral infection followed by GFP-positive FACS isolation. In each case the method of selection matches the selectable marker on the vector used. For experiments discussed in Appendices A & B, some lines were infected by retrovirus with puro-selectable vectors, and thus selected by puromycin selection.

4.3.1.1 Electroporated lines

2.5e7 Ba/F3 cells were electroporated in a 0.4mm GenePulser Cuvette (Bio-Rad, Hercules, California) at 300V for two 25ms pulses (GenePulser MXcell, Bio-Rad) with 40µg of plasmid. Stably transfected cells were selected using two weeks of continual 2µg/ml puromycin dihydrochloride selection (ThermoFisher Scientific, Gibco) in R10 + WEHI media.

4.3.1.2 Retrovirally infected lines

Retroviruses were created by transfecting plasmids into 293T/17 cells along with the pIK6.1MCV.ecopac.UTD helper plasmid using FuGENE 6 transfection reagent (Promega, Madison, Wisconsin). After confirming GFP expression in 293T/17 cells by confocal microscopy 72 h post-transfection, viral supernatant was harvested and filtered. 1ml Fresh virus was added to $1.5x10^6$ Ba/F3 cells in 1ml R10 + Wehi, with 30µl 1M HEPES (ThermoFisher Scientific, Gibco) and 2µl polybrene (10mg/ml Santa Cruz Biotechnology,

Dallas, Texas) prior to spin inoculation at 1500rcf for 90 min at 37°C. Following spinoculation, cells recovered for 4 h at 37°C 5% CO_2, and underwent a second spinoculation to ensure high rates of infection (1ml media removed, 1ml fresh viral supernatant added, spin). Cells recovered in R10 + WEHI media. 48 h post-infection, infected Ba/F3 cells were resuspended in R10 media[26] and then selected by GFP-positive fluorescent activated cell sorting (BD FACSAria IIIu, ThermoFisher Scientific, BD Biosciences).

4.3.1.3 IL-3 withdrawal

Selected Ba/F3 cells were split 24 h prior to factor withdrawal to ensure cells were in exponential growth. Cells were counted, pelleted and resuspended 3 times in RPMI-1640, pelleted again and resuspended in R10 media at $4x10^5$/ml. Withdrawn lines were counted daily for 1 week, and then every 2 days for 2 additional weeks. Additional R10 media was added to cultures as necessary to support growth (target concentrations $1x10^5 – 5x10^5$ cells/ml).

4.3.2 Genomic DNA extraction and Sanger sequencing

For extraction of genomic DNA, $1x10^6$ cells were pelleted, flash frozen in liquid nitrogen, and stored at -80°C. Genomic DNA was extracted using DNeasy Blood and Tissue Kit

[26] This step is necessary to remove exogenous WEHI-CM from the limiting dilution plates created immediately after sorting.

(Qiagen) and quantified on a Nanodrop ND-1000. Transgenic DNA was amplified using vector specific primers (MigFwd – CCCTTTGTACACCCTAAGCCTCCGCC, MigRev – GGAAAGACCCCTAGAATGCTCGTCAA) and AccuPrime Taq with a slowdown PCR protocol. Sanger sequencing was performed (Eurofins) and analyzed (LaserGene) as described above.

4.3.3 Protein lysis and immunoblot

For protein lysis, $5x10^6$ cells were pelleted, washed in DPBS, pelleted and flash frozen before storage at -80°C. Lysis was performed by addition of 1x Cell Lysis Buffer (Cell Signaling Technologies, Danvers, Massachusetts), 10% phenylmethylsulfonyl floride (Sigma-Aldrich, St. Louis, Missouri), 10% Phosphatase Inhibitor Cocktail 2 (Sigma-Aldrich), and 1x cOmplete, Mini, EDTA-free Protease Inhibitor Cocktail (Roche, Sigma-Aldrich). Protein concentration was quantified using the Bradford-based Protein Assay Dye Reagent (Bio-Rad) measured relative to a standard curve.

Prior to loading, protein lysis was mixed with a loading dye (final solution: 2% SDS, 50mM Tris (pH 6.8), 10% glycerol, 360µg/ml bromophenol blue) and 2-mercaptoethanol (final concentration 0.38mM). Lysates were heated at 95°C for 10 min, spun down and loaded in Criterion Precast Gels (4-15% gradient, Tris-HCL, Bio-Rad). SeeBlue Pre-stained Protein Standard was used for a molecular ladder (ThermoFisher Scientific, Invitrogen). Electrophoresis was performed at 190V for 55 min (PowerPac HC power supply, Bio-Rad; CRITERION Cell, Bio-Rad). Transfer to methanol activated Imobilon-P PVDF membrane

(EMD Millipore) was performed overnight with 0.1% SDS, 20% methanol transfer buffer in a Criterion Blotter (Bio-Rad) at 20V.

Membranes were blocked for 1 h while shaking in 5% bovine serum albumin (BSA, Sigma-Aldrich) then probed with primary antibodies listed in Table 2-2 overnight at 4°C while shaking. Membranes were washed 3x in TBST, probed with HRP-conjugated secondary antibodies in 5% BSA for 1 h, washed again and then visualized using Clarity Western ECL Substrate (Bio-Rad) on a ChemiDoc MP Imaging System (Bio-Rad) with the Image Lab Software (version 5.1, Bio-Rad).

Immunoprecipitations were performed with 500µg protein and anti-CSF2RB or rabbit IgG isotype control overnight at 4°C before adding BSA-blocked protein A-sepharose 4B conjugate beads (ThermoFisher Scientific, Invitrogen). Input, unbound, and bound samples were mixed with loading dye and handled as above.

Non-reducing immunoblots were run as above but without addition of 2-mercaptoethanol in the loading dye, and modification of sample boiling prior to loading as indicated (Figure 2-7).

4.3.4 Cycloheximide timecourse

Ba/F3 cells were treated with 100µg/ml cycloheximide in DMSO for the indicated times before washing in DPBS with 0.5% FBS and staining for 45 minutes with PE-conjugated

anti-CSF2RB antibody. Cells were analyzed by flow cytometry (BD FACSAria IIIu and BD LSR II) for mean fluorescence intensity and normalized to untreated controls.

4.3.5 Flow cytometry staining for CSF2RB

As above, cells were washed in DPBS with 0.5% FBS and stained for 45 minutes with PE-conjugated anti-CSF2RB antibody, then analyzed by flow cytometry for percent positivity and mean fluorescence intensity.

4.3.6 Small molecule inhibitor screen

A library (previously described[121]) of 104 small-molecule kinase inhibitors across three 384-well plates was used to determine inhibitors that specifically inhibited the growth of R461C-expressing cells. Cells were maintained in their culture media, where only WT cells were supplemented with 15% WEHI-conditioned media. Cells were plated at 400 cells per well in 50µl total volume (8,000 cells per mL) and incubated for 3 days at 37°C, 5% CO_2 and then subjected to a CellTiter 96 AQ_{ueous} One solution, tetrazolium-based, cell proliferation assay (Promega). All values were normalized to cells incubated in the absence of drug and IC_{50} values were calculated from the resulting kill curves of each drug gradient. Biologically replicate WT and R461C lines were run on this assay, with R461C-specific drugs identified as drugs with the largest percent difference in IC_{50} between WT and R461C cells.

4.3.7 Drug curves and Annexin-V readouts

Individual drug curves for JAK-inhibitors were plated using an HP D300 Digital Dispenser (Hewlett-Packard, Palo Alto, California) with conditions matching those in the screen above. Plates were analyzed after 3 days using CellTiter 96 AQ_{ueous} One solution (Promega). Annexin-V staining was determined using Guava Nexin Reagent and a Guava Personal Cell Analysis cytometer (EMD Millipore).

4.3.8 6-thioguanine survival assay

Ba/F3 cells were cultured in HAT-supplemented media (100μM sodium hypoxanthine, 0.4μM aminopterin, 16μM thymidine, Gibco) for 4 days to select for HPRT-expressing cells. Cells were then allowed to recover for 5 days in HT-supplemented media (100μM sodium hypoxanthine, 16μM thymidine, Gibco) prior to culturing in regular R10 + WEHI media. Ba/F3 cells were infected with retrovirus 14 days prior to 6-TG exposure. Positive control cells were treated overnight with 50μg/ml ENU 6 days prior to 6-TG exposure. Biologically replicate lines were screened for 6-TG survival in the following conditions: 2 96-well plates seeded at 1 cell per well without 6-TG (plating efficiency calculations), 2 96-well plates at 1000 cells per well with 20μM 6-TG, and 2 96-well plates at 5000 cells per well with 20μM 6-TG. Wells were visually assessed for growth 14 days later and the number of cells surviving through HPRT-inactivation was determined using ELDA.

4.3.9 Limiting dilution plates

Cells were counted and resuspended in IL-3 free media prior to dilution. Each line was seeded on three plates, 1 cell/well in R10 + WEHI, 1 cell/well in R10, and a final R10 plate with 24-wells at 100 cells/well, 24-wells at 1,000 cells/well, and 48-wells at 10,000 cells/well. Plates were prepared with media (180µl/well for 1 cell/well plates, 100µl/well for other plates) using a Multidrop Combi reagent dispenser (ThermoFisher Scientific). Cells were diluted to 1 cell per 20µl, then added to 1 cell/well plates using the Multidrop Combi dispenser. For the final plate, cells were diluted to desired number of cells per 100µl, and then 100µl was added to each well using a multidrop pipette.

Plates were visually inspected once a week for three weeks to identify growing wells. Suspicious growths were inspected microscopically and contaminated wells were censored from final analysis in R (described below).

4.4 Computational analysis and modeling

4.4.1 Statistical analysis

Statistically significant differences for cycloheximide timepoints, CSF2RB MFI, and differences in IC_{50} to targeted inhibitors were calculated by an unpaired Student's t-test using Prism (version 6, GraphPad, La Jolla, California).

4.4.2 Transmembrane domain prediction

Consensus coding sequences for wildtype and R461C CSF2RB were analyzed by the indicated modeling programs (websites and references in Figure 2-6). Top predictions that maintained a single transmembrane domain and type-I orientation are listed.

4.4.3 Multiple sequence alignment

The sequence for human CSF2RB on UniProt (P32927)[99] was BLAST searched against proteins in other species. Nine additional genes were selected for percent similarity with the human sequence (ideally 60-80% matched) and for a variety of genetically diverse species. Once selected the group of genes was not altered, even though the bovine genome did not match other species at arginine-461 (Figure 2-2). Alignment performed using CLUSTALO, 25.2% of positions were identical.

4.4.4 Extreme limiting dilution analysis

All analysis for limiting dilution plates was performed using R (version 3.3.2) and the elda() function in the statmod package (version 1.4.26)[163]. 1 cell/well R10 + WEHI plates were used to calculate plating efficiency in the R10 plates. The estimated frequency of transforming cells and 95% confidence intervals are presented (Figure 3-4).

4.4.5 Meta-literature review

PubMed searches were performed on October 26, 2016 for all studies matching the terms "Ba/F3" or "Baf3" and published between 2014 and 2016. Abstracts were read to identify

studies using Ba/F3 cells for the purpose of establishing the transformative capacity of a gene product. Every study fitting these criteria was included in the final analysis.

The methods in relevant studies were read, as well as the full text searched for terms including "sequence", "sequenced", or "sequencing" and then read for context to determine if transgenes in cells were sequenced following transformation. Method of introducing the transgene to Ba/F3 cells (viral, electroporation) was also determined by reading methods and searching for terms.

5 Conclusions and Future Directions

The identification and characterization of rare, activating mutations in individual cancers is a necessary step towards a future of personalized, targeted therapy. This includes both the work on characterizing the transformative capacity of individual mutations and work towards improving the reliability and speed of models used to test mutations. The data presented in this dissertation contributes to this knowledge base and to the continued basic research of characterizing the receptor CSF2RB.

5.1 Identification of R461C as the first CSF2RB-activating mutation in humans

CSF2RB R461C is a transmembrane domain variant found in the germline of a pediatric T-ALL patient. This variant results in ligand-independent signaling and receptor stabilization *in vitro*, and is sensitive to JAK-inhibitors. Given the wide range of roles CSF2RB serves hematopoietic regulation, it is surprising that this represents the first report of an activating mutation in CSF2RB; the only other functional CSF2RB variants reported in humans are loss-of-function mutations resulting in pulmonary alveolar proteinosis. This is particularly striking given CSF2RB R461C is a germline variant found in the general population.

5.1.1 CSF2RB R461C is a rare, germline variant

CSF2RB R461C is reported as a SNP (rs371045078) with a minor allele frequency less than 0.0003. The 1000 genomes project reports 5 individuals heterozygous for R461C worldwide, 4 of those are of South Asian descent[27][112]. Similarly, the Exome Aggregation Consortium (ExAC) reports 33 heterozygous individuals, 18 of South Asian descent[28][113]. A cohort of 103 Gujarati Indians[29] living in Houston, Texas have submitted samples for whole genome sequencing as part of the HapMap project. 3 of those 103 individuals are heterozygous for R461C, which represents the only known population highly enriched for this variant[113]. There is no data indicating the frequency of CSF2RB R461C in leukemia as prior studies have filtered out germline mutations that were not previously described as functional[114].

As of yet there is no evidence that individuals carrying CSF2RB R461C are at increased risk for leukemia or present with any other hematological abnormalities. Epidemiological investigation of enriched populations would provide a better understanding of the impacts of this variant. Additionally, studies involving the whole genome sequencing of leukemia patients should modify their germline variant exclusion criteria for CSF2RB R461C.

---

[27] South Asian MAF = 0.004, 978 individuals
[28] South Asian MAF = 0.0011, 8,248 individuals
[29] South Asian Indians with ancestry to the Gujarat region in northwest India. Individuals in this cohort were self-identified as Gujarati (3 of 4 grandparents were Gujarati), and no attempts were made to clarify that status[170].

The characterization of this variant supports additional investigation into the clinical relevance of CSF2RB-targeted therapeutics. No small-molecule inhibitor exists for CSF2RB, and for 15 years the only monoclonal antibody that targeted CSF2RB was BION-1, which suffered from low-affinity[171]. A recent publication detailed a new human monoclonal antibody, CSL311, with picomolar affinity for CSF2RB and inhibiting signaling from all 3 CSF2RB ligands. Future research should determine whether CSL311 can block ligand-independent growth in CSF2RB R461C transformed cell lines and represents an improvement on JAK-inhibitors.

5.1.2 The implications of CSF2RB R461C for basic research

The exact mechanism by which R461C drives ligand-independent signaling in CSF2RB is unclear. The novel cysteine may participate in intermolecular disulfide bonds, resulting in CSF2RB dimers, or the disruption of the charged arginine near the transmembrane boundary may activate signaling even in the absence of disulfide bonds. Considerable research and discussion towards this concept is detailed in Appendix A. My working hypothesis is that R461C activates CSF2RB through the loss of the positively-charged arginine near the membrane-spanning boundary and that the novel cysteine is unnecessary for receptor activation. Additional investigation is required to test this hypothesis and determine the nature of the intermolecular disulfide-bonded complexes observed in Figure 2-7, which could still be a result of CSF2RB activation.

The role of the CSF2RB transmembrane domain in receptor oligomerization is poorly understood. Indeed, even the boundaries of the transmembrane domain remain undefined with the modeling performed in this dissertation standing as the most thorough investigation to date (Figure 2-6). The characterization of R461C and other CSF2RB-activating, transmembrane domain mutations found *in vitro* are tools for future research into the role the transmembrane domain plays in CSF2RB signaling. Of particular interest is the possibility that CSF2RB R461C is incapable of interacting with CSF2RA, as proposed based on observations in Appendix B. I hypothesize the CSF2RA G343D variant (described in Appendix B) constitutively dimerizes and activates CSF2RB signaling, but fails to do so with CSF2RB R461C. These variants give binary positive and negative controls for future mutational-based experiments modeling the intramembrane orientation of activated CSF2RB and CSF2RA transmembrane domains.

5.2 The continued use of the Ba/F3 transformation assay

Using Ba/F3 cells to screen for gene products driving factor-independent growth has been, and remains, an essential assay for cancer researchers. This dissertation covers the potential of this assay to test the functionality of cancer mutations but also raises concern that this method is susceptible to the previously unreported tendency of acquiring mutations in the transgene of interest. As the research community continues to characterize mutations found within the long tail of cancer we will need to determine what relevance weak transforming mutations have for patients.

5.2.1 Acquired mutations in transformed Ba/F3 cells

The discovery that Ba/F3 cells expressing activating variants of CSF2RB and CSF3R frequently acquire additional mutations in the transgene of interest during the course of a transformation assay raises concerns of scientific reproducibility. Short of reproducing every study using the Ba/F3 assay, it is impossible to determine how many findings could be affected by this phenomenon. From 2014-2016[30] there have been 142 studies mentioning Ba/F3[31], and during a literature review I determined that 24 of these made use of Ba/F3 cells to determine the transforming potential of a gene product (Table 3-1, Table 3-2). However, several additional studies used transformed Ba/F3 cells to test therapeutic inhibitors, and these lines could also carry acquired mutations.

Beyond the risk for incorrect conclusions from flawed experiments and the lost time of researchers, these mutations could have outsized impacts on drug development. In 2007, Novartis published a panel of kinase-activated Ba/F3 cells they use to characterize kinase inhibitor specificity[46]. If these cell lines acquired additional kinase mutations during the course of outgrowth, then hundreds of inhibitors could be tailored towards artificial targets. This would be unlikely to affect patients as these errors would be corrected for in higher model systems, but the inefficient use of finances and researcher effort could be detracting from other targets.

---

[30] As of 10-26-16 when the review was performed
[31] Or the similar, though incorrect, "Baf3"

Acquired mutations are most likely the result of using retroviruses for the infection of Ba/F3 cells, but there is insufficient evidence to determine if plasmid electroporation reduces mutations. Additional studies should compare retroviral and lentiviral infection against electroporation and lipofection to determine if a particular transfection method results in an improvement of assay fidelity. The use of CRISPR targeting would be problematic in Ba/F3 cells, both because it is difficult to scale and because every human mutation would need to be translated to a murine equivalent that might not represent the original variant. The Ba/F3 assay would also benefit from the investigation of basic scientists to develop effective methods for reliably transfecting Ba/F3 cells.

Further investigation will determine if mutations acquired during Ba/F3 transformation represent independently transforming mutations, functional mutations that synergize with the original variant, or inconsequential passenger mutations. While this represents a substantial undertaking, constructs would be created carrying either the original variant, the acquired mutation, or both and then tested for transformation rate by limiting dilution analysis. Limiting dilution transformation rate would be preferred here as the results are minimally influenced mutational subpopulations. Should only one mutation transform and not the other, the conclusion would be clear as to which is oncogenic. If, however, the combination of mutations transforms at a higher rate, then the synergistic interaction of these mutations would allow for a fascinating investigation into protein function and compound mutations in cancer.

It is possible that these mutations are limited, confined to only CSF2RB, CSF3R and a few other cytokine receptors[32]. To determine the actual breadth of this artifact, additional studies must be performed on a wider range of oncogenes. These studies, if similarly constructed to those used in this dissertation, could also determine how robust the correlation is between mutational gain and transformation rate. If acquired mutations are a frequent artifact, but confined to weak transforming mutations, then the field faces a different set of challenges; namely, what does it mean for a mutation to be weakly transforming?

5.2.2 Relevance of weak transforming mutations

CSF2RB R461C, a germline variant discovered in a pediatric patient with T-ALL, is a weakly transforming mutation providing factor independence to roughly 1 in every 60,000 infected cells (Figure 3-4), an order of magnitude above WT CSF2RB. What remains unclear is whether CSF2RB R461C has any functional impact on the patient's leukemia. The patient's leukemic blasts contained somatic mutations in Notch1 and PTEN (Table 2-1), both recurrent and leukemia-associated mutations. These mutations likely represent the driving mutational events in this leukemia, though CSF2RB R461C could contribute to signaling through the PTEN-regulated PI3K/AKT pathway. CSF2RB R461C could also be

[32] One study reported IL9R mutants that, following transition to IL-9-supplemented media and then weaning to cytokine-free media, could result in factor-independent Ba/F3 cells. 80% of these clones acquired activating mutations in endogenous JAK1[167]. This is a dramatically different type of experiment than those described above, but could result in a similar phenotype.

one of a growing group of cancer-predisposing, germline variants found in over 1% of the general population[33][114], though that conclusion would require further epidemiological research. This all leads to the question of how to interpret the discovery of weak transforming mutations.

In the course of this work variants that result in transformation rates of less than 1 in every 200 cells have been classified as "weak" based on the stratification of rates observed and the frequency of acquired mutations in this group. This is an arbitrary threshold and additional research would determine if more robust thresholds exist. Based on this classification, CSF2RB R461C, CSF3R W791X and IL7R Ins243PPCL could be considered weak transforming mutations[34]. Prior research has established functional impacts for all three of these variants *in vitro*[36, 100, 115, 119, 161, 162]. More importantly, CSF3R truncations are frequently observed in CNL/aCML patients[36], and expression of truncated forms of CSF3R are linked with pediatric MDS and AML[172]. IL7R mutations altering the number of cysteines near the transmembrane domain are a recognized driving event in pediatric T-ALL[173]. While it is unclear whether every weakly transforming mutation has translational relevance, weak transforming mutations also cannot be simply dismissed as model system artifacts.

---

[33] These germline variants are enriched to over 8% in pediatric cancer patients

[34] CSF3R WT also lands in this classification. This is important to consider as the baseline potential for CSF3R to transform Ba/F3 cells, however it's not relevant to think of a WT gene product as a transforming variant but rather a proto-oncogene. CSF3R W791X appears to still show a functional advantage as it transforms cells at double the rate observed in CSF3R WT.

Instead, the question of why some mutations are weakly transforming requires additional investigation. Why does a mutation like CSF2RB R461C or IL7R Ins243PPCL provide factor-independent growth to only 1 in 60,000 or 1 in 100 cells, and not the 1 in every 2 cells observed with CSF3R T618I? One possibility is that the weaker mutations extend cell viability after IL-3 withdrawal long enough for additional mutational events to occur and transform the cells. While the data presented does not rule out this possibility, it does demonstrate that the expressed transgene does not undergo additional mutagenesis following IL-3 withdrawal (Table 3-4).

Another explanation is that weak transforming mutations require highly favorable circumstances to drive factor-independent growth. This could be high expression of the transgene, a requirement for cells to be in a specific metabolic or cell cycle state when IL-3 is withdrawn, or a requirement that certain regulators of cell signaling are expressed at a specific level. These factors could be experimentally tested by individually controlling for transgene expression or cell cycle status prior to withdrawal but the experiments would be open-ended and time consuming.

Another final explanation is that the signals generated by CSF2RB, IL7R or some CSF3R variants differ from the pathways that maintain Ba/F3 viability in IL-3 culture. This change in signaling mechanisms would require the cell to alter expression of signaling members or regulators of this new pathway, and only a small proportion of cells are capable of living long enough to complete this change. Or in terms of Waddington's epigenetic landscape,

there is a large hill or barrier between the state of Ba/F3 cells growing in IL-3 and those capable of surviving on the new oncogene. This theory of pathway transition lag is supported by the findings that FLT3 and KIT-activated Ba/F3 cells demonstrate differing phenotypes when cultured in presence or absence of IL-3[164]. These strong oncogenes, when cultured 1-2 weeks without IL-3, increase phosphorylation of the transgenic receptor, are more proliferative, and grow faster in cytokine-free media[164].

However, this pathway transition hypothesis is problematic in the case of CSF2RB R461C, which results in constitutive activation of the receptor responsible for IL-3 signaling, seemingly not a substantial change in pathways. This theory could be tested by comparing expression profiling of weak transformants and strong transformants both before and after achieving factor-independent growth. While not fully conclusive, a theoretical finding that CSF3R T618I and BCR-ABL minimally alter gene expression following factor withdrawal compared with large-scale changes in CSF3R W791X or CSF2RB R461C would support this hypothesis.

Regardless of the nature of weak transforming mutations, the field would greatly benefit from implementing limiting dilution analysis as a standard part of the Ba/F3 transformation assay. The data generated is inherently more quantitative than flask-based culture assays and less susceptible to skewing by a minority population of cells. Additionally, if every study describing a Ba/F3 transforming mutation included a transformation rate then the field could develop robust classifiers for weak and strong transforming mutations. Eventually,

this would answer the question of what role do weak transforming mutations play in individual patients.

5.3 Summary

Targeted therapy in cancer has been a remarkable achievement of modern medicine, and to extend this treatment to all cancer patients will require a comprehensive understanding of both common and rare functional mutations in each patient. The work described here showcases the role Ba/F3 transformation assays play in the discovery of functional mutations in leukemia and presents suggestions to improve this assay in the future.

CSF2RB R461C is a rare germline variant found in a pediatric patient with T-ALL. *In vitro,* this variant transforms cells to factor-independent growth through activation and stabilization of CSF2RB. While it is not clear what role CSF2RB R461C plays in patients, the signal could be blocked by JAK-inhibitors making this a potentially actionable mutation. CSF2RB R461C is observed in an estimated 2.9% of individuals in one population of South Asian Indians, which represents an opportunity for further epidemiological research.

Additionally, the finding that the transmembrane R461C activates CSF2RB, and leads to potentially altered interactions with CSF2RA, should spur on basic research into the CSF2RB transmembrane domain. It appears that R461C does not activate CSF2RB through the inclusion of a novel cysteine but rather through the loss of a positively charged arginine

at the transmembrane domain border, indicating that this domain may have a larger role in CSF2RB activation than previously understood.

During the course of characterizing CSF2RB R461C, the frequent tendency for Ba/F3 cells to acquire additional mutations in CSF2RB during the factor withdrawal assay was also observed. This observation was repeated in additional experiments including other receptor activating mutations. The presence of acquired mutations in the Ba/F3 assay could affect an entire field of studies screening for functional mutations in cancer. These effects could be as severe as false positive reports and mischaracterized kinase inhibitors, or as minor as improper characterization of downstream signaling pathways.

The data from these experiments indicate that acquired mutations are largely confined to weak transforming mutations, an ambiguous term that while useful should be refined by further studies into this phenomenon. Additional research should also determine if using non-viral methods for transgene expression reduce the incidence of these acquired mutations.

The Ba/F3 transformation assay would be substantially improved by two changes. First, every transformed Ba/F3 cell line should be sequenced for the full length of the transgene of interest. This step is simple, affordable, and would reduce the potential of publishing irreproducible results. Second, researchers should adopt limiting dilution assays of Ba/F3 cells when characterizing transforming mutations, and then report rates of transformation.

It is unclear at this time what relevance a mutation's rate of transformation has on disease, but that question will only be answered by additional data on a wide range of mutations.

This dissertation represents one study conducted in the pursuit of understanding the functional impact of rare mutations in cancer. To fully understand and target each individual cancer, hundreds more studies will be conducted. These will include the identification and characterization of rare mutations, like CSF2RB R461C, as well as modifications and improvements on the methods used in that pursuit. The Ba/F3 transformation assay remains a flexible, essential, and robust model for characterizing activating mutations, but future researchers should be receptive to adopt improvements and consider the implications of weak transforming mutations. As researchers continue to characterize variants in the long tail of cancer-associated mutations, this question of weak but reliably transforming mutations will become even more pressing and relevant.

6 Appendix A: Alternate CSF2RB mutations at residue 461

6.1 Background

A germline SNV in CSF2RB coding for the R461C substitution was found in a pediatric T-ALL patient[100]. *In vitro,* this variant results in ligand-independent signaling, increased receptor stability, and the formation of novel, high molecular weight, disulfide-linked complexes[100]. Mutations in other receptors that alter the number of cysteine residues in and around the TM domain have been shown to result in ligand-independent activation through the creation of disulfide-linked dimers[64, 119, 120]. Accordingly, it would seem likely that the R461C variant activates signaling by inducing novel disulfide-linked dimers.

Alternatively, the hydrophilic arginine replaced in R461C appears to lie at the boundary between membrane-spanning and cytoplasmic residues (Figure 2-6), and the loss of a charged residue could alter the position or configuration of the transmembrane domain and activate downstream signaling. The observation of larger, disulfide-linked complexes (Figure 2-7A) could be the result of either an accumulation of CSF2RB on the cell surface (Figure 2-5), or of ligand-independent activation (Figure 2-7B).

Ultimately, the role or importance of a cysteine at position 461 has not been determined. Understanding the mechanism and cause behind this receptor-activating variant is important as it will allow us to predict the functional impact of other possible mutations in the same region of CSF2RB. A few experiments were conducted to address this question but

ultimately did not prove conclusive or relevant enough for either manuscript detailed in this dissertation, and I present them here.

6.2 Results

Two additional CSF2RB constructs—R461A and R461S—were cloned into a pMXs-IRES-Puro vectors using site-directed mutagenesis. The former mimics the loss of both a hydrophilic residue and bulky side-chain, while the latter contains an uncharged polar residue similar in size to cysteine. These constructs would be compared to R461C to determine if receptor function was altered.

When tested in a Ba/F3 transformation assay, all 3 biologically replicate lines expressing R461A and R461S achieved factor-independent growth at rates similar to those observed in R461C (Figure 6-1). Given the capacity for CS2RB WT to occasionally transform through the acquisition of additional mutations, this result alone was not proof that R461A/R461S activated receptor signaling. However, CSF2RB WT results in successful transformation in 50% or fewer of tested lines, therefore the 100% success of R461A/R461S (6/6) behaves more similarly to R461C. Genomic DNA extracts were taken from these outgrown lines but sequencing was never performed. In theory, sequencing data could indicate if these lines transformed through the acquisition of mutations commonly found in transformed CSF2RB WT lines (e.g. V449E), but even a finding of divergent mutations similar to those in CSF2RB R461C would still not address the underlying hypothesis.

Another phenotype observed in CSF2RB R461C expressing cells was the increased level of surface CSF2RB. Ba/F3 cells stained for surface hCSF2RB prior to factor withdrawal showed that while equivalent portions of each line were expressing hCSF2RB, R461C cells reliably had substantially higher mean fluorescent intensities (MFIs, Figure 2-5). This data was further supported by Western blots that also showed increased hCSF2RB expression in R461C cells compared to WT (Figure 2-3B).

Ba/F3 cells infected with CSF2RB R461A or R461S were compared to R461C and WT expressing cells by FACS after staining for surface hCSF2RB. All four lines had comparable percentages of cells expressing hCSF2RB, indicating similar infection efficiency (Figure 6-2A). The portion of cells stained for CSF2RB were compared by MFI, and R461A/R461S showed MFIs comparable with R461C and significantly greater than WT (Figure 6-2B). While this would suggest that the cysteine is not essential for receptor surface accumulation there were insufficient WT replicates to firmly make this conclusion. However, the trend between R461C and WT observed in this experiment is consistent with other experiments (Figure 2-5), suggesting that this single WT observation is not an outlier.

6.3 Discussion

Changing the cysteine in R461C to an alanine or a serine does not change the capacity for mutant CSF2RB to transform Ba/F3 lines or accumulate on the cell surface. Individually, each of these conclusions have minor caveats outlined above (limited sample size, the ability for WT CSF2RB to mimic the same phenotype), which prevents the formation of a firm

conclusion on the necessity of this cysteine. However, the preponderance of evidence suggests that the loss of the charged arginine at the membrane border drives receptor accumulation and activation.

This hypothesis calls into question the role and nature of disulfide-linked complexes observed in R461C-transformed cells (Figure 2-7A). It is possible that these complexes are the result of signal activation, and therefore were not observed in cells expressing WT CSF2RB. Another possibility is that R461C does induce novel disulfide-linked complexes, but these complexes are inconsequential for receptor accumulation and activation. Lastly, the disulfide bonds could form as a result of the disruption of the membrane-spanning domain due to loss of the charged arginine. These questions would be addressed by investigation of R461A/R461S expressing cells on a non-reducing Western blot. Additionally, cells with activated WT CSF2RB would address whether the bonds form as a result of signaling or TM-domain disruption, but this experiment would require the introduction of a human alpha chain receptor (CSF2RA or IL3RA), which could confound results. These results also emphasize the lack of understanding surrounding the transmembrane domain of CSF2RB[71, 100] which could be improved by additional basic research.

6.4 Figures

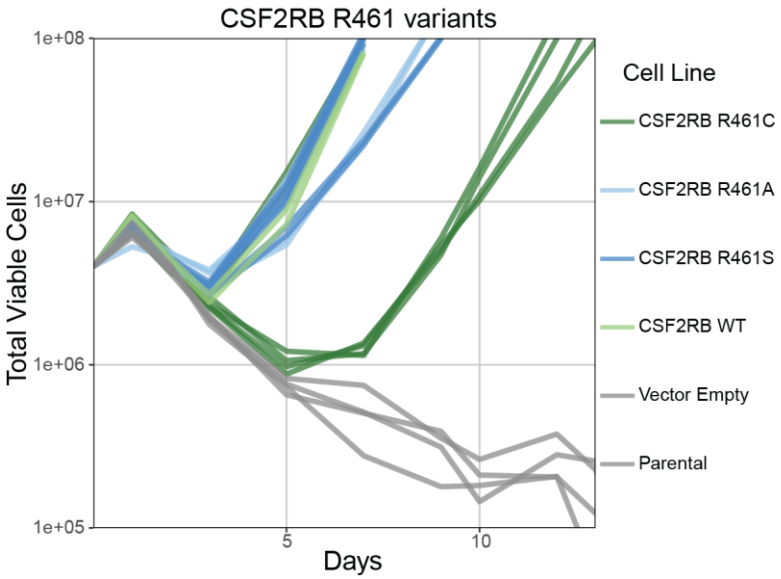

Figure 6-1 R461A and R461S drive factor-independent growth in Ba/F3 cells.

CSF2RB variants (R461C, R461A, R461S) were expressed by Ba/F3 cells and assayed for transformation. Each variant was expressed in 3 biologically replicate lines, and each line was tested for transformation in 2 technically replicate flasks. CSF2RB WT was only tested in one cell line (2 replicates). All three CSF2RB variants achieved factor independence in every line, with R461A and R461S generally growing earlier than R461C (one CSF2RB R461C line grew just as quickly but is obscured in this graph). CSF2RB WT transformed and upon sequencing presented with the activating V449E point mutation.

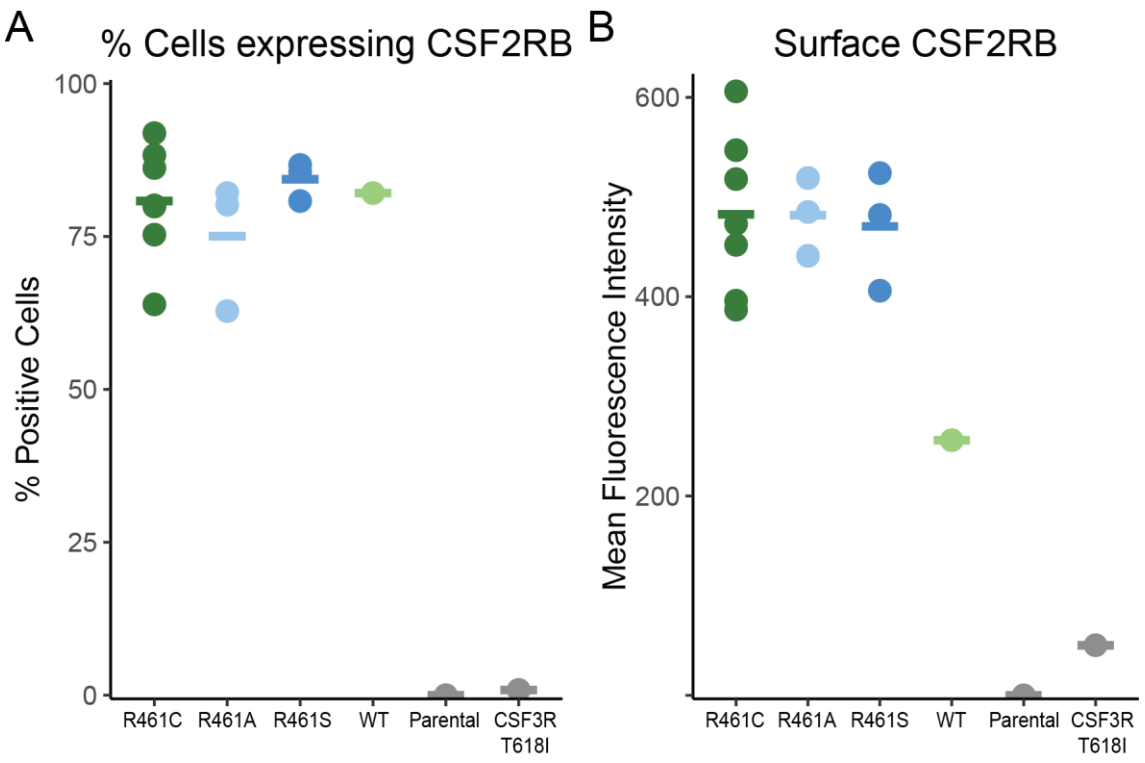

Figure 6-2 CSF2RB R461A and R461S drive surface accumulation similar to R461C.

(A) Pre-transformation Ba/F3 cells grown in IL-3 supplemented media expressing CSF2RB variants stained for hCSF2RB. Percent of cells positively staining for CSF2RB is shown for each cell line. Uninfected Ba/F3 cells, as well as those expressing CSF3R T618I, showed minimal staining for hCSF2RB (R461C n=7, R461A n=3, R461S n=3, WT n=1, Parental n=1, CSF3R T618I n=1). (B) Geometric mean fluorescence intensity for hCSF2RB-positive cells in each line.

7 Appendix B: Discovery of a CSF2RA mutation inducing dimerization with CSF2RB

7.1 Background

The trimerization of CSF2RB to CSF2RA and GM-CSF ligand is an essential step in the activation of GM-CSF signaling. Significant work has been done to explore the extracellular interactions of these three molecules but none have investigated interactions between the TM-domains of CSF2RA and CSF2RB[71, 100]. Investigation of these domains would improve structural modeling of these receptors and our understanding of how extracellular events influence cytoplasmic orientation. While performing preliminary experiments not detailed in this dissertation I happened upon an artifact that could shed light on this matter.

During the identification of R461C as an activating variant in CSF2RB, 7 other CSF2RB variants were tested in a series of Ba/F3 transformation assays (Table 2-4)[100]. None of these additional variants could reliably transform Ba/F3 cells, but it was unknown if these variants could induce alpha-beta chain dimerization and transform cells if co-expressed with CSF2RA.

7.2 Results

Ba/F3 cells were infected to express hCSF2RA with a pMX-IRES-Puro vector, followed by selection in puromycin. CSF2RA-expressing Ba/F3 cells were split and infected with CSF2RB MSCV-IRES-GRP retroviruses driving expression of WT or one of 8 different

CSF2RB variants. Infected cells were selected by GFP-positive FACS and then assayed for factor-independent growth. Cells expressing CSF2RA and an empty-vector GFP construct failed to transform while every combination of CSF2RB and CSF2RA succeeded (Figure 7-1A). Other groups have published results indicating that WT CSF2RA and CSF2RB in combination form a receptor capable of binding hGM-CSF, but absent GM-CSF are unable to drive factor-independent growth in Ba/F3 cells[174]. Notably, every CSF2RA + CSF2RB line transformed faster than CSF2RA + CSF2RB R461C in this experiment (Figure 7-1A), and also faster than what is typically seen in other CSF2RB R461C lines (Figure 2-3, Figure 3-2). Genomic DNA taken from transformed lines was sequenced and revealed a transmembrane CSF2RA point mutation (G343D) in every line except CSF2RA + CSF2RB R461C (Figure 7-1B). CSF2RB R461C carried novel acquired mutations in both transgenes.

7.3 Discussion

It is possible that in this experiment the co-expression of CSF2RA and CSF2RB alone was sufficient to transform Ba/F3 cells, but that would not explain the CSF2RA mutational enrichment or differential rate of outgrowth. It is also possible that the mutations acquired in the CSF2RB R461C line (in both CSF2RA and CSF2RB) resulted in the slower outgrowth and failure to enrich CSF2RA G343D, but that would be highly coincidental.

The most comprehensive conclusion is that CSF2RA G343D is a point mutation that results in constitutive dimerization with CSF2RB and ligand-independent activation. This mutation

must have been present in the original CSF2RA-expressing line prior to the addition of CSF2RB, as the alternative explanation that it independently and identically occurred in 8 of 9 flasks is exceedingly improbable. Therefore, this mutation was present in the CSF2RA + empty vector line, which did not transform, so the point mutation cannot independently transform without CSF2RB. We are then left with a conundrum, that a CSF2RA point mutation—which drives transformation faster than CSF2RB R461C—was present in the CSF2RB R461C population and ultimately not selected for. The residue affected by G343D lies in the transmembrane domain of CSF2RA, near the cytoplasmic end as predicted by UniProt (TM domain 321-346)[99].

I hypothesize that CSF2RA G343D results in constitutive dimerization with and activation of CSF2RB signaling. CSF2RB R461C, also mutated at the cytoplasmic end of the transmembrane domain, is unable to interact with mutant CSF2RA. The simplest explanation is that the negatively-charged aspartate formed in CSF2RA G343D causes dimerization through interaction with the positively-charged arginine-461 in WT CSF2RB. This conclusion would shed further light on the specific boundaries of the CSF2RB TM domain, which are in question[100], and the specific orientation of TM domain interaction in CSF2RB-CSF2RA dimerization. Another explanation for these data is that the CSF2RB R461C mutation results in either constitutive formation of another CSF2RB complex that out competes the formation of a dimer with CSF2RA G343D, or the CSF2RB mutation results in a substantial alteration of the CSF2RB TM domain such that it loses the ability to

bind with CSF2RA. Future studies could determine if CSF2RB R461C co-expressed with CSF2RA is capable of forming a functional receptor for GM-CSF by assaying proliferation over a ligand dose curve.

These hypotheses are made on the limited observations of a preliminary experiment and require repeat experiments to validate. The conclusions drawn above are admittedly zealous, but they also represent the most consistent and logical accounting for every observation. Furthermore, while these conclusions are minimally relevant to the direct discovery of driving mutations in leukemia, they could prove highly useful in the basic science characterizations of CSF2RB structure and binding to CSF2RA.

7.4 Figures

A

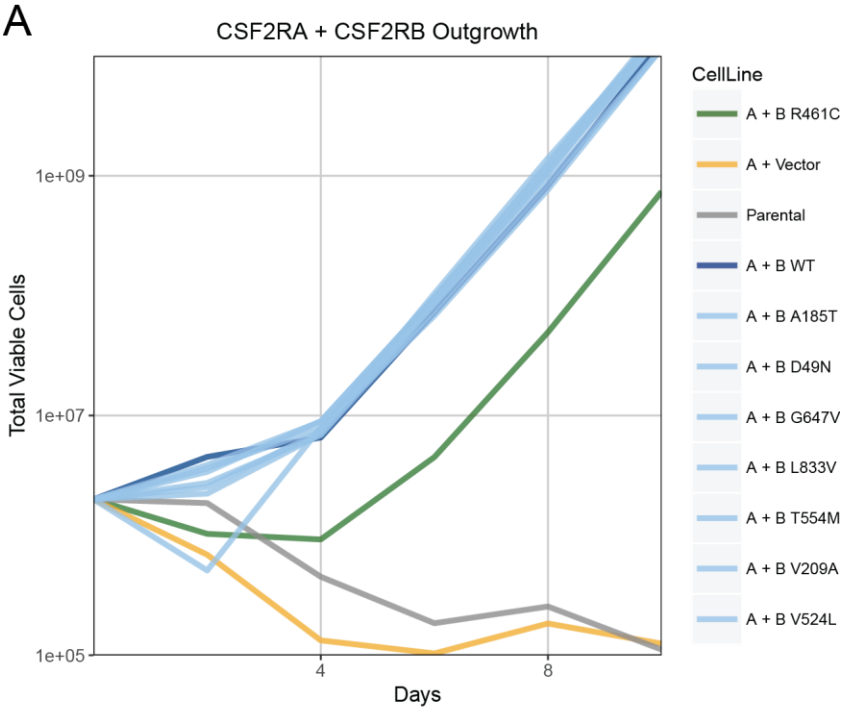

B

Sequence results of outgrown Ba/F3 lines

CSF2RA	CSF2RB	Outgrowth speed	CSF2RA mutations	CSF2RB mutations
-	-	n/a	n/a	n/a
+	-	n/a	n/a	n/a
+	R461C	Slow	A121T E200K	V73L
+	WT	Fast	G343D	✓
+	A185T	Fast	G343D	✓
+	D49N	Fast	G343D	✓
+	G647V	Fast	G343D	✓
+	L833V	Fast	G343D	✓
+	T554M	Fast	G343D	✓
+	V209A	Fast	G343D	✓
+	V524L	Fast	G343D	✓

✓ - Full transgene sequenced, no variants detected

Figure 7-1 CSF2RA G343D results in Ba/F3 transformation when combined with functional CSF2RB.

(A) Ba/F3 cells expressing CSF2RA and CSF2RB variants tested for factor-independent growth. CSF2RA alone (empty vector) failed to transform Ba/F3 cells, but when combined with any CSF2RB construct cells rapidly transformed. CSF2RB R461C was notably slower to transform than other CSF2RB variants when paired with CSF2RA. (B) Sequence results for outgrown cell lines. CSF2RA acquired mutations in every outgrown line, but in 8 of 9 lines the exact same G343D mutation was detected. CSF2RB R461C presented with novel acquired mutations in both transgenes.

8 References

1. Network, C.G.A.R., *Genomic and epigenomic landscapes of adult de novo acute myeloid leukemia.* N Engl J Med, 2013. **368**(22): p. 2059-74.
2. Moore, P.S. and Y. Chang, *Why do viruses cause cancer? Highlights of the first century of human tumour virology.* Nat Rev Cancer, 2010. **10**(12): p. 878-89.
3. Epstein, M.A., B.G. Achong, and Y.M. Barr, *VIRUS PARTICLES IN CULTURED LYMPHOBLASTS FROM BURKITT'S LYMPHOMA.* Lancet, 1964. **1**(7335): p. 702-3.
4. *Peyton Rous - Facts*. 2014 [cited 2016 11/28/2016]; Available from: http://www.nobelprize.org/nobel_prizes/medicine/laureates/1966/rous-facts.html.
5. Stehelin, D., et al., *DNA related to the transforming gene(s) of avian sarcoma viruses is present in normal avian DNA.* Nature, 1976. **260**(5547): p. 170-3.
6. Vogt, P.K., *Retroviral Oncogenes: A Historical Primer.* Nat Rev Cancer, 2012. **12**(9): p. 639-48.
7. Ames, B.N., et al., *Carcinogens are mutagens: a simple test system combining liver homogenates for activation and bacteria for detection.* Proc Natl Acad Sci U S A, 1973. **70**(8): p. 2281-5.
8. Daley, G.Q. and D. Baltimore, *Transformation of an interleukin 3-dependent hematopoietic cell line by the chronic myelogenous leukemia-specific P210bcr/abl protein.* Proc Natl Acad Sci U S A, 1988. **85**(23): p. 9312-6.
9. Heisterkamp, N., et al., *Structural organization of the bcr gene and its role in the Ph' translocation.* Nature, 1985. **315**(6022): p. 758-761.
10. Abelson, H.T. and L.S. Rabstein, *Lymphosarcoma: virus-induced thymic-independent disease in mice.* Cancer Res, 1970. **30**(8): p. 2213-22.
11. Rowley, J.D., *Letter: A new consistent chromosomal abnormality in chronic myelogenous leukaemia identified by quinacrine fluorescence and Giemsa staining.* Nature, 1973. **243**(5405): p. 290-3.
12. Nowell, P.C. and D.A. Hungerford, *Minute chromosome in human chronic granulocytic leukemia*. 1960: Amer Assoc Advancement Science. p. 1497-1497.
13. Zhao, X., et al., *Structure of the Bcr-Abl oncoprotein oligomerization domain.* Nat Struct Biol, 2002. **9**(2): p. 117-20.
14. Jainchill, J.L., S.A. Aaronson, and G.J. Todaro, *Murine sarcoma and leukemia viruses: assay using clonal lines of contact-inhibited mouse cells.* J Virol, 1969. **4**(5): p. 549-53.
15. Todaro, G.J. and H. Green, *Quantitative studies of the growth of mouse embryo cells in culture and their development into established lines.* J Cell Biol, 1963. **17**: p. 299-313.
16. Aaronson, S.A. and G.J. Todaro, *Development of 3T3-like lines from Balb-c mouse embryo cultures: transformation susceptibility to SV40.* J Cell Physiol, 1968. **72**(2): p. 141-8.

17. Copeland, N.G., A.D. Zelenetz, and G.M. Cooper, *Transformation of NIH/3T3 mouse cells by DNA of Rous sarcoma virus.* Cell, 1979. **17**(4): p. 993-1002.
18. Daley, G.Q., et al., *The CML-specific P210 bcr/abl protein, unlike v-abl, does not transform NIH/3T3 fibroblasts.* Science, 1987. **237**(4814): p. 532-5.
19. McLaughlin, J., E. Chianese, and O.N. Witte, *In vitro transformation of immature hematopoietic cells by the P210 BCR/ABL oncogene product of the Philadelphia chromosome.* Proc Natl Acad Sci U S A, 1987. **84**(18): p. 6558-62.
20. Pierce, J.H., et al., *Neoplastic transformation of mast cells by Abelson-MuLV: abrogation of IL-3 dependence by a nonautocrine mechanism.* Cell, 1985. **41**(3): p. 685-93.
21. Oliff, A., et al., *Friend murine leukemia virus-immortalized myeloid cells are converted into tumorigenic cell lines by Abelson leukemia virus.* Proc Natl Acad Sci U S A, 1985. **82**(10): p. 3306-10.
22. Greenberger, J.S., et al., *Interleukin 3-dependent hematopoietic progenitor cell lines.* Fed Proc, 1983. **42**(10): p. 2762-71.
23. Cook, W.D., et al., *Malignant transformation of a growth factor-dependent myeloid cell line by Abelson virus without evidence of an autocrine mechanism.* Cell, 1985. **41**(3): p. 677-83.
24. Cook, W.D., et al., *Abelson virus transformation of an interleukin 2-dependent antigen-specific T-cell line.* Mol Cell Biol, 1987. **7**(7): p. 2631-5.
25. Palacios, R. and M. Steinmetz, *Il-3-dependent mouse clones that express B-220 surface antigen, contain Ig genes in germ-line configuration, and generate B lymphocytes in vivo.* Cell, 1985. **41**(3): p. 727-34.
26. Palacios, R., C. Fernandez, and P. Sideras, *Development and continuous growth in culture of interleukin 2-producer lymphocytes from athymic nu/nu mice.* Eur J Immunol, 1982. **12**(9): p. 777-82.
27. Ralph, P., M.A. Moore, and K. Nilsson, *Lysozyme synthesis by established human and murine histiocytic lymphoma cell lines.* J Exp Med, 1976. **143**(6): p. 1528-33.
28. Warner, N.L., M.A. Moore, and D. Metcalf, *A transplantable myelomonocytic leukemia in BALB-c mice: cytology, karyotype, and muramidase content.* J Natl Cancer Inst, 1969. **43**(4): p. 963-82.
29. Palacios, R., *Conditions for the Establishment in Vitro of Interleukin 3-Dependent Murine B Cell Precursor Lines*, in *Immunological Methods*, I.P. Lefkovits, B., Editor. 1985, Academic Press, Inc. p. 265-278.
30. Mathey-Prevot, B., et al., *Abelson virus abrogation of interleukin-3 dependence in a lymphoid cell line.* Mol Cell Biol, 1986. **6**(11): p. 4133-5.
31. Didion, J.P., et al., *SNP array profiling of mouse cell lines identifies their strains of origin and reveals cross-contamination and widespread aneuploidy.* BMC Genomics, 2014. **15**: p. 847.
32. Nakamura, Y. *The information about Ba/F3*. 2012 [cited 2016 11/30/16]; Available from: http://cell.brc.riken.jp/en/rcb/baf3.

33. Krapf, G., et al., *ETV6/RUNX1 abrogates mitotic checkpoint function and targets its key player MAD2L1.* Oncogene, 2010. **29**(22): p. 3307-12.
34. Fest, T., et al., *c-MYC overexpression in Ba/F3 cells simultaneously elicits genomic instability and apoptosis.* Oncogene, 2002. **21**(19): p. 2981-90.
35. Pikman, Y., et al., *MPLW515L is a novel somatic activating mutation in myelofibrosis with myeloid metaplasia.* PLoS Med, 2006. **3**(7): p. e270.
36. Maxson, J.E., et al., *Oncogenic CSF3R mutations in chronic neutrophilic leukemia and atypical CML.* N Engl J Med, 2013. **368**(19): p. 1781-90.
37. Mullighan, C.G., et al., *JAK mutations in high-risk childhood acute lymphoblastic leukemia.* Proc Natl Acad Sci U S A, 2009. **106**(23): p. 9414-8.
38. Walters, D.K., et al., *Activating alleles of JAK3 in acute megakaryoblastic leukemia.* Cancer Cell, 2006. **10**(1): p. 65-75.
39. Mullighan, C.G., et al., *Rearrangement of CRLF2 in B-progenitor- and Down syndrome-associated acute lymphoblastic leukemia.* Nat Genet, 2009. **41**(11): p. 1243-6.
40. Lacronique, V., et al., *A TEL-JAK2 fusion protein with constitutive kinase activity in human leukemia.* Science, 1997. **278**(5341): p. 1309-12.
41. Hirota, S., et al., *Gain-of-function mutations of c-kit in human gastrointestinal stromal tumors.* Science, 1998. **279**(5350): p. 577-80.
42. Hirota, S., et al., *Gain-of-function mutations of platelet-derived growth factor receptor alpha gene in gastrointestinal stromal tumors.* Gastroenterology, 2003. **125**(3): p. 660-7.
43. Corless, C.L., et al., *PDGFRA mutations in gastrointestinal stromal tumors: frequency, spectrum and in vitro sensitivity to imatinib.* J Clin Oncol, 2005. **23**(23): p. 5357-64.
44. George, R.E., et al., *Activating mutations in ALK provide a therapeutic target in neuroblastoma.* Nature, 2008. **455**(7215): p. 975-8.
45. Greulich, H., et al., *Functional analysis of receptor tyrosine kinase mutations in lung cancer identifies oncogenic extracellular domain mutations of ERBB2.* Proc Natl Acad Sci U S A, 2012. **109**(36): p. 14476-81.
46. Warmuth, M., et al., *Ba/F3 cells and their use in kinase drug discovery.* Curr Opin Oncol, 2007. **19**(1): p. 55-60.
47. Zhang, W., et al., *Mutant FLT3: a direct target of sorafenib in acute myelogenous leukemia.* J Natl Cancer Inst, 2008. **100**(3): p. 184-98.
48. Gozgit, J.M., et al., *Ponatinib (AP24534), a multitargeted pan-FGFR inhibitor with activity in multiple FGFR-amplified or mutated cancer models.* Mol Cancer Ther, 2012. **11**(3): p. 690-9.
49. Quintas-Cardama, A., et al., *Preclinical characterization of the selective JAK1/2 inhibitor INCB018424: therapeutic implications for the treatment of myeloproliferative neoplasms.* Blood, 2010. **115**(15): p. 3109-17.
50. Costa, D.B., et al., *BIM mediates EGFR tyrosine kinase inhibitor-induced apoptosis in lung cancers with oncogenic EGFR mutations.* PLoS Med, 2007. **4**(10): p. 1669-79; discussion 1680.

51. Schnittger, S., et al., *KIT-D816 mutations in AML1-ETO-positive AML are associated with impaired event-free and overall survival.* Blood, 2006. **107**(5): p. 1791-9.
52. Bradeen, H.A., et al., *Comparison of imatinib mesylate, dasatinib (BMS-354825), and nilotinib (AMN107) in an N-ethyl-N-nitrosourea (ENU)-based mutagenesis screen: high efficacy of drug combinations.* Blood, 2006. **108**(7): p. 2332-8.
53. O'Hare, T., et al., *AP24534, a pan-BCR-ABL inhibitor for chronic myeloid leukemia, potently inhibits the T315I mutant and overcomes mutation-based resistance.* Cancer Cell, 2009. **16**(5): p. 401-12.
54. Graham, F.L. and A.J. van der Eb, *A new technique for the assay of infectivity of human adenovirus 5 DNA.* Virology, 1973. **52**(2): p. 456-67.
55. Poste, G. and D. Papahadjopoulos, *Lipid vesicles as carriers for introducing materials into cultured cells: influence of vesicle lipid composition on mechanism(s) of vesicle incorporation into cells.* Proc Natl Acad Sci U S A, 1976. **73**(5): p. 1603-7.
56. Fraley, R., et al., *Studies on the mechanism of membrane fusion: role of phosphate in promoting calcium ion induced fusion of phospholipid vesicles.* Biochemistry, 1980. **19**(26): p. 6021-9.
57. Wong, T.K., C. Nicolau, and P.H. Hofschneider, *Appearance of beta-lactamase activity in animal cells upon liposome-mediated gene transfer.* Gene, 1980. **10**(2): p. 87-94.
58. Neumann, E., et al., *Gene transfer into mouse lyoma cells by electroporation in high electric fields.* Embo j, 1982. **1**(7): p. 841-5.
59. Mansky, L.M., *Retrovirus mutation rates and their role in genetic variation.* J Gen Virol, 1998. **79 (Pt 6)**: p. 1337-45.
60. Lang, R.A., et al., *Expression of a hemopoietic growth factor cDNA in a factor-dependent cell line results in autonomous growth and tumorigenicity.* Cell, 1985. **43**(2 Pt 1): p. 531-42.
61. Laker, C., et al., *Autocrine stimulation after transfer of the granulocyte/macrophage colony-stimulating factor gene and autonomous growth are distinct but interdependent steps in the oncogenic pathway.* Proc Natl Acad Sci U S A, 1987. **84**(23): p. 8458-62.
62. Stocking, C., et al., *Identification of genes involved in growth autonomy of hematopoietic cells by analysis of factor-independent mutants.* Cell, 1988. **53**(6): p. 869-79.
63. Stocking, C., et al., *Distinct classes of factor-independent mutants can be isolated after retroviral mutagenesis of a human myeloid stem cell line.* Growth Factors, 1993. **8**(3): p. 197-209.
64. Hannemann, J., et al., *Sequential mutations in the interleukin-3 (IL3)/granulocyte-macrophage colony-stimulating factor/IL5 receptor beta-subunit genes are necessary for the complete conversion to growth autonomy mediated by a truncated beta C subunit.* Mol Cell Biol, 1995. **15**(5): p. 2402-12.
65. Prassolov, V., et al., *Functional identification of secondary mutations inducing autonomous growth in synergy with a truncated interleukin-3 receptor: implications for multi-step oncogenesis.* Exp Hematol, 2001. **29**(6): p. 756-65.

66. Horn, S., et al., *An increase in the expression and total activity of endogenous p60(c-Src) in several factor-independent mutants of a human GM-CSF-dependent leukemia cell line (TF-1).* Oncogene, 2003. **22**(46): p. 7170-80.
67. Schwieger, M., et al., *A dominant-negative mutant of C/EBPalpha, associated with acute myeloid leukemias, inhibits differentiation of myeloid and erythroid progenitors of man but not mouse.* Blood, 2004. **103**(7): p. 2744-52.
68. Li, Z., et al., *Predictable and efficient retroviral gene transfer into murine bone marrow repopulating cells using a defined vector dose.* Exp Hematol, 2003. **31**(12): p. 1206-14.
69. Meyer, J., et al., *Activation of the gene for the PDGF receptor beta1 (PDGFRbeta) in interleukin-3-dependent myeloid cells by retroviral insertional mutagenesis: implications for the transforming potential of PDGFRbeta.* Growth Factors, 2002. **20**(3): p. 131-40.
70. Murphy, J.M. and I.G. Young, *IL-3, IL-5, and GM-CSF signaling: crystal structure of the human beta-common receptor.* Vitam Horm, 2006. **74**: p. 1-30.
71. Broughton, S.E., et al., *The betac receptor family - Structural insights and their functional implications.* Cytokine, 2015.
72. Brooks, A.J., et al., *Mechanism of activation of protein kinase JAK2 by the growth hormone receptor.* Science, 2014. **344**(6185): p. 1249783.
73. Lantz, C.S., et al., *Role for interleukin-3 in mast-cell and basophil development and in immunity to parasites.* Nature, 1998. **392**(6671): p. 90-3.
74. Lopez, A.F., et al., *Recombinant human interleukin 5 is a selective activator of human eosinophil function.* J Exp Med, 1988. **167**(1): p. 219-24.
75. Armitage, J.O., *Emerging applications of recombinant human granulocyte-macrophage colony-stimulating factor.* Blood, 1998. **92**(12): p. 4491-508.
76. Garcia-Carbonero, R., et al., *Granulocyte colony-stimulating factor in the treatment of high-risk febrile neutropenia: a multicenter randomized trial.* J Natl Cancer Inst, 2001. **93**(1): p. 31-8.
77. Cebon, J.S. and G.J. Lieschke, *Granulocyte-macrophage colony-stimulating factor for cancer treatment.* Oncology, 1994. **51**(2): p. 177-88.
78. Desai, A.V., et al., *Pharmacokinetics of the chimeric anti-GD2 antibody, ch14.18, in children with high-risk neuroblastoma.* Cancer Chemother Pharmacol, 2014. **74**(5): p. 1047-55.
79. Zittoun, R., et al., *Granulocyte-macrophage colony-stimulating factor associated with induction treatment of acute myelogenous leukemia: a randomized trial by the European Organization for Research and Treatment of Cancer Leukemia Cooperative Group.* J Clin Oncol, 1996. **14**(7): p. 2150-9.
80. Kanerva, A., et al., *Antiviral and antitumor T-cell immunity in patients treated with GM-CSF-coding oncolytic adenovirus.* Clin Cancer Res, 2013. **19**(10): p. 2734-44.
81. Thorne, S.H., *The role of GM-CSF in enhancing immunotherapy of cancer.* Immunotherapy, 2013. **5**(8): p. 817-9.
82. Becher, B., S. Tugues, and M. Greter, *GM-CSF: From Growth Factor to Central Mediator of Tissue Inflammation.* Immunity. **45**(5): p. 963-973.

83. Pylayeva-Gupta, Y., et al., *Oncogenic Kras-Induced GM-CSF Production Promotes the Development of Pancreatic Neoplasia.* Cancer Cell. **21**(6): p. 836-847.
84. Bayne, Lauren J., et al., *Tumor-Derived Granulocyte-Macrophage Colony-Stimulating Factor Regulates Myeloid Inflammation and T Cell Immunity in Pancreatic Cancer.* Cancer Cell. **21**(6): p. 822-835.
85. Hunt, S., et al., *A crazy cause of dyspnea.* N Engl J Med, 2010. **363**(25): p. e38.
86. Patel, S.M., et al., *Pulmonary alveolar proteinosis.* Canadian Respiratory Journal : Journal of the Canadian Thoracic Society, 2012. **19**(4): p. 243-245.
87. Michaud, G., C. Reddy, and A. Ernst, *Whole-lung lavage for pulmonary alveolar proteinosis.* Chest, 2009. **136**(6): p. 1678-81.
88. Ohashi, K., et al., *Direct evidence that GM-CSF inhalation improves lung clearance in pulmonary alveolar proteinosis.* Respir Med, 2012. **106**(2): p. 284-93.
89. Tanaka, T., et al., *Adult-onset hereditary pulmonary alveolar proteinosis caused by a single-base deletion in CSF2RB.* J Med Genet, 2011. **48**(3): p. 205-9.
90. Takaki, M., et al., *Recurrence of pulmonary alveolar proteinosis after bilateral lung transplantation in a patient with a nonsense mutation in CSF2RB.* Respiratory Medicine Case Reports, 2016. **19**: p. 89-93.
91. Robb, L., et al., *Hematopoietic and lung abnormalities in mice with a null mutation of the common beta subunit of the receptors for granulocyte-macrophage colony-stimulating factor and interleukins 3 and 5.* Proc Natl Acad Sci U S A, 1995. **92**(21): p. 9565-9.
92. Nicola, N.A., et al., *Functional inactivation in mice of the gene for the interleukin-3 (IL-3)-specific receptor beta-chain: implications for IL-3 function and the mechanism of receptor transmodulation in hematopoietic cells.* Blood, 1996. **87**(7): p. 2665-74.
93. Mach, N., et al., *Involvement of interleukin-3 in delayed-type hypersensitivity.* Blood, 1998. **91**(3): p. 778-83.
94. Gainsford, T., et al., *Cytokine production and function in c-mpl-deficient mice: no physiologic role for interleukin-3 in residual megakaryocyte and platelet production.* Blood, 1998. **91**(8): p. 2745-52.
95. Nishinakamura, R., et al., *Hematopoiesis in mice lacking the entire granulocyte-macrophage colony-stimulating factor/interleukin-3/interleukin-5 functions.* Blood, 1996. **88**(7): p. 2458-64.
96. Riccioni, R., et al., *Interleukin (IL)-3/granulocyte macrophage-colony stimulating factor/IL-5 receptor alpha and beta chains are preferentially expressed in acute myeloid leukaemias with mutated FMS-related tyrosine kinase 3 receptor.* Br J Haematol, 2009. **144**(3): p. 376-87.
97. Testa, U., et al., *Elevated expression of IL-3Ralpha in acute myelogenous leukemia is associated with enhanced blast proliferation, increased cellularity, and poor prognosis.* Blood, 2002. **100**(8): p. 2980-8.
98. Jenkins, B.J., T.J. Blake, and T.J. Gonda, *Saturation mutagenesis of the beta subunit of the human granulocyte-macrophage colony-stimulating factor receptor shows clustering of*

constitutive mutations, activation of ERK MAP kinase and STAT pathways, and differential beta subunit tyrosine phosphorylation. Blood, 1998. **92**(6): p. 1989-2002.
99. The UniProt Consortium, *UniProt: a hub for protein information.* Nucleic Acids Research, 2015. **43**(D1): p. D204-D212.
100. Watanabe-Smith, K., et al., *Discovery and functional characterization of a germline, CSF2RB-activating mutation in leukemia.* Leukemia, 2016. **30**(9): p. 1950-3.
101. Bargmann, C.I., M.C. Hung, and R.A. Weinberg, *Multiple independent activations of the neu oncogene by a point mutation altering the transmembrane domain of p185.* Cell, 1986. **45**(5): p. 649-57.
102. Forbes, L.V., et al., *An activating mutation in the transmembrane domain of the granulocyte colony-stimulating factor receptor in patients with acute myeloid leukemia.* Oncogene, 2002. **21**(39): p. 5981-9.
103. Webster, M.K. and D.J. Donoghue, *Constitutive activation of fibroblast growth factor receptor 3 by the transmembrane domain point mutation found in achondroplasia.* EMBO J, 1996. **15**(3): p. 520-7.
104. Cerami, E., et al., *The cBio cancer genomics portal: an open platform for exploring multidimensional cancer genomics data.* Cancer Discov, 2012. **2**(5): p. 401-4.
105. Gao, J., et al., *Integrative analysis of complex cancer genomics and clinical profiles using the cBioPortal.* Sci Signal, 2013. **6**(269): p. pl1.
106. Forbes, S.A., et al., *COSMIC: exploring the world's knowledge of somatic mutations in human cancer.* Nucleic Acids Res, 2015. **43**(Database issue): p. D805-11.
107. Tyner, J.W., *Functional genomics for personalized cancer therapy.* Sci Transl Med, 2014. **6**(243): p. 243fs26.
108. Hansen, G., et al., *The structure of the GM-CSF receptor complex reveals a distinct mode of cytokine receptor activation.* Cell, 2008. **134**(3): p. 496-507.
109. Perugini, M., et al., *Alternative modes of GM-CSF receptor activation revealed using activated mutants of the common beta-subunit.* Blood, 2010. **115**(16): p. 3346-53.
110. Hercus, T.R., et al., *Signalling by the betac family of cytokines.* Cytokine Growth Factor Rev, 2013. **24**(3): p. 189-201.
111. D'Andrea, R., et al., *A mutation of the common receptor subunit for interleukin-3 (IL-3), granulocyte-macrophage colony-stimulating factor, and IL-5 that leads to ligand independence and tumorigenicity.* Blood, 1994. **83**(10): p. 2802-8.
112. The 1000 Genomes Project Consortium, *A global reference for human genetic variation.* Nature, 2015. **526**(7571): p. 68-74.
113. Lek, M., et al., *Analysis of protein-coding genetic variation in 60,706 humans.* bioRxiv, 2015.
114. Zhang, J., et al., *Germline Mutations in Predisposition Genes in Pediatric Cancer.* N Engl J Med, 2015. **373**(24): p. 2336-46.
115. Dong, F., et al., *Mutations in the gene for the granulocyte colony-stimulating-factor receptor in patients with acute myeloid leukemia preceded by severe congenital neutropenia.* N Engl J Med, 1995. **333**(8): p. 487-93.

116. McMahon, D.P., et al., *Congenital Neutrophilia Arising from a T618I Germline Mutation in the CSF3R Gene.* Blood, 2015. **126**(23): p. 1623-1623.
117. Sokol, L., et al., *Primary familial polycythemia: a frameshift mutation in the erythropoietin receptor gene and increased sensitivity of erythroid progenitors to erythropoietin.* Blood, 1995. **86**(1): p. 15-22.
118. Ding, J., et al., *Familial essential thrombocythemia associated with a dominant-positive activating mutation of the c-MPL gene, which encodes for the receptor for thrombopoietin.* Blood, 2004. **103**(11): p. 4198-200.
119. Zenatti, P.P., et al., *Oncogenic IL7R gain-of-function mutations in childhood T-cell acute lymphoblastic leukemia.* Nat Genet, 2011. **43**(10): p. 932-9.
120. Kjaer, S., et al., *Self-association of the transmembrane domain of RET underlies oncogenic activation by MEN2A mutations.* Oncogene, 2006. **25**(53): p. 7086-95.
121. Tyner, J.W., et al., *Kinase pathway dependence in primary human leukemias determined by rapid inhibitor screening.* Cancer Res, 2013. **73**(1): p. 285-96.
122. Rawlings, J.S., K.M. Rosler, and D.A. Harrison, *The JAK/STAT signaling pathway.* J Cell Sci, 2004. **117**(Pt 8): p. 1281-3.
123. Hofmann, K. and W. Stoffel, *TMBASE - A database of membrane spanning protein segments.* Biol. Chem. Hoppe-Seyler, 1993. **374**(166).
124. White, S.H. and W.C. Wimley, *Hydrophobic interactions of peptides with membrane interfaces.* Biochim Biophys Acta, 1998. **1376**(3): p. 339-52.
125. Jones, D.T., W.R. Taylor, and J.M. Thornton, *A model recognition approach to the prediction of all-helical membrane protein structure and topology.* Biochemistry, 1994. **33**(10): p. 3038-49.
126. Jones, D.T., *Improving the accuracy of transmembrane protein topology prediction using evolutionary information.* Bioinformatics, 2007. **23**(5): p. 538-44.
127. Nugent, T. and D.T. Jones, *Transmembrane protein topology prediction using support vector machines.* BMC Bioinformatics, 2009. **10**: p. 159.
128. Buchan, D.W., et al., *Scalable web services for the PSIPRED Protein Analysis Workbench.* Nucleic Acids Res, 2013. **41**(Web Server issue): p. W349-57.
129. Kall, L., A. Krogh, and E.L. Sonnhammer, *A combined transmembrane topology and signal peptide prediction method.* J Mol Biol, 2004. **338**(5): p. 1027-36.
130. Kall, L., A. Krogh, and E.L. Sonnhammer, *Advantages of combined transmembrane topology and signal peptide prediction--the Phobius web server.* Nucleic Acids Res, 2007. **35**(Web Server issue): p. W429-32.
131. Jones, D.T., *Protein secondary structure prediction based on position-specific scoring matrices.* J Mol Biol, 1999. **292**(2): p. 195-202.
132. Krogh, A., et al., *Predicting transmembrane protein topology with a hidden Markov model: application to complete genomes.* J Mol Biol, 2001. **305**(3): p. 567-80.
133. Sonnhammer, E.L., G. von Heijne, and A. Krogh, *A hidden Markov model for predicting transmembrane helices in protein sequences.* Proc Int Conf Intell Syst Mol Biol, 1998. **6**: p. 175-82.

134. Tsirigos, K.D., et al., *The TOPCONS web server for consensus prediction of membrane protein topology and signal peptides.* Nucleic Acids Res, 2015. **43**(W1): p. W401-7.
135. Ben-Neriah, Y., et al., *The chronic myelogenous leukemia-specific P210 protein is the product of the bcr/abl hybrid gene.* Science, 1986. **233**(4760): p. 212-214.
136. Yuzugullu, H., et al., *NTRK2 activation cooperates with PTEN deficiency in T-ALL through activation of both the PI3K-AKT and JAK-STAT3 pathways.* Cell Discov, 2016. **2**: p. 16030.
137. Cante-Barrett, K., et al., *MEK and PI3K-AKT inhibitors synergistically block activated IL7 receptor signaling in T-cell acute lymphoblastic leukemia.* Leukemia, 2016. **30**(9): p. 1832-43.
138. White, Y., et al., *KRAS insertion mutations are oncogenic and exhibit distinct functional properties.* Nat Commun, 2016. **7**: p. 10647.
139. Ishibashi, T., et al., *Ph-like ALL-related novel fusion kinase ATF7IP-PDGFRB exhibits high sensitivity to tyrosine kinase inhibitors in murine cells.* Exp Hematol, 2016. **44**(3): p. 177-88.e5.
140. Yang, S., et al., *Activating JAK1 mutation may predict the sensitivity of JAK-STAT inhibition in hepatocellular carcinoma.* Oncotarget, 2016. **7**(5): p. 5461-9.
141. Reshetnyak, A.V., et al., *Augmentor alpha and beta (FAM150) are ligands of the receptor tyrosine kinases ALK and LTK: Hierarchy and specificity of ligand-receptor interactions.* Proc Natl Acad Sci U S A, 2015. **112**(52): p. 15862-7.
142. Kiessling, M.K., et al., *Mutant HRAS as novel target for MEK and mTOR inhibitors.* Oncotarget, 2015. **6**(39): p. 42183-96.
143. Arts, F.A., et al., *PDGFRB mutants found in patients with familial infantile myofibromatosis or overgrowth syndrome are oncogenic and sensitive to imatinib.* Oncogene, 2016. **35**(25): p. 3239-48.
144. Cheng, H., et al., *RICTOR Amplification Defines a Novel Subset of Patients with Lung Cancer Who May Benefit from Treatment with mTORC1/2 Inhibitors.* Cancer Discov, 2015. **5**(12): p. 1262-70.
145. Roncero, A.M., et al., *Contribution of JAK2 mutations to T-cell lymphoblastic lymphoma development.* Leukemia, 2016. **30**(1): p. 94-103.
146. Kobayashi, Y., et al., *EGFR Exon 18 Mutations in Lung Cancer: Molecular Predictors of Augmented Sensitivity to Afatinib or Neratinib as Compared with First- or Third-Generation TKIs.* Clin Cancer Res, 2015. **21**(23): p. 5305-13.
147. Lindblad, O., et al., *PI3 kinase is indispensable for oncogenic transformation by the V560D mutant of c-Kit in a kinase-independent manner.* Cell Mol Life Sci, 2015. **72**(22): p. 4399-407.
148. Grubbs, E.G., et al., *RET fusion as a novel driver of medullary thyroid carcinoma.* J Clin Endocrinol Metab, 2015. **100**(3): p. 788-93.
149. Stockklausner, C., et al., *The thrombopoietin receptor P106L mutation functionally separates receptor signaling activity from thrombopoietin homeostasis.* Blood, 2015. **125**(7): p. 1159-69.

150. Schinnerl, D., et al., *The role of the Janus-faced transcription factor PAX5-JAK2 in acute lymphoblastic leukemia.* Blood, 2015. **125**(8): p. 1282-91.
151. Capelletti, M., et al., *Identification of recurrent FGFR3-TACC3 fusion oncogenes from lung adenocarcinoma.* Clin Cancer Res, 2014. **20**(24): p. 6551-8.
152. Degryse, S., et al., *JAK3 mutants transform hematopoietic cells through JAK1 activation, causing T-cell acute lymphoblastic leukemia in a mouse model.* Blood, 2014. **124**(20): p. 3092-100.
153. Yin, C., C. Sandoval, and G.H. Baeg, *Identification of mutant alleles of JAK3 in pediatric patients with acute lymphoblastic leukemia.* Leuk Lymphoma, 2015. **56**(5): p. 1502-6.
154. Kiel, M.J., et al., *Integrated genomic sequencing reveals mutational landscape of T-cell prolymphocytic leukemia.* Blood, 2014. **124**(9): p. 1460-72.
155. Janke, H., et al., *Activating FLT3 mutants show distinct gain-of-function phenotypes in vitro and a characteristic signaling pathway profile associated with prognosis in acute myeloid leukemia.* PLoS One, 2014. **9**(3): p. e89560.
156. Marty, C., et al., *Germ-line JAK2 mutations in the kinase domain are responsible for hereditary thrombocytosis and are resistant to JAK2 and HSP90 inhibitors.* Blood, 2014. **123**(9): p. 1372-83.
157. Tomita, O., et al., *Sensitivity of SNX2-ABL1 toward tyrosine kinase inhibitors distinct from that of BCR-ABL1.* Leuk Res, 2014. **38**(3): p. 361-70.
158. Bossi, D., et al., *Functional characterization of a novel FGFR1OP-RET rearrangement in hematopoietic malignancies.* Mol Oncol, 2014. **8**(2): p. 221-31.
159. Velghe, A.I., et al., *PDGFRA alterations in cancer: characterization of a gain-of-function V536E transmembrane mutant as well as loss-of-function and passenger mutations.* Oncogene, 2014. **33**(20): p. 2568-76.
160. Jenkins, B.J., R. D'Andrea, and T.J. Gonda, *Activating point mutations in the common beta subunit of the human GM-CSF, IL-3 and IL-5 receptors suggest the involvement of beta subunit dimerization and cell type-specific molecules in signalling.* EMBO J, 1995. **14**(17): p. 4276-87.
161. Gits, J., et al., *Multiple pathways contribute to the hyperproliferative responses from truncated granulocyte colony-stimulating factor receptors.* Leukemia, 2006. **20**(12): p. 2111-8.
162. Shochat, C., et al., *Gain-of-function mutations in interleukin-7 receptor- α (IL7R) in childhood acute lymphoblastic leukemias.* The Journal of Experimental Medicine, 2011. **208**(5): p. 901-908.
163. Hu, Y. and G.K. Smyth, *ELDA: extreme limiting dilution analysis for comparing depleted and enriched populations in stem cell and other assays.* J Immunol Methods, 2009. **347**(1-2): p. 70-8.

164. Kazi, J.U., J. Sun, and L. Ronnstrand, *The presence or absence of IL-3 during long-term culture of Flt3-ITD and c-Kit-D816V expressing Ba/F3 cells influences signaling outcome.* Exp Hematol, 2013. **41**(7): p. 585-7.
165. Drake, J.W., *Rates of spontaneous mutation among RNA viruses.* Proc Natl Acad Sci U S A, 1993. **90**(9): p. 4171-5.
166. Davidson, C.J., et al., *Improving the limit of detection for Sanger sequencing: A comparison of methodologies for KRAS variant detection.* Biotechniques, 2012. **2012**.
167. Hornakova, T., et al., *Oncogenic JAK1 and JAK2-activating mutations resistant to ATP-competitive inhibitors.* Haematologica, 2011. **96**(6): p. 845-53.
168. Hawley, R.G., et al., *Versatile retroviral vectors for potential use in gene therapy.* Gene Ther, 1994. **1**(2): p. 136-8.
169. Frey, U.H., et al., *PCR-amplification of GC-rich regions: 'slowdown PCR'.* Nat Protoc, 2008. **3**(8): p. 1312-7.
170. *NHGRI Collection - Gujarati Indians in Houston, Texas, USA*. HapMap Collections 12-22-2016]; Available from: https://catalog.coriell.org/1/NHGRI/Collections/HapMap-Collections/Gujarati-Indians-in-Houston-TX-USA-GIH.
171. Sun, Q., et al., *Simultaneous antagonism of interleukin-5, granulocyte-macrophage colony-stimulating factor, and interleukin-3 stimulation of human eosinophils by targetting the common cytokine binding site of their receptors.* Blood, 1999. **94**(6): p. 1943-51.
172. Mehta, H.M., et al., *Alternatively spliced, truncated GCSF receptor promotes leukemogenic properties and sensitivity to JAK inhibition.* Leukemia, 2014. **28**(5): p. 1041-51.
173. Roberts, K.G., et al., *Targetable kinase-activating lesions in Ph-like acute lymphoblastic leukemia.* N Engl J Med, 2014. **371**(11): p. 1005-15.
174. Watanabe, S., et al., *Reconstituted human granulocyte-macrophage colony-stimulating factor receptor transduces growth-promoting signals in mouse NIH 3T3 cells: comparison with signalling in BA/F3 pro-B cells.* Mol Cell Biol, 1993. **13**(3): p. 1440-8.